

# UC Berkeley

## UC Berkeley Electronic Theses and Dissertations

### Title

Designing and Evaluating Novel Approaches to Nitrogen Recovery from Source-Separated Urine

### Permalink

<https://escholarship.org/uc/item/0hv961hw>

### Author

Tarpeh, William Abraham

### Publication Date

2017

Peer reviewed|Thesis/dissertation

Designing and Evaluating Novel Approaches to Nitrogen Recovery from  
Source-Separated Urine

By  
William Abraham Tarpeh

A dissertation submitted in partial satisfaction of the  
requirements for the degree of  
Doctor of Philosophy  
in  
Engineering – Civil and Environmental Engineering  
and the Designated Emphasis  
in  
Development Engineering  
in the  
Graduate Division  
of the  
University of California, Berkeley

Committee in charge:

Professor Kara L. Nelson, Chair  
Professor David Sedlak  
Professor Alice Agogino

Summer 2017

Designing and Evaluating Novel Approaches to Nitrogen Recovery from  
Source-Separated Urine

Copyright 2017  
by  
William Abraham Tarpeh

## Abstract

### Designing and Evaluating Novel Approaches to Nitrogen Recovery from Source-Separated Urine

By

William Abraham Tarpeh

Doctor of Philosophy in Civil & Environmental Engineering

University of California, Berkeley

Professor Kara Nelson, Chair

Urine is a “waste” stream that contains the majority of nitrogen, phosphorus, and potassium present in domestic wastewater. Separate collection and treatment of urine can potentially reduce treatment costs, environmental pollution due to nutrient discharges, and dependence on energy-intensive synthetic fertilizers. Closing the nitrogen loop between conventional fertilizer production and wastewater treatment can improve system efficiencies in industrialized settings and generate revenue that can be used to enhance sanitation access in developing communities. Harnessing the benefits of urine separation requires selective separation of nitrogen from other urine constituents. In this dissertation, two unit processes were characterized to recover nitrogen as ammonium from urine: ion exchange and electrochemical stripping. Observations were made at several scales, from molecular-scale mechanisms to process performance metrics and systems-level evaluation. In sum, this dissertation furthers understanding of two processes for recovering nitrogen as ammonium from urine as well as the overall source separation and resource recovery paradigm.

Ion exchange is an established technique for separating charged species from solutions and has recently been applied to urine. Household cartridges could be employed to concentrate nitrogen at the source of urine production. Four adsorbents were compared using equilibrium isotherms and fixed-bed columns; Dowex Mac 3, a synthetic ammonium-specific resin, exhibited the highest adsorption density and regeneration efficiency. Based on comparing synthetic urine solutions of increasing complexity and similarity to real urine, competition from sodium and potassium did not significantly decrease ammonium adsorption. Because urine composition varies, several models were compared to experimental data to predict adsorption isotherms. Flow

rate did not significantly affect ammonium adsorption nor regeneration; higher ammonium concentration in urine and proton activity in regenerants increased adsorption and regeneration efficiencies. Only trace organics that were positively charged at urine pH values (~9) adsorbed, and only two of ten compounds studied were detected in the ammonium sulfate product. Potassium recovery via cation exchange and phosphate recovery via struvite precipitation and anion exchange did not significantly affect ammonium adsorption, indicating potential implementation of complete nutrient recovery treatment trains.

Electrochemical stripping was shown to recover nitrogen as ammonium sulfate from urine based on the charge and volatility of ammonia. This novel approach combines electro dialysis with membrane stripping and selectively recovered 93% of nitrogen in batch studies at lower energy consumption than conventional ammonia stripping. Based on continuous-flow nitrogen fluxes, transport from the cathode to the trap chamber was identified as the rate-limiting step of electrochemical stripping. Synthetic urine solutions were used to determine the effects of urine composition and operating parameters on nitrogen flux, recovery efficiencies, and competing reactions. Electrochemically produced chlorine was found to be a loss mechanism for nitrogen but was mitigated by organic compounds present in urine. Nitrogen was selectively separated from other urine constituents, including sodium, potassium, inorganic anions, trace organic compounds, and metals.

Building on the molecular and process-scale insights in the laboratory, ion exchange for nitrogen recovery was evaluated in a container-based sanitation system in Nairobi, Kenya. No losses in performance metrics were observed over ten adsorption-regeneration cycles or with locally-produced columns ten times larger than lab scale. Parameters that can be economically and regularly measured to indicate process performance, such as absorbance and electrical conductivity, were identified as useful proxies for urine and ammonium breakthrough. While ammonium sulfate produced from urine was slightly more expensive than trucking urine to a local waste treatment facility, urine-derived fertilizers could be produced for less than conventional fertilizers in Kenya. Producing fertilizer from waste could reduce costs of sanitation provision and increase access to fertilizer.

Insights from this dissertation are useful to researchers and practitioners interested in closing loops to generate revenue from “waste” streams and reduce environmental impacts of excreta treatment. Adding fundamental understanding of two nitrogen recovery processes informs the design of pilot and demonstration scale installations to separately collect and treat urine at household and building scales. Beyond urine treatment, ion exchange and electrochemical stripping can be applied to other nitrogen-rich waste streams such as anaerobic digester effluent, landfill leachate, and food processing wastes.

## Acknowledgments

Although this dissertation bears my name, an entire village has contributed to this work and the completion of my PhD. I am extremely grateful to all of those who supported me in this journey. First I thank my wife Rachel Terrell-Perica and my mother Cheryl Walters, two stalwart women who have shown me so much about the world. Rachel, thank you for your unwavering support, for the late-night coffee, your patience with my midnight lab runs, and your steadfast love. Mums, thank you for passing your indomitable grit and endurance on to me, for praying and believing in me despite all odds, and for reminding me to never forget where I come from. To my siblings Wilson and Lisa, thank you for being role models and supporting me in all of my endeavors, no matter how crazy they seem. I also owe thanks to my families away from home, including Sequoyah Community Church, 360Church, and the Black Graduate Engineering Students Society. Above all, I am thankful to God for the opportunity and resources to pursue my interests while improving life for marginalized people.

Thank you to Dr. Kara Nelson, my advisor, for believing in me, patiently training me, and instilling high standards that became attainable. I am also grateful to David Sedlak, Alice Agogino, Oscar Dubón, Isha Ray, Baoxia Mi, and Ashok Gadgil for supporting me by asking challenging questions, sharpening my focus, and enriching my research and professional development with their own experiences. Mimi Jenkins was also instrumental in helping me secure my first research funding for preliminary studies. I am extremely grateful to co-authors Kai Udert, Ileana Wald, Maja Wiprächtiger, James Barazesh, Tzahi Cath, Micael Otieno Omollo, and Timothy Egan for their contributions to this dissertation. Thank you to my fellow graduate students, especially Madeline Foster-Martinez, Rachel Allen, Chelsea Preble, Rachel Dzombak, and Katya Cherukumilli, for spurring me on and making my experience at Berkeley unforgettable.

I cannot overstate the impact of communities that helped me thrive despite obstacles associated with being one of few African-American scholars in my field. The Ford Foundation network has been especially valuable and encouraging to me; the support I received made me believe that I belong in academia. Thank you to Project Touchdown, Urban Life, and SMASH Academy for giving me hope that I can bring others with me to diversify the academy. I hope to live up to the challenge from Ron Brown, the first African-American Secretary of Commerce: “When you reach that level of success, keep the door open and the ladder down for others to follow.”

Lastly, I am grateful to several institutions that funded my dissertation research, making it possible for me to complete this dissertation. The National Science Foundation Graduate Research fellowship, the Ford Foundation Pre-Doctoral Fellowship, the Harvey Fellowship, the Jack Kent Cooke Graduate Fellowship, and the UC Chancellor’s Fellowship allowed me the flexibility to research the questions that interested me most. The Development Impact Lab at Berkeley, the Andrew and Virginia Rudd Family Foundation, and the Blum Center for Developing Economies funded several trips to Kenya that helped me propose and complete my research on sanitation in developing communities. My laboratory work was supported by the NSF-funded engineering research center for Re-inventing the Nation’s Urban Water Infrastructure, or ReNUWIt.

## Table of Contents

<b>Chapter 1. Introduction .....</b>	<b>1</b>
<b>1.1 Resource Recovery from Wastewater .....</b>	<b>1</b>
<b>1.2 Source Separation.....</b>	<b>1</b>
<b>1.3 Nutrient Recovery from Urine .....</b>	<b>3</b>
<b>1.4 Evaluating novel approaches to nitrogen recovery .....</b>	<b>5</b>
<b>1.5 Dissertation Outline.....</b>	<b>6</b>
<b>Chapter 2. Comparing ion exchange adsorbents for nitrogen recovery from source-separated urine.....</b>	<b>8</b>
<b>1. INTRODUCTION .....</b>	<b>8</b>
<b>2. MATERIALS AND METHODS.....</b>	<b>10</b>
2.1 Description of Adsorbents.....	10
2.2 Solution Types .....	10
2.3 Batch Adsorption Experiments .....	11
2.4 Continuous Adsorption Experiments .....	11
2.5 Continuous Regeneration Experiments.....	11
2.6 Modeling .....	12
2.7 Statistical Analysis .....	13
<b>3. RESULTS AND DISCUSSION.....</b>	<b>14</b>
3.1 Comparison of Adsorbents at pH 4.....	14
3.2 Effect of pH on Ammonium Adsorption .....	14
3.3 Effect of Competition on Ammonium Adsorption .....	16
3.4 Adsorption in Real Urine .....	17
3.5 Comparison of Solutions.....	19
3.6 Continuous Flow Adsorption .....	20
3.7 Regeneration .....	20
3.8 Feasibility Assessment.....	21
3.9 Potential Implications for Urine Treatment .....	22
<b>Chapter 3. Effects of operating and design parameters on ion exchange columns for nutrient recovery from urine .....</b>	<b>23</b>
<b>1. INTRODUCTION .....</b>	<b>23</b>
<b>2. MATERIALS AND METHODS.....</b>	<b>25</b>
2.1 Column setup .....	25
2.2 Combined nutrient recovery.....	25
2.3 Operating Conditions and Adsorption .....	26
2.4 Operating Conditions and Regeneration .....	26
2.5 Trace organic contaminants .....	27
2.6 Chemical Analysis .....	27
2.7 Modeling Breakthrough Curves.....	28
2.8 Statistical Analysis .....	28
<b>3. RESULTS AND DISCUSSION.....</b>	<b>28</b>
3.1 Combined nitrogen and phosphorus recovery.....	28
3.2 Effects of operating conditions on adsorption .....	30
3.3 Effects of operating conditions on regeneration .....	32
3.4 Comparing regenerants .....	33
3.5 Fate of indicator trace organics .....	34
<b>4. CONCLUSIONS.....</b>	<b>35</b>
<b>Chapter 4. Electrochemical stripping to recover nitrogen from source-separated urine....</b>	<b>37</b>

<b>1. INTRODUCTION .....</b>	<b>37</b>
<b>2. MATERIALS AND METHODS .....</b>	<b>38</b>
2.1 Electrochemical Stripping Setup .....	38
2.2 Electrolysis Operation .....	39
2.3 Electrolysis solutions .....	40
2.4 Chemical Analysis .....	40
2.5 Statistical Analysis .....	41
<b>3. RESULTS AND DISCUSSION .....</b>	<b>41</b>
3.1 Nitrogen recovery from real urine in batch experiments .....	41
3.2 Continuous electrochemical stripping with real urine .....	42
3.3 Electrochemical oxidation reactions .....	43
3.4 Mechanisms of ammonia transformation .....	44
3.5 Fate of trace organic contaminants .....	45
3.6 Implications for urine treatment .....	47
<b>Chapter 5. Evaluating ion exchange for nitrogen recovery from source-separated urine in Nairobi, Kenya .....</b>	<b>49</b>
<b>CHAPTER 6. Conclusion .....</b>	<b>61</b>
<b>6.1 Ion Exchange .....</b>	<b>61</b>
6.1.1 Main Findings .....	61
6.1.2 Future Research .....	62
<b>6.2 Electrochemical Stripping .....</b>	<b>63</b>
6.2.1 Main Findings .....	63
6.2.2 Future Work .....	63
<b>6.3 Nitrogen Recovery and Development Engineering .....</b>	<b>64</b>
6.3.1 Main Findings .....	64
6.3.2 Future Work .....	65
<b>6.4 Characterizing Source Separation and Resource Recovery .....</b>	<b>65</b>
<b>REFERENCES .....</b>	<b>67</b>
<b>APPENDICES .....</b>	<b>78</b>
<b>A. Comparing ion exchange adsorbents for nitrogen recovery from source-separated urine .....</b>	<b>78</b>
A1. EQUATIONS .....	78
A2. TABLES .....	82
A3. FIGURES .....	85
<b>B. Effects of operating and design parameters on ion exchange columns for nutrient recovery from urine .....</b>	<b>90</b>
B1. EQUATIONS .....	90
B2. TABLES .....	92
B3. FIGURES .....	97
<b>C. Electrochemical stripping to recover nitrogen from urine .....</b>	<b>102</b>
C1. EQUATIONS .....	102
C2. TABLES .....	105
C3. FIGURES .....	109
<b>D. Evaluating ion exchange for nitrogen recovery from source-separated urine in Nairobi, Kenya .....</b>	<b>116</b>
D1. EQUATIONS .....	116
D2. TABLES .....	120
D3. FIGURES .....	121



# **Chapter 1. Introduction**

## **1.1 RESOURCE RECOVERY FROM WASTEWATER**

Despite its current categorization as waste, municipal wastewater contains resources such as energy,<sup>1</sup> water,<sup>2</sup> nutrients,<sup>3,4</sup> and metals<sup>5</sup> that can be recovered as valuable products. Energy recovered from carbon in wastewater can be used to power treatment operations and even lead to energy-positive treatment plants.<sup>6</sup> Potable reuse, or converting wastewater to drinking water, has become technically feasible and is being tested at pilot and full scale in water-constrained regions.<sup>7,8</sup> While energy and water recovery processes are already well-established, nutrients and metals have generally been targets for removal rather than recovery. In the case of nutrients like phosphorus and nitrogen, fertilizer inputs are currently identified as contaminants in wastewater effluents due to their contribution to eutrophication, which damages aquatic ecosystems. Similarly, metals in sewage are valued at \$13 million per year for wastewater collected from 1 million people.<sup>5</sup> Because contaminants in one waste stream can be valuable inputs to other sectors, wastewater treatment plants are shifting toward simultaneous resource recovery and treatment.

This dissertation focuses on the recovery of nutrients and specifically nitrogen from wastewater. In regions with centralized wastewater treatment, the motivation for recovering nutrients from wastewater is primarily environmental protection. Reducing nitrogen and phosphorus in waterways can reduce the rate of eutrophication, which affects over 70% of U.S. lakes and costs more than \$2.2 billion due to losses in recreation, livelihood, and remediation.<sup>9</sup> For the 2.6 billion people around the world without access to improved sanitation,<sup>10</sup> creating valuable products from excreta can reduce costs of sanitation provision. Transforming toilets from waste disposal installations to raw material collection centers could increase demand for excreta collection, maximizing health benefits of improved sanitation. In addition to safeguarding public health and environmental quality, recovering resources from wastewater can ultimately increase the sustainability of treating wastewater and producing valuable products like fertilizer. Recovering nitrogen from wastewater can reduce treatment energy and costs.<sup>11-13</sup> By closing loops between fertilizer production and wastewater treatment, resource recovery can remove redundancies and increase overall system efficiency.

## **1.2 SOURCE SEPARATION**

Separating urine at the toilet, or source separation, facilitates recovery of compounds that are found at high concentrations in urine. Source separation hinges on the realization that different waste streams have unique compositions and can be treated accordingly to optimize recovery efficiency (Figure 1.1). Whereas greywater produced from showers and laundry machines is an

ideal stream for recovering water, feces contains the majority of carbon present in wastewater, making feces a target for energy recovery. Urine contains 80% of wastewater nitrogen, 70% of P, and 50% of K but is only 1% of wastewater volume (Figure 1.2).<sup>14</sup> Urine is a low-volume, highly concentrated stream well suited for nutrient recovery.

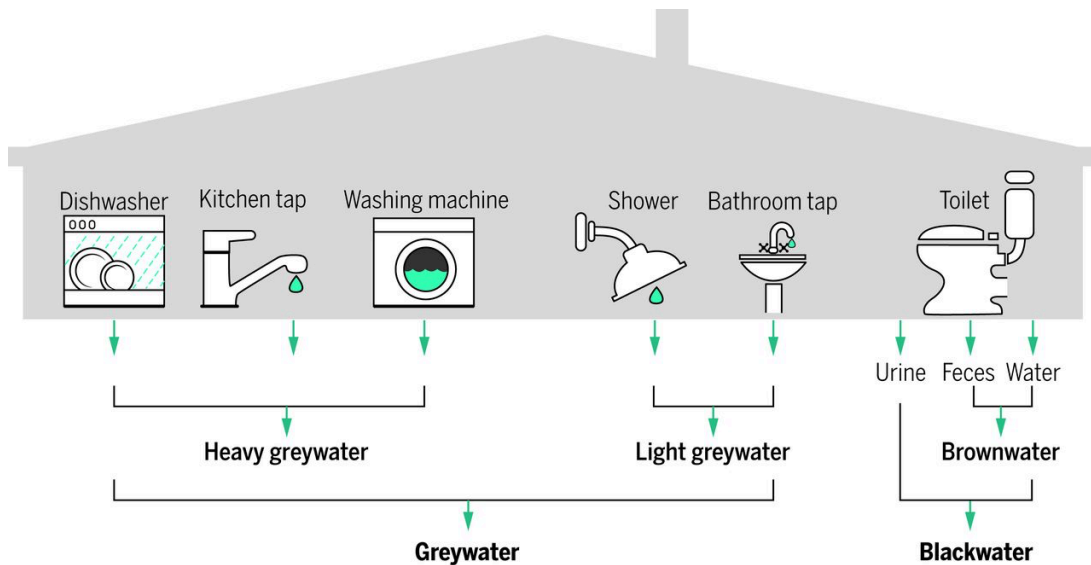


Figure 1.1. Source separation of domestic wastewater. From Larsen et al 2016.<sup>15</sup>

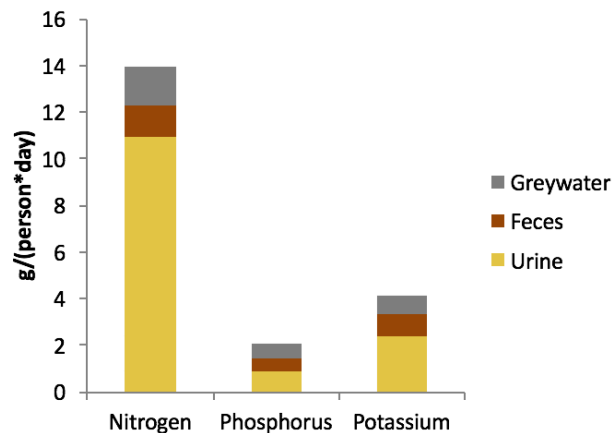


Figure 1.2. Nutrient load in different wastewater streams. Original figure; data from Jonsson et al 2005.<sup>16</sup>

Urine separation requires toilets that passively separate urine from feces and flushwater (Figure 1.3). Urine is already collected separately from feces in men’s urinals; waterless urinals avoid dilution. NoMix flush toilets can also be used, which have a barrier in the toilet chamber that excludes urine from feces. In unsewered settings, urine-diverting dry toilets (UDDTs) are an option. Many sanitation providers in developing communities have employed UDDTs to avoid

adding liquids to feces, which enhances the efficiency of drying processes for creating compost, solid fuel, and other value-added products from feces.<sup>17-20</sup>



Figure 1.3. Urine-diverting toilets. From left to right: waterless urinal, NoMix flush toilet, urine-diverting dry toilet.

By increasing the efficiency of nutrient recovery from wastewater, urine separation also augments the benefits of resource recovery. In particular, urine separation allows for resource recovery to happen at various scales, such as the toilet, building, or block level. At current growth rates, less than 50% of people in Africa and Asia will have access to centralized wastewater treatment by 2050,<sup>15</sup> smaller-scale solutions will be required to completely address sanitation needs. Depending on the scale of recovery, infrastructure can be adapted to include pipes or trucks; this additional flexibility may allow for more tailored solutions suitable for varying settings from densely populated urban slums to remote rural communities.

### 1.3 NUTRIENT RECOVERY FROM URINE

Urine composition must be well characterized to identify potential processes to recover nutrients. Several key reactions cause the composition of fresh and stored urine to differ significantly (Table 1.1). Stored urine has a lower urea concentration and higher pH, total ammonia, total carbonate, and alkalinity values than fresh urine. The predominant reaction responsible for the differences between fresh and stored urine is urea hydrolysis (Equation 1.1), in which the bacterial enzyme urea converts urea into ammonia/ammonium and carbonate. As a result of urea hydrolysis, pH and alkalinity increase and phosphate precipitates out with calcium and/or magnesium to form hydroxyapatite and struvite. Urea hydrolysis occurs spontaneously because urease-containing bacteria are ubiquitous in the environment.<sup>21,22</sup>

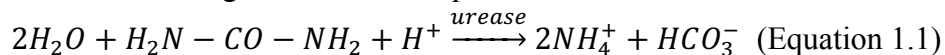


Table 1.1. Urine composition. From Udert 2006.<sup>23</sup>

	Fresh Urine	Stored Urine
pH	6	9
<b>Species</b>	<b>Concentrations (mM)</b>	
Urea	300	0
Cl <sup>-</sup>	100	100
Na <sup>+</sup>	100	100
K <sup>+</sup>	60	60
Total Ammonia	30	600
NH <sub>4</sub> <sup>+</sup>	30	400
Total Phosphate	25	20
SO <sub>4</sub> <sup>-2</sup>	15	15
Ca <sup>+2</sup>	5	0
Mg <sup>+2</sup>	5	0
NH <sub>3</sub>	0	200
Total carbonate	0	300
Alkalinity	22	500

Urine has been used as a fertilizer because it is inexpensive and contains all three major macronutrients: nitrogen, phosphorus, and potassium. Historically, farmers have primarily used their urine to grow crops for their own consumption<sup>24</sup>. Several studies have examined the effect of urine on plant growth,<sup>25,26</sup> but most have not considered the engineered systems for collecting and transporting urine as fertilizer. Recently, higher-density pilot systems have been constructed to collect and apply separately collected urine to fields.<sup>27,28</sup> Transporting urine at large scales may be prohibitively expensive because urine is 96% water.<sup>29</sup> This obstacle constrains the use of urine as fertilizer to areas where urine production occurs close to croplands. Using urine without treatment may also lead to application of chemical contaminants (e.g., pharmaceuticals such as sulfamethoxazole, trimethoprim)<sup>30</sup> and biological contaminants (e.g., *Clostridium*).<sup>30</sup> Pasteurization has been documented to reduce high bacterial concentrations in stored urine (~10<sup>9</sup> cells/mL),<sup>31</sup> but is unlikely to reduce chemical constituents such as trace organic contaminants. Recovering targeted resources from urine could reduce transport costs and reduce or eliminate contaminants from value-added products.

Phosphorus is the most valuable component of urine per mass. Two major approaches have been used to recover phosphorus: struvite precipitation and anion exchange. Struvite, or magnesium ammonium phosphate (MgNH<sub>4</sub>PO<sub>4</sub>), is a slow-release fertilizer that can be recovered from urine by magnesium addition and filtration of solids.<sup>3,32</sup> Anion exchange resins have also been used to recover phosphorus from urine;<sup>33</sup> ferrous iron nanoparticle-coated anion exchange resins are demonstrably selective for phosphate over chloride and sulfate,<sup>34,35</sup> which are also present in urine.

In comparison to phosphorus, nitrogen recovery from urine has not been extensively studied.<sup>36</sup> Nitrification-distillation, a biological process that converts half of total ammonia to nitrate to

produce ammonium nitrate, is the most mature unit process that effectively recovers nitrogen from urine.<sup>37,38</sup> Other wastewater nitrogen removal processes, such as ammonia stripping<sup>39</sup> and electrodialysis,<sup>40</sup> have been applied to urine. *Recovery* is distinguished from *removal* by the separation of nitrogen as a valuable product in addition to removal from the main treatment stream.

This dissertation adds to the body of literature on nitrogen recovery from urine by characterizing two novel processes for recovering nitrogen as ammonia from source-separated urine: ion exchange and electrochemical stripping. Both techniques target nitrogen as total ammonia, thus requiring the use of hydrolyzed (stored) urine. While several techniques to prevent urea hydrolysis have been explored,<sup>41,42</sup> this body of research assumes that spontaneous urea hydrolysis has occurred, as is typical in urine collection systems.<sup>21</sup> Total ammonia speciation depends on pH and temperature, where ammonia ( $\text{NH}_3$ ) is a volatile neutral species and ammonium ( $\text{NH}_4^+$ ) is a cation ( $\text{pK}_a$  9.25). In this dissertation most measurements are total ammonia nitrogen (TAN), the sum of both ammonia and ammonium concentrations. In both ion exchange and electrochemical stripping, ammonium ( $\text{NH}_4^+$ ) is recovered based on electrostatic interactions. During ion exchange ammonium adsorbs to negatively charged sites on adsorbents; electrochemical stripping employs a cation exchange membrane to selectively transport ammonium.

## 1.4 EVALUATING NOVEL APPROACHES TO NITROGEN RECOVERY

To inform the choice between source separation/resource recovery and existing wastewater management, technologies must be more rigorously characterized. Biological nitrogen removal has been successfully implemented at many wastewater treatment plants to reduce effluent nitrogen discharges.<sup>43</sup> Upgrading an existing treatment plant to convert ammonium ( $\text{NH}_4^+$ ) to dinitrogen gas ( $\text{N}_2$ ) via nitrification-denitrification requires additional costs and energy inputs. Paradoxically,  $\text{N}_2$  is converted to  $\text{NH}_4^+$  fertilizers during the Haber-Bosch process, which consumes about 1% of global energy.<sup>44</sup> In addition, nitrification-denitrification operates best in centralized treatment processes;<sup>45</sup> however, 25% of the United States population<sup>46</sup> and most people with sanitation access in developing regions<sup>10</sup> use on-site sanitation systems. In high-income countries, recovering nitrogen directly from wastewater could close the loop between fertilizer production and wastewater treatment, reducing the costs and energy required to prevent environmentally harmful discharges. In low and middle income countries, 90% of human excreta is discharged to the environment without treatment,<sup>47</sup> threatening aquatic ecosystems and public health; resource recovery from urine can incentivize excreta management.

Thus far, most research on nitrogen management technologies has focused on designing bench-scale systems. A well-informed comparison between conventional nitrogen management and source separation with resource recovery requires improved understanding of life-cycle impacts

and costs. Standard metrics for comparing approaches, such as energy demand, cost, and greenhouse gas emissions, are needed. Robustness, or repeatable performance in different settings and with different operating parameters (e.g., varying urine composition, other waste streams) is another important aspect of processes for resource recovery. Finally, context can influence technology choice through optimal scale, effluent treatment options, and combining processes into treatment trains. Ion exchange has been evaluated in Nairobi through field testing and in San Francisco with life-cycle cost and environmental assessment.<sup>48</sup> In San Francisco, decentralized household ion exchange cartridges could recover nitrogen at lower cost, greenhouse gas emissions, and energy demand than conventional nitrogen management.<sup>48\*</sup>

Conducting systems-level analysis while the development of novel unit processes is still at bench-scale helps identify research priorities, evaluate potential tradeoffs early in the technology development process, quantify potential benefits before scaling up, and improve the likelihood of progression to full-scale implementation. For example, sulfuric acid for regeneration was a significant contributor to emissions and energy demand for household ion exchange cartridges;<sup>48</sup> laboratory experiments exploring alternative regenerants were subsequently conducted (chapter 3). Iterative design and evaluation is especially valuable because evaluation in one setting can enhance design in another. For example, practical experience from producing fertilizers from urine, packing and applying them, and comparing them to industrial fertilizer could prove useful. Pilot-scale implementation of urine separation and nitrogen recovery would also increase understanding of practical issues such as long-term system performance, maintenance issues, odor, and user experience. A growing body of literature is connecting bench-scale characterization with systems-level evaluation of resource recovery technologies.

## **1.5 DISSERTATION OUTLINE**

The remainder of this dissertation consists of five chapters. In Chapter 2, four cation exchange adsorbents (clinoptilolite, biochar, Dowex 50, and Dowex Mac 3) were compared in terms of their adsorption capacity and regeneration efficiency for recovering nitrogen from urine as ammonium sulfate. Effects of urine composition on adsorption were characterized by comparing real and synthetic urine solutions and fitting with single-solute and competitive Langmuir models. Relationships between maximum adsorption density, regeneration lifetime, and cost were determined. Process modeling conducted in this study can also be used to specify adsorption capacities and regeneration lifetimes required for newly developed adsorbents to be cost-effective for nitrogen recovery from urine.

In Chapter 3, bench-scale development of nitrogen recovery via ion exchange was evaluated through continuous-flow experiments. Effects of operating conditions on adsorption and

---

\* William Tarpeh contributed to the submitted manuscript as second author; however, the study is not included in this dissertation.

regeneration were evaluated, along with the potential and optimization of combined phosphorus and nitrogen recovery. Regenerants were compared in terms of recovery efficiency and the fate of pharmaceuticals commonly found in urine was investigated during the ion exchange process.

Electrochemical stripping, a second unit process for recovering nitrogen from urine, is described in Chapter 4. Most importantly, nitrogen recovery efficiencies and mechanisms were investigated by comparing real and synthetic urine solutions; product and effluent streams were characterized with an emphasis on trace organics and metals. Electrochemical stripping was also compared to conventional nitrogen management in terms of energy required. In addition to validating this novel unit process, this chapter provides mechanistic understanding of parameters that reduce and facilitate nitrogen migration.

In Chapter 5 ion exchange is evaluated through technical validation and economic assessment in Nairobi, Kenya. Field and lab-scale studies were connected through demonstrating nitrogen recovery and validating field measurement methods. Process robustness was evaluated in terms of urine composition, process indicators, and scalability. For economic assessment, ion exchange costs were compared to current excreta management and fertilizer production practices in Kenya.

Overall, major findings are summarized in Chapter 6, the conclusion. Implications for both future research and practical implementation are also described. Finally, observations on the emerging paradigm of resource recovery from liquid waste streams are offered.

## **Chapter 2. Comparing ion exchange adsorbents for nitrogen recovery from source-separated urine.**

The following chapter is adapted from Tarpeh et al. (2017) Comparing ion exchange adsorbents for nitrogen recovery from source-separated urine. *Environmental Science & Technology* (51) 4, 2373-2381, with permission from Kai M. Udert and Kara L. Nelson. Copyright 2017, ACS Publications.

### **1. INTRODUCTION**

Source separation, in which urine and feces are separated at the toilet, has recently emerged as a potential alternative to conventional wastewater management, in which all wastewater is combined and treated together.<sup>47</sup> Separately collecting and treating distinct waste streams could allow for more optimal approaches to recover embedded resources,<sup>11</sup> and reduce energy and financial costs for wastewater treatment.<sup>12,13</sup> Conventional biological treatment removes nitrogen as dinitrogen gas (N<sub>2</sub>); this process simply reverses energy-intensive fertilizer production via the Haber-Bosch process, from which most of the wastewater nitrogen was derived.<sup>49</sup> Recovering reduced nitrogen directly from wastewater closes the loop between fertilizer production and wastewater treatment more efficiently than using N<sub>2</sub> as an intermediate. Urine has emerged as a waste stream of increasing interest because it comprises only 1% of wastewater volume but contains the majority of excreted macronutrients.<sup>47</sup> Furthermore, nitrogen-based fertilizers and disinfectants could potentially be a revenue source;<sup>50,51</sup> this creation of valuable products distinguishes recovery from removal.

Source separation could potentially be integrated into existing centralized wastewater infrastructure to reduce nutrient loads on wastewater treatment plants.<sup>52</sup> For example, as San Francisco and Paris are facing potential large capital investments to remove nitrogen from wastewater to reduce eutrophication in receiving waters,<sup>53,54</sup> source separation and resource recovery technologies are being considered.<sup>55</sup> Source separation could also be used to reduce nitrogen loads from on-site sanitation due to failing septic systems,<sup>13</sup> and in urban areas that lack formal infrastructure, such as the decentralized approaches being pursued by Sanergy in low-income, high-density settlements in Nairobi, Kenya<sup>56</sup> and the Valorization of Urine Nutrients (VUNA) project in Durban, South Africa.<sup>57</sup> To inform the choice between source separation/resource recovery and current wastewater management approaches, technologies that enable the new paradigm must be further developed and more rigorously characterized.

Ion exchange is a promising technology for nitrogen recovery from source-separated urine. During urine storage, urea is hydrolyzed to ammonium (NH<sub>4</sub><sup>+</sup>),<sup>22</sup> which can adsorb onto materials with negatively charged sites. Although cation exchange has been studied for removing



$\text{NH}_4^+$  from  $\text{NH}_4\text{Cl}$  solutions,<sup>58</sup> drinking water,<sup>59</sup> and landfill leachate<sup>60</sup> at concentrations less than 800 mg N/L, it has only been preliminarily documented for urine treatment, which has  $\text{NH}_4^+$  concentrations of around 5000 mg N/L.<sup>61</sup> Multiple studies have examined sorption of phosphate and pharmaceuticals from synthetic urine by anion exchange resins.<sup>33,62</sup> Cation exchange adsorbents could also be used for potassium recovery. Suitable adsorbents can be selected and combined to remove the resources or pollutants of interest. As a physicochemical process, sorption may be more stable than biological nitrogen removal. Because the required adsorbent mass and reactor size are proportional to the mass of compound removed, sorption can be applied at varying scales. Sorption's selective, stable, and scalable nature make it a promising option for resource recovery from urine.<sup>63</sup>

To our knowledge, this investigation is the first to compare the feasibility of a diverse set of ion exchange adsorbents for cation recovery from source-separated urine. Four ion exchange adsorbents were tested: clinoptilolite, biochar, Dowex 50, and Dowex Mac 3. Clinoptilolite is extremely abundant, naturally-occurring, and has been documented for removing ammonium from drinking water,<sup>64</sup> wastewater,<sup>64,65</sup> and, preliminarily, source-separated urine.<sup>66</sup> Biochar is already being used as a soil conditioner for nutrient and moisture retention and can be produced economically from a variety of feedstocks.<sup>67,68</sup> One such feedstock is feces, which could make possible a scheme in which feces-based biochar is used to recover ammonium from separately collected urine. Dowex 50 is a standard synthetic cation exchange resin, and Dowex Mac 3 is another synthetic cation resin with purported ammonium specificity,<sup>69</sup> suggesting it may be particularly suited to ammonium recovery from source-separated urine.

In this study, factors affecting ammonium adsorption were explored in solutions of increasing complexity: pure salt, synthetic urine, and real urine. Experiments were designed to measure two major determinants of feasibility: adsorption capacity and regeneration potential. Adsorption capacity describes how much nitrogen can be captured each sorption cycle per mass of adsorbent (before regeneration) and can be used to determine minimum reactor size. Regeneration potential influences adsorbent lifetime, and therefore how much urine the adsorbent can treat before replacement. The specific objectives of this study were to: (i) characterize adsorption in ideal solutions with respect to the Langmuir parameters maximum adsorption density,  $q_{\text{max}}$ , and affinity constant,  $K_{\text{ads}}$ ; (ii) characterize adsorption isotherms in synthetic and real urine, including the effect of sodium and potassium competition on ammonium adsorption; (iii) determine adsorption capacity and regeneration efficiency in column experiments; and (iv) estimate adsorbent costs and reactor volume to preliminarily assess the feasibility of ion exchange for nitrogen recovery from source-separated urine.

## 2. MATERIALS AND METHODS

### 2.1 Description of Adsorbents

Four adsorbents were examined in this study: clinoptilolite (Multavita, Castle Valley, MT), biochar (Ithaca Institute, Ayent, Switzerland), Dowex 50 (Alfa Aesar, Ward Hill, MA), and Dowex Mac 3 (Sigma Aldrich, St. Louis, MO). Clinoptilolite is an aluminosilicate zeolite with negatively charged sites due to the isomorphous substitution of trivalent aluminum for tetravalent silicate groups. As the most abundant natural zeolite, it is isolated from naturally occurring mineral deposits in many countries, including Turkey, South Africa, Australia, China, and the United States.<sup>64</sup> Biochar is a carbon-rich product made by thermal decomposition of organic material under limited supply of oxygen and at a temperature greater than 700°C.<sup>70</sup> Within this definition, biochar varies extensively in form, feedstock, and processing method. The biochar used in this study was from wood husks (950°C for 2 hours, no pretreatment); similar biochars have carboxyl functional groups.<sup>68</sup> The adsorption sites of Dowex 50 and Dowex Mac 3 are sulfonic acid and carboxylic acid moieties, respectively. This difference in functional groups makes Dowex 50 effective over a wider pH range than Dowex Mac 3.<sup>69,71</sup> Both Dowex resins are available with protons initially adsorbed to functional sites. Dowex Mac 3 is marketed as an ammonium-specific cation exchange resin produced from a polyacrylic matrix and added carboxylate moieties.<sup>69</sup> For further information on adsorbents see Table A1.

### 2.2 Solution Types

To examine the factors and mechanisms affecting adsorption in urine, four solutions were used, ranging from ideal to real: (i) NH<sub>4</sub>Cl without pH adjustment; (ii) NH<sub>4</sub>Cl at pH 9; (iii) synthetic stored urine (pH ~ 9); and (iv) real stored urine (pH ~ 9). Because NH<sub>4</sub><sup>+</sup> is a weak acid (pK<sub>a</sub> 9.25)<sup>72</sup>, the pH of the 9000 mg N/L NH<sub>4</sub>Cl solution without adjustment was 4.72. For ease of reference, we call these “pH 4 experiments.” The effect of pH on ammonium adsorption was elucidated by comparison with pH 9 NH<sub>4</sub>Cl, which is closer to the pH of stored urine and the NH<sub>4</sub><sup>+</sup>/NH<sub>3</sub> pK<sub>a</sub>. Synthetic stored urine was used to observe the effect of competition on ammonium adsorption by other cations, such as Na<sup>+</sup> and K<sup>+</sup>. We used an existing synthetic urine recipe based on real urine concentrations (Table A2).<sup>23</sup> Organic acids are the primary organic constituent of urine;<sup>23</sup> acetic acid is used in synthetic urine to represent organic acids. Finally, real source-separated urine from NoMix toilets and waterless urinals was used.<sup>51</sup> The real urine was from the men’s collection tank of the Swiss Federal Institute of Aquatic Sciences and Technology’s (Eawag) main building *Forum Chriesbach* (composition in Table A3). Given the extended storage time, urea was completely hydrolyzed to ammonia/ammonium and magnesium and calcium concentrations were negligible due to struvite and hydroxyapatite precipitation.<sup>73</sup> In addition to the four solution types above, NaCl and KCl solutions were also prepared without pH adjustment. These results served as inputs for competitive adsorption models to which synthetic urine results were compared. All experiments were conducted at room temperature (23 ± 2 °C) with nanopure water and analytical grade chemicals.

### 2.3 Batch Adsorption Experiments

Batch adsorption experiments were conducted by adding 0.015 g adsorbent to 1.5 mL of solution and continuously mixing for 24 hours to ensure equilibration (based on preliminary experiments). Samples were then centrifuged at 2000 rpm for five minutes to separate adsorbent and solution. Aliquots from the initial solution and the supernatant were analyzed for  $\text{NH}_4^+$ ,  $\text{Na}^+$ , and  $\text{K}^+$  concentrations via ion chromatography (Metrohm chromatograph, IonPac CS12 column, 30 mM methanesulfonic acid eluent, 1.0 mL/min, 30 °C). A six-cation chloride calibration standard ( $\text{LiCl}$ ,  $\text{NaCl}$ ,  $\text{NH}_4\text{Cl}$ ,  $\text{KCl}$ ,  $\text{MgCl}_2$ ,  $\text{CaCl}_2$ ) was diluted 100, 50, 20, 10, and 6.25 times to generate a calibration curve. A mass balance was used to calculate the final adsorption density ( $q_f$ ) at equilibrium according to Equation 1:

$$V_L(C_0 - C_f) = W(q_f - q_0) \quad (\text{Equation 2.1})$$

where  $V_L$  is solution volume (L),  $C_0$  is initial concentration of adsorbate (mg  $\text{NH}_4^+$ -N,  $\text{Na}^+$ , or  $\text{K}^+$ /L),  $C_f$  is adsorbate concentration at equilibrium (mg  $\text{NH}_4^+$ -N,  $\text{Na}^+$ , or  $\text{K}^+$ /L),  $W$  is adsorbent mass (g), and  $q_0$  is the initial adsorption density (mg  $\text{NH}_4^+$ -N,  $\text{Na}^+$ , or  $\text{K}^+$ /g adsorbent). To compare adsorption densities between cation species, molar mass was used to convert adsorption densities to mmol/g adsorbent.

For pH 4 experiments, 16 initial  $\text{NH}_4\text{Cl}$  solutions with total ammonia concentrations varying from 25-9000 mg N/L were prepared without pH adjustment. For pH 9 experiments,  $\text{NH}_4\text{OH}$  was added to increase pH. For synthetic and real urine experiments, one master solution was made and diluted to 15 different concentrations to generate adsorption curves. Real urine was filtered (0.47  $\mu\text{m}$ ) to exclude precipitates that might have interfered with adsorption. Although initial pH differed for each dilution in a given adsorption curve, we refer collectively to each set of experiments by the pH of the most concentrated initial solution. For example, we refer collectively to samples prepared from the 9000 mg N/L  $\text{NH}_4\text{Cl}$  at pH 9 as “pH 9 experiments” although pH was less than 9 for many dilutions.

### 2.4 Continuous Adsorption Experiments

Upflow continuous adsorption experiments were performed in PVC columns (2.54-cm diameter, 16-cm length) packed with each adsorbent, sponges to retain media, and pretreated with 1 M borate buffer. Synthetic urine was pumped through each column at 4.5 mL/min for 6 hours, and samples from the end of the column were collected every 20 minutes and analyzed for ammonium and chloride (used as a conservative tracer) via ion chromatography. Adsorption densities were calculated by numerically integrating breakthrough curves and dividing by adsorbent mass (Equation A6).

### 2.5 Continuous Regeneration Experiments

Regeneration experiments were similar to adsorption experiments, except with 0.1 M  $\text{H}_2\text{SO}_4$  pumped at 22.5 mL/min for 2 hours and samples collected every 10 minutes. Regeneration

efficiencies were calculated by dividing moles of ammonium eluted (integration of elution curve, Figure A1) by the moles adsorbed (Equation A7).

## 2.6 Modeling

To account for non-ideality of concentrated ionic solutions, PHREEQC software<sup>74</sup> was used to determine Pitzer activity coefficients based on the concentrations in each initial solution. Cation chromatography measures total ammonia concentrations. Ammonia/ammonium speciation was determined according to Equations 2-4 using measured values of pH and temperature:<sup>75</sup>

$$K_{NH_4^+|T_2} = K_{NH_4^+|T_1} x \exp \left[ \frac{\Delta H_R}{R} \left( \frac{1}{T_1} - \frac{1}{T_2} \right) \right] \quad (\text{Equation 2.2})$$

$$[NH_4^+] = \frac{N_{tot}}{1 + \gamma_{NH_4^+} 10^{\frac{pH - pK_{NH_4^+}}{pH - pK_{NH_4^+}}}} \quad (\text{Equation 2.3})$$

$$\{NH_4^+\} = \gamma_{NH_4^+} [NH_4^+] \quad (\text{Equation 2.4})$$

where  $K_{NH_4^+}$  is the ammonium acid dissociation constant at 25 °C (9.25),<sup>72</sup> R is the universal gas constant, T is temperature,  $N_{TOT}$  is total ammonia concentration,  $[\ ]$  denotes molar concentration,  $\{ \}$  denotes chemical activity, and  $\gamma_{NH_4^+}$  is the Pitzer activity coefficient for ammonium.

Adsorption curves were fit to the single-solute Langmuir model for each adsorbent (Equation 5, where  $n=1$ ).<sup>76</sup>  $q_f$  is the adsorption density (mmol  $NH_4^+$ ,  $Na^+$ , or  $K^+$ /g adsorbent),  $q_{max}$  is maximum adsorption density,  $K_{ads}$  is the affinity constant, and  $\{A\}$  denotes the chemical activity of species A. Although many previous studies have used linearization to determine maximum adsorption density and affinity constants, this approach can introduce statistical biases.<sup>77,78</sup> Thus, we used a non-linear regression to determine maximum adsorption density and affinity constants with ISOFIT (Isotherm Fitting Tool).<sup>79</sup>

For synthetic urine, experimental results were evaluated with three competitive adsorption models. The first was the competitive Langmuir model (Equation 5, where  $n=3$  for  $NH_4^+$ ,  $Na^+$ , and  $K^+$ ).<sup>76</sup> The values of  $q_{max}$  and  $K_{ads}$  calculated from the single-cation adsorption experiments were used as inputs to the competitive Langmuir model, which was plotted for various activities using non-linear parameterization in MATLAB (8.3.0 R2014A). The second was a three-solute competitive adsorption model based on Jain and Snoeyink (Equation 6, see section A1.1 for more detail);  $q_{max}$  and  $K_{ads}$  for each cation were from single-cation adsorption experiments, and numerical subscripts denote each cation from lowest (1) to highest (3) maximum adsorption density.<sup>80</sup> The third was the empirical Langmuir-Freundlich model (Equation 7), in which  $K_{ads}$  values were from single-solute experiments, and  $n$  and  $q_{max}$  (one value for all cations) were determined by nonlinear regression on synthetic urine data. For all three models, adsorption densities were calculated using the experimentally measured equilibrium activities in synthetic urine. To predict equilibrium adsorption densities and activities in undiluted real urine, we used

initial activities and model parameters to solve a system of six equations containing model predictions for each cation and mass balances on each cation (section A1.1).

$$q_{f,i} = \frac{K_{ads,i}q_{max,i}\{A_i\}}{1+\sum_{n=1} K_{ads,n}\{A_n\}} \quad (\text{Equation 2.5})$$

$$q_{f,3} = \frac{q_{max,1}K_{ads,3}\{A_3\}}{1+K_{ads,1}\{A_1\}+K_{ads,2}\{A_2\}+K_{ads,3}\{A_3\}} + \frac{(q_{max,2}-q_{max,1})K_{ads,3}\{A_3\}}{1+K_{ads,2}\{A_2\}+K_{ads,3}\{A_3\}} + \frac{(q_{max,3}-q_{max,2})K_{ads,3}\{A_3\}}{1+K_{ads,3}\{A_3\}} \quad (\text{Equation 2.6})$$

$$q_{f,i} = \frac{K_{ads,i}q_{max}\{A_i\}^n}{1+\sum_{n=1} K_{ads,n}\{A_i\}^n} \quad (\text{Equation 2.7})$$

Material cost for different adsorbents was evaluated as an initial analysis of feasibility. Three major determinants of adsorbent cost per gram nitrogen recovered ( $P_N$ ) were considered: specific adsorbent price ( $P_{\text{adsorbent}}$ , in USD/kg resin), adsorption capacity ( $q_0$  in mmol N/g adsorbent), and number of uses before adsorbent replacement ( $N$ ) (Equation 8, where  $MW_N$  is the molecular weight of nitrogen). Adsorption capacities were the highest values measured in undiluted real urine; resin prices were determined from literature (Table A5). Adsorbent cost per gram nitrogen was also converted to cost per liter of urine treated ( $P_U$ ) by considering the total ammonia concentration in urine in mg N/L ( $[\text{NH}_3]_{\text{tot}}=[\text{NH}_4^+] + [\text{NH}_3]$ , Equation 9).

$$P_N = \frac{P_{\text{adsorbent}}}{Nq_0MW_N} \quad (\text{Equation 2.8})$$

$$P_U = P_N[\text{NH}_3]_{\text{tot}} \quad (\text{Equation 2.9})$$

For each adsorbent tested, experimental adsorption density values were used to determine the reactor volume (Equation 10).  $D_U$  is urine production rate per person (L urine/(person\*day)),  $P_H$  is average household size (people/household),  $t_c$  is time between collection,  $q$  is experimental adsorption density (mg  $\text{NH}_4^+$ -N/g adsorbent), and  $\rho_b$  is bulk density (g adsorbent/L reactor volume). We assumed that the ion exchange cartridge would be replaced weekly and treat 28 liters of urine per week for a household with four people each producing one liter of urine each day. Bulk densities were determined by weighing known volumes of packed adsorbents.

$$V_R = \frac{D_U * P_H * t_c * [\text{NH}_3]_{\text{tot}}}{q * \rho_b} \quad (\text{Equation 2.10})$$

## 2.7 Statistical Analysis

Best-fit Langmuir parameters ( $q_{\text{max}}$  and  $K_{\text{ads}}$ ) determined from non-linear regression were compared for each pair of adsorbents with a one-way ANOVA and paired t-tests. A similar analysis was performed to compare solutions (pure salt, synthetic urine, and real urine). The single-solute Langmuir isotherm was applied to all solutions for consistency in the statistical analysis (Table A6). Although both  $q_{\text{max}}$  and  $K_{\text{ads}}$  were compared for each isotherm, only  $q_{\text{max}}$  was reported because it was a more conservative indicator of significant differences and was more relevant to high ammonium concentrations in urine. Ammonium adsorption densities in experimental triplicates with undiluted real urine for each adsorbent were also compared with a one-way ANOVA and paired t-tests.

### 3. RESULTS AND DISCUSSION

#### 3.1 Comparison of Adsorbents at pH 4

Based on experiments with  $\text{NH}_4\text{Cl}$  at pH 4, the four adsorbents exhibited different adsorption capacities (Figure 2.1a); however, the best-fit maximum adsorption densities were not statistically different ( $p > 0.05$ ). More variability was observed at high concentrations because of high dilution factors (e.g., 1:1000 for highest concentrations); they were accepted because of the redundancy present with sixteen points per adsorption curve. The Langmuir model was used because we expected a finite number of identical adsorption sites for zeolite and the synthetic resins and previous studies reported it had the best fit for the adsorbents tested.<sup>58,65,68,81</sup> Best-fit maximum adsorption densities and affinity constants are summarized in Table A4 and Figure A2. A similar analysis was performed for NaCl and KCl to determine Langmuir parameters for later use in the competitive adsorption model (Figure A3).

Overall, the adsorption capacities and affinity constants for pH 4  $\text{NH}_4\text{Cl}$  from this study were higher than those in literature (Table A1, Table A4).<sup>64,65,68,69,71</sup> For natural adsorbents, different sources (e.g. clinoptilolite from Turkey or USA)<sup>64</sup> and pretreatment (pyrolysis temperature and time)<sup>68</sup> could contribute to variation in best-fit Langmuir parameters between studies. For all adsorbents, variation could be due to operation at much higher concentrations that show more of the adsorption curve and the use of non-linear regression for fitting ( $q_{\text{max}}$  values determined by linearization of the Langmuir isotherm were lower; data not shown). Note that the estimate for the maximum ammonium adsorption capacity for Dowex Mac 3 was significantly higher than the highest value measured directly, which is one limitation of using best-fit parameters to compare isotherms.

#### 3.2 Effect of pH on Ammonium Adsorption

Adsorption results for the pH 9  $\text{NH}_4\text{Cl}$  solutions are presented in Figure 2.1b. Although the adsorption densities were higher for the synthetic resins than the natural adsorbents, there were no statistically significant differences between adsorbents due to the high variability observed. Ammonium adsorption isotherms at pH 4 and pH 9 were also not significantly different for any adsorbent, but several observations can be made about the effects of pH on adsorption sites and ammonia speciation. Cation adsorption sites are most effective when negatively charged, which occurs when solution pH exceeds the surface point of zero charge. This effect was especially apparent for Dowex Mac 3, which has a reported  $\text{pK}_a$  of 5 (Table A1), which is between the two pH values tested for  $\text{NH}_4\text{Cl}$  solutions. In the pH 4 solutions, substantially fewer sites were deprotonated than in the pH 9 solutions. Accordingly, fewer sites were available for ammonium adsorption and lower adsorption densities were observed, especially at low equilibrium activities. Similar trends have been reported for clinoptilolite.<sup>82</sup>

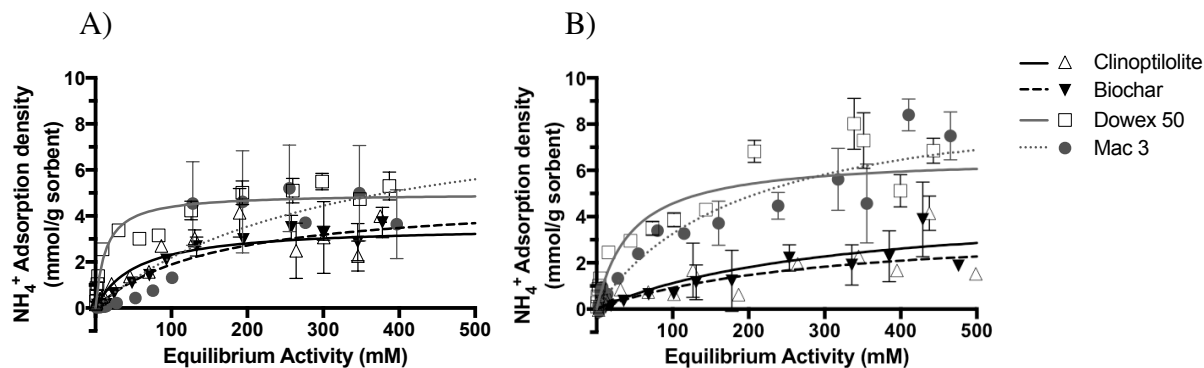


Figure 2.1  $\text{NH}_4^+$  adsorption in  $\text{NH}_4\text{Cl}$  (a) without pH adjustment and (b) for pH 9 solutions. Error bars represent one standard deviation above and below mean of dilution triplicates ( $n=3$ ) for high activities ( $> 100$  mM). Curves show best-fit Langmuir isotherms based on non-linear regression of experimental data.

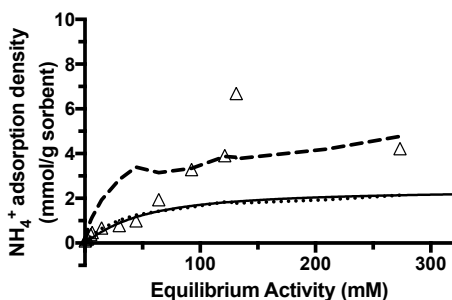
The solution pH also impacted  $\text{NH}_4^+$  adsorption by affecting ammonia speciation. Given the proximity of the pH in pH 9  $\text{NH}_4\text{Cl}$ , synthetic urine, and real urine experiments to the  $\text{NH}_3/\text{NH}_4^+$   $pK_a$  (9.25), up to 35% of total ammonia was present as  $\text{NH}_3$ . Because  $\text{NH}_3$  is uncharged and thus does not participate in cation exchange, we expected the adsorption density to be lower for the pH 9 solutions than the pH 4 solutions. Although this was the trend for the natural adsorbents, it was not the case for the synthetic resins. One possible reason for the difference is that natural adsorbents have more heterogeneous adsorption sites and initial adsorbates and therefore more complex pH effects (Figure A4).

In interpreting the pH results, it is important to note that the final pH of the solutions, after adsorption equilibrium was established, was different in some cases than the initial solution pH; the equilibrium pH values of the highest concentrations tested for each solution are shown in Figure A5. The equilibrium pH was affected by two competing phenomena. The first was sorption of  $\text{NH}_4^+$ , which removes it from solution and shifts the  $\text{NH}_3/\text{NH}_4^+$  equilibrium, causing protonation of some  $\text{NH}_3$  and increasing solution pH. The second was desorption of protons due to exchange with other cations, which decreases solution pH. For the pH 4 solutions, the solution pH decreased after equilibrating with the synthetic resins, indicating that desorption of protons was the dominant effect. With natural adsorbents exposed to pH 4 solutions, the pH increased, indicating that  $\text{NH}_3/\text{NH}_4^+$  equilibrium dominated. In addition, natural adsorbents were initially loaded with a mixture of protons and other cations, leading to relatively fewer  $\text{H}^+$  desorbing. Batch experiments with sulfuric acid confirmed this phenomenon, as  $\text{Na}^+$ ,  $\text{K}^+$ , and  $\text{Ca}^{2+}$  ions desorbed from natural adsorbents but not from synthetic resins (Figure A4). At pH 9, the  $\text{NH}_3/\text{NH}_4^+$  pair buffered the pH and only small pH changes were observed (Figure A5). Synthetic urine and real urine pH values also increased (slightly) for natural adsorbents and decreased for synthetic resins (Figure A5).

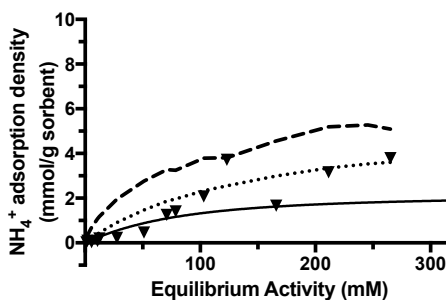
### 3.3 Effect of Competition on Ammonium Adsorption

The effect of competition was investigated by performing adsorption experiments in synthetic urine, in which  $\text{Na}^+$  and  $\text{K}^+$  competed with  $\text{NH}_4^+$  for adsorption sites (Figure 2.2). Again, the synthetic resins adsorbed more ammonium per gram than the natural adsorbents. In particular, the maximum adsorption density ( $q_{\text{max}}$  from best-fit single-solute Langmuir isotherm) of Dowex Mac 3 was significantly higher than the other three adsorbents ( $p < 0.01$  with Dowex 50;  $p < 0.0001$  with clinoptilolite and biochar). There was no significant difference between adsorption capacities for the pure  $\text{NH}_4\text{Cl}$  and synthetic urine solutions ( $p > 0.05$ ), indicating that the presence of other constituents, including competing ions, did not decrease the adsorption density of ammonium on any of the adsorbents.

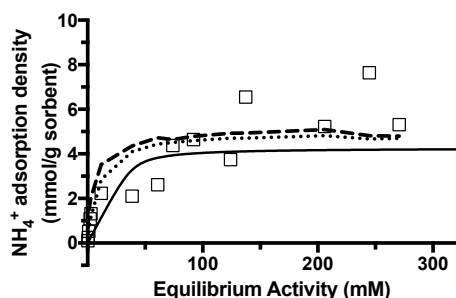
A) Clinoptilolite



B) Biochar



C) Dowex 50



D) Dowex Mac 3

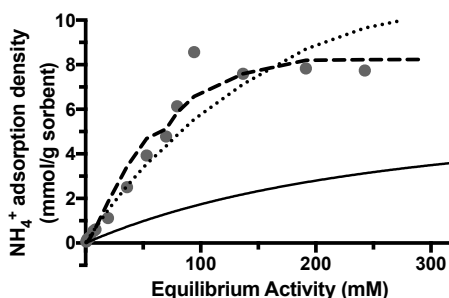


Figure 2.2 Comparison of  $\text{NH}_4^+$  adsorption in synthetic urine and competitive Langmuir, competitive Langmuir-Freundlich, and Jain-Snoeyink models for (a) clinoptilolite, (b) biochar, (c) Dowex 50, and (d) Dowex Mac 3. Insets of lower equilibrium activities are in Figure A6.

Synthetic urine adsorption data were fitted to three models: competitive Langmuir, trisolute Jain/Snoeyink, and competitive Langmuir-Freundlich (Figure 2.2) and the average relative error and sum of squared error (SSE) were determined. For clinoptilolite, Dowex 50, and Dowex Mac 3, the Langmuir-Freundlich model had the lowest SSE and best overall fit to synthetic urine data (Table A7), although it overestimated adsorption for clinoptilolite and Dowex 3 at low equilibrium activities (Figure A6). It is not surprising that the Langmuir-Freundlich model was superior because the parameters  $q_{\text{max}}$  and  $n$  (Equation 2.7) were determined by fitting to the



synthetic urine data (using nonlinear regression), whereas the Jain-Snoeyink and competitive models were based exclusively on the  $q_{\max}$  and  $K_{\text{ads}}$  parameters determined from single-solute Langmuir fits. For biochar, competitive Langmuir was the best fit overall (Table A7), but it overestimated adsorption at low equilibrium activities (Figure A6). The Jain-Snoeyink model assumes competitive Langmuir behavior below the maximum adsorption densities of sodium and potassium and single-solute Langmuir for ammonium above those adsorption densities. There was not much difference between the competitive Langmuir and Jain-Snoeyink isotherms, primarily because single-solute  $q_{\max}$  values for  $\text{Na}^+$  and  $\text{NH}_4^+$  differed by at most 0.74 mmol N/g adsorbent (Dowex 50, Table A4).

The fact that the competitive Langmuir model predicted lower adsorption densities in synthetic urine than were measured could be due to overestimating the impact of competitor cations or because other constituents in the synthetic urine increased adsorption (such as acetate; see section 3.5). Single solute ammonium adsorption densities, which isolate the former effect, were higher than competitive Langmuir models for clinoptilolite (38%), biochar (64%), Dowex 50 (75%), and Dowex Mac 3 (18%). Larger differences between competitive and single-solute models may indicate less homogeneous sites and thus more selectivity for ammonium. Even if adsorption sites are identical, access to them may vary based on macroscopic pore size distributions. Hydrated ionic radius is one proxy for access to adsorption sites;<sup>83</sup> ammonium and potassium ions have smaller radii than sodium ions,<sup>84</sup> allowing the former species to diffuse through smaller pores and access more exchange sites. However, the  $q_{\max}$  values for  $\text{NH}_4^+$  and  $\text{Na}^+$  from single-solute experiments were similar (Table A4), suggesting that differences in hydrated ionic radius did not completely explain differential adsorption of cations.

### 3.4 Adsorption in Real Urine

The isotherm trends observed in synthetic urine adsorption were similar to those in real urine (Figure 2.3a, Dowex Mac 3 > Dowex 50 > clinoptilolite ~biochar). Maximum ammonium adsorption densities ( $q_{\max}$  from best-fit single-solute Langmuir isotherm) were significantly different for all adsorbent pairs except clinoptilolite and biochar. The Dowex Mac 3 adsorption isotherm had the highest maximum adsorption density ( $p < 0.001$  for pair-wise comparison with all other adsorbents). To provide a more direct comparison between the adsorbents for the specific case of real urine, and to overcome the variability observed in the isotherms, triplicate adsorption experiments were conducted with undiluted real urine (Figure 2.3b). Dowex Mac 3 had a statistically higher  $\text{NH}_4^+$  adsorption density than all other adsorbents ( $p < 0.001$  for clinoptilolite and biochar;  $p < 0.05$  for Dowex 50). Together, these results support the conclusion that Dowex Mac 3 exhibited a higher adsorption density than clinoptilolite, biochar, and Dowex 50. Given its manufactured nature, Dowex Mac 3 was expected to have a higher maximum adsorption density than the heterogeneous natural adsorbents; it was also expected to have a higher maximum adsorption density than Dowex 50 because of its aliphatic resin structure and

macropores, which have more surface area available for adsorption than the polystyrene backbone of Dowex 50 (Table A1).

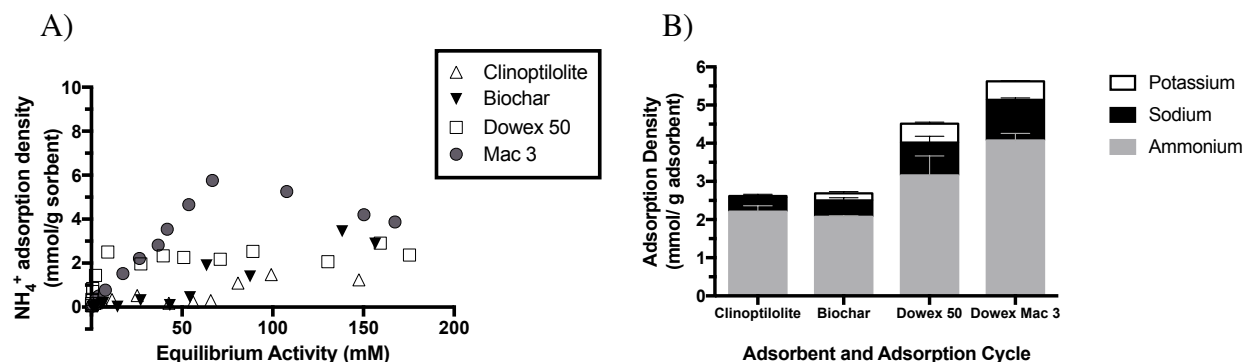


Figure 2.3 (a)  $\text{NH}_4^+$  adsorption isotherm for real urine. (b) Adsorption density of  $\text{NH}_4^+$ ,  $\text{Na}^+$ , and  $\text{K}^+$  in undiluted real urine. Error bars represent one standard deviation above and below mean for experimental triplicates ( $n=3$ ), and in some cases are too small to be shown.

The three competitive models from synthetic urine isotherms were also applied to adsorption in undiluted real urine (Table A8). The Jain-Snoeyink model was best for predicting adsorption densities in real urine. The main reason is because the adsorption density in real urine was lower than that measured in synthetic urine at similar equilibrium activity levels (even though the differences were not statistically significant; see next section). Thus, the Langmuir-Freundlich overestimated adsorption density in undiluted real urine.

To provide more insight into the differential adsorption of competitor cations (Figure 2.3b), the adsorption isotherms for  $\text{NH}_4^+$ ,  $\text{Na}^+$ , and  $\text{K}^+$  in real urine on Dowex Mac 3 are shown in Figure 2.4a. As expected given its sixfold (relative to  $\text{Na}^+$ ) or tenfold (relative to  $\text{K}^+$ ) higher molar concentration in urine, ammonium occupied the majority of available sites. Preferential adsorption of  $\text{NH}_4^+$  was also observed, as seen by the higher adsorption density of ammonium compared to the other cations at the same equilibrium activity. Similar trends were observed for the other adsorbents, even though they are not reported to have higher affinities for ammonium.

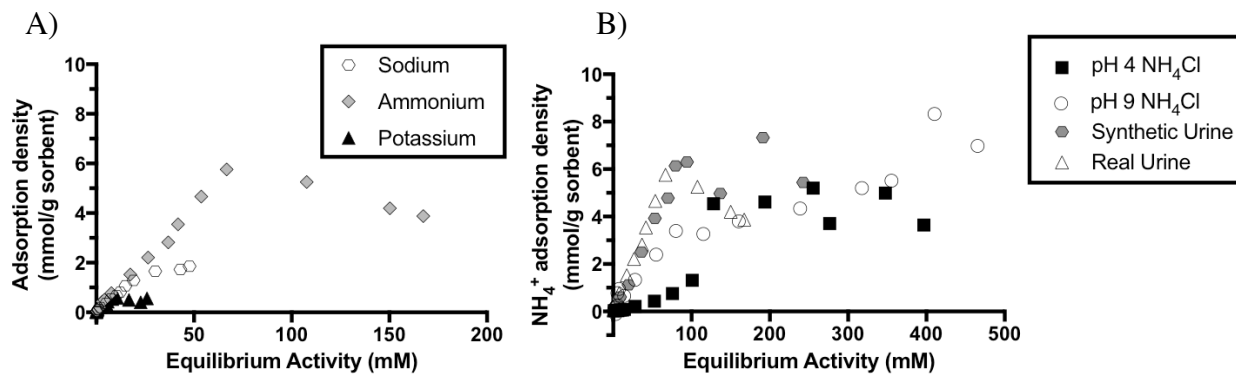


Figure 2.4 (a) Dowex Mac 3  $\text{NH}_4^+$ ,  $\text{Na}^+$ , and  $\text{K}^+$  adsorption in real urine. (b) Dowex Mac 3  $\text{NH}_4^+$  adsorption for all solutions.

To confirm that ion exchange was the primary sorption mechanism in real urine, the characteristic free energy of adsorption in undiluted real urine was determined using the Dubinin-Radushkevich isotherm. The free energy of adsorption for every adsorbent was in the ion exchange range ( $>8$  kJ/mol),<sup>77</sup> indicating that ion exchange was a more significant factor than van der Waals interactions (Figure A7).

### 3.5 Comparison of Solutions

For all adsorbents, there were no statistically significant differences between ammonium adsorption curves in different solutions (Figure 2.3b, Dowex Mac 3; all other resins, Figure A8,  $p>0.05$ ). Given the higher ionic strength in urine compared to  $\text{NH}_4\text{Cl}$ , we expected less adsorption in real and synthetic urine than the pure salt solutions due to charge screening.<sup>85</sup> However,  $\text{NH}_4^+$  adsorption densities in urine solutions were not significantly different than in pure salt solutions when plotted relative to both equilibrium concentration and equilibrium activity, which accounts for ionic strength differences (Figure A9,  $p>0.05$ ). Charge screening can be complicated by several factors: the presence of macropores, because sites deep within macropores are less affected by solution characteristics; net surface charge and the distribution of charged surface moieties; and electrostatic effects of previously adsorbed molecules.<sup>86</sup>

In addition to ionic strength, the presence of organics may also affect ammonium adsorption. Organics have been documented to lead to higher  $\text{NH}_4^+$  uptake by ion exchange materials due to a reduction in surface tension that increases access to macroporous sites.<sup>65</sup> In our experiments, synthetic urine contained only acetic acid whereas real urine is known to contain acetic acid as well as amino acids; organic acids have been shown to decrease the surface tension of water.<sup>87,88</sup> Jorgensen and Weatherley also determined that the enhancement of ammonium adsorption was not as large at higher adsorption densities,<sup>65</sup> which is the same trend observed when comparing synthetic and real urine with pure salt solutions. Thus, organic compounds present in synthetic and real urine but absent in pure salt solutions may enhance adsorption density for macroporous sites. Real and synthetic urine adsorption curves were not significantly different ( $p>0.05$ ),

indicating that synthetic urine was a sufficient proxy and that the more heterogeneous mixture of organics in real urine did not significantly affect ammonium adsorption.

### 3.6 Continuous Flow Adsorption

While batch experiments were useful for characterizing adsorption isotherms, nutrient recovery from urine using ion exchange would most likely be implemented in continuous-flow column configuration. To complement the batch data, breakthrough curves in continuous-flow columns were generated to compare adsorbents (Figure 2.5a). In control columns with no resin,  $\text{NH}_4^+$  and  $\text{Cl}^-$  mass balances were within 5% (Figure A10). Calculated adsorption densities were 1.91 mmol N/g for biochar, 2.00 for clinoptilolite, 2.74 for Dowex 50, and 4.23 for Dowex Mac 3.

These results are similar to batch results (e.g., Fig 2.3b), confirming that Dowex Mac 3 had the highest adsorption capacity. Importantly, the total ammonia concentrations measured during column experiments were less variable than those measured during batch experiments. Possible reasons include the use of lower dilution factors (e.g., note that less variability is observed for the lowest concentrations, similar to the batch experiments) and the potential for more ammonia volatilization to occur during the 24-h batch tests.

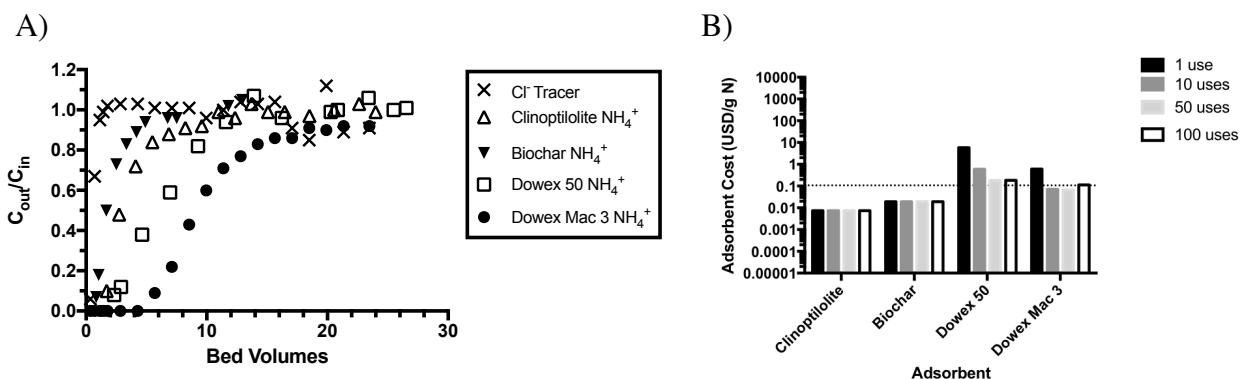


Figure 2.5 (a) Adsorption breakthrough curves in continuous-flow columns. (b) Comparison of adsorbent cost for all four resins (in USD/g N) assuming 100% regeneration ( $r=1$ ). The dotted line is the cost of conventional biological nitrogen removal per gram nitrogen removed (horizontal line).<sup>89</sup>

### 3.7 Regeneration

Column regeneration was performed for one cycle as a proof-of-concept and regeneration efficiencies were calculated for each adsorbent. The synthetic resins both showed almost 100% regeneration (Dowex 50 95%, Dowex Mac 3 99%). Clinoptilolite had a regeneration efficiency of 43%, indicating that not all ammonium was eluted; biochar had a regeneration over 100%, indicating elution of initially loaded ammonium or biochar decomposition. These natural adsorbents may still be promising for direct application as a solid fertilizer.<sup>90,91</sup>

### 3.8 Feasibility Assessment

As an initial assessment of feasibility, adsorbent cost was determined for recovering nitrogen by ion exchange according to Equation 8. Material cost for each adsorbent was determined from literature values and the adsorption densities were those determined from the triplicate batch experiments in undiluted real urine (Table A5). Based on the low recovery of ammonium from clinoptilolite, it would likely only be used once; however, better regeneration may be possible with other regenerants or other conditions. Thus, for comparison with synthetic resins, we show adsorbent costs for a single use up to 100 uses assuming 100% regeneration efficiency (Figure 5).

For a single use, clinoptilolite had the lowest adsorbent cost/g N because of its low material cost, even though its adsorption capacity is lower than the synthetic resins. However, a more expensive adsorbent can result in a lower treatment cost if it is more regenerable. For example, if clinoptilolite is used once, treatment would cost \$7.40/kg N; if Dowex Mac 3 is used 100 times, treatment would cost \$6.00/kg N.

Adsorbent costs (\$/g N) were compared to the cost of conventional nitrogen removal (Figure 5b, dotted line).<sup>89</sup> We are currently investigating other regenerants (e.g., HCl, HNO<sub>3</sub>) over many regeneration cycles to more conclusively evaluate long-term regeneration potential and costs. With 100% regeneration efficiency, material costs are at or below the cost of biological nitrogen removal if Dowex Mac 3 is used as few as ten times; the natural adsorbents used only once still have a lower material cost than conventional nitrogen removal. In addition, we expect nitrogen recovery to have additional benefits compared to removal, including revenue generated from value-added products like fertilizer. The same data in Figure 2.5b can also be calculated per liter of urine using Equation 2.9 (Figure A11).

Reactor volume will also impact process costs and feasibility. To treat the urine produced by a family of four over one week, the reactor volume required for Dowex Mac 3 was the lowest (5.3 L), followed by Dowex 50 (5.8 L), clinoptilolite (8.9 L), and biochar (19 L)(Figure A12). Biochar required a much larger reactor volume because of its markedly lower bulk density (Table A5).

This analysis illustrates that the adsorbent costs and reactor volumes may be feasible and that further analysis of the potential for ion exchange adsorbents is warranted. Multicomponent models like the Jain-Snoeyink can help predict adsorption capacities based on influent urine concentrations, which can vary (Figure A13). Many other factors besides regeneration potential and adsorption density will affect the cost of recovering nitrogen via ion exchange, including other materials for producing cartridges and regeneration facilities, whether the adsorbents are installed at individual toilets or at the building scale, the cost of regenerant, transport distances, and the final fertilizer product quality and market value. Because the other factors are relatively

independent of adsorbent material, however, the simple analysis presented here is useful for comparing adsorbents used in the same configuration, which was the overall objective of this investigation.

### **3.9 Potential Implications for Urine Treatment**

Characterization of four different ion exchange adsorbents has provided a proof-of-concept for nitrogen recovery from source-separated urine via ion exchange. Once their adsorption capacity is reached, natural adsorbents like clinoptilolite and biochar could be applied directly as fertilizer, assuming pathogen concerns can be addressed. Alternatively, ammonium concentrate could be produced by eluting ammonium from any adsorbent. The process modeling conducted in this study can also be used to specify adsorption capacities and regeneration lifetimes required for newly developed adsorbents to be cost effective for nitrogen recovery from urine.

Several process engineering questions are recommended for future research, including optimizing elution of the ammonium to produce a concentrated solution that can feed into fertilizer or other products, and how to combine ion exchange with other nutrient recovery processes, like struvite precipitation. These questions are best investigated using column operation. Additional post-treatment, such as pharmaceutical removal from the eluent or eluate, or converting liquid fertilizer to solid, may be desirable and will affect process costs.

Ion exchange adsorbents could be employed in on-site or centralized wastewater treatment. A decentralized scheme might involve a service provider that regularly collects and replaces household cartridges and transports them to a centralized regeneration facility. Alternatively, cation exchange adsorbents could be used and regenerated on-site at a central facility at which source-separated urine is collected (by manual transport, such as high-density slums, or via dedicated pipes in a large building). Other implementation factors to consider include variability in urine composition, location of treatment facilities, method and cost of transport, and degree of centralization. For example, lifecycle impacts and costs have recently been modeled for phosphate recovery and trace organic removal via ion exchange.<sup>92</sup>

Because source separation has not yet been widely adopted, resource recovery technologies like ion exchange can potentially influence the design and scale of source separation systems. In this study we have demonstrated that ammonium can be recovered from urine using ion exchange and compared the efficacy of natural and synthetic adsorbents. Further work on continuous-flow recovery, optimal scale, and integration with other processes will add to the base of knowledge for potential application of novel technologies for nitrogen recovery from source-separated urine. Another promising direction for future research is the recovery of ammonium from other high-strength wastes, such as digestate and agricultural waste streams.

# **Chapter 3. Effects of operating and design parameters on ion exchange columns for nutrient recovery from urine**

The following chapter is adapted from a co-authored manuscript in preparation with permission from Ileana Wald, Maja Wiprächtiger, and Kara L. Nelson.

## **1. INTRODUCTION**

Effluent from centralized wastewater treatment plants is a significant source of nutrients, which contribute to the accelerated eutrophication of natural water bodies. Separate collection and treatment of urine at the toilet is a potential alternative to biological nutrient removal at wastewater treatment plants. When coupled with nutrient recovery strategies, fertilizer can be produced to supplement energy-intensive synthetic fertilizers.<sup>32</sup> Furthermore, revenue generated from the sale of urine-derived fertilizers could offset the cost of excreta collection and treatment services. Nutrient recovery from human urine has garnered increasing interest because urine contributes approximately 80% of the nitrogen (N), 50% of the phosphorus (P), and 70% of the potassium (K) load in municipal wastewater streams, but comprises only 1% of the liquid volume.<sup>93</sup>

Several studies have focused on recovery of either nitrogen or phosphorus from urine; combining treatment technologies into a full urine treatment train is a logical next step. Phosphorus is often recovered via precipitation of struvite ( $\text{MgNH}_4\text{PO}_4 \cdot 6\text{H}_2\text{O}$ ), a slow-release fertilizer.<sup>31,32,94</sup> Anion exchange for phosphorus removal has also been explored,<sup>33</sup> both phosphorus recovery techniques could be combined with nitrogen recovery via cation exchange. Thus far, potassium recovery from urine has not been extensively explored. Ultimately, selective recovery of nitrogen, phosphorus, and potassium could lead to tailored fertilizer production from urine.

Phosphorus recovery by struvite precipitation in urine has been well-characterized in terms of magnesium dosage, mixing, and precipitation mechanisms.<sup>32,95,96</sup> Similarly, equilibrium and kinetic models for adsorption and regeneration of anion exchange resins for urine treatment have been developed.<sup>33,97</sup> In comparison, design and operating parameters have not been optimized for nitrogen recovery via cation exchange, although the approach is a promising option for extracting nitrogen from concentrated streams.<sup>59,60,98</sup> In freshly excreted urine nitrogen is predominately in the form of urea; during storage, the microbial enzyme urease hydrolyzes urea to ammonia.<sup>99</sup> Cation adsorption can be used to transfer ammonium from urine to a selective ion exchange resin. Once saturated, the resin can be regenerated to produce a concentrated ammonia solution, a potential liquid fertilizer or disinfectant.

In a previous study, we compared synthetic and natural adsorbents and demonstrated the recovery of ammonium from urine. The commercial resin Dowex Mac 3 had the highest adsorption density ( $4.23 \text{ mmol N g resin}^{-1}$ ) and regeneration efficiency ( $>99\%$ ).<sup>98</sup> While useful for comparing adsorbents and characterizing adsorption isotherms, batch studies give limited kinetic information and make it difficult to maintain constant pH,<sup>34</sup> which can impact ammonia speciation and sorption. A more appropriate configuration for implementing ion exchange is a flow-through, fixed-bed reactor. In this study, we used continuous-flow column experiments to investigate the impact of operating conditions (e.g., flow rate, concentration) and other design parameters on adsorption of urine constituents (N, P, K, trace organic compounds) by ion exchange resins and regeneration of the adsorbents.

In addition to nutrients, urine contains trace organic compounds (TrOCs), many of which are contaminants of emerging concern. Many trace organic compounds are present in urine at concentrations 100-10,000 times that of wastewater.<sup>100</sup> While urine separation can effectively avoid input of TrOCs to bulk wastewater, their fate in urine treatment technologies, such as nitrification-distillation,<sup>30</sup> urine storage,<sup>30</sup> and anion exchange, is under investigation.<sup>101</sup> For cation exchange, organic compounds could end up in the urine effluent (which could be discharged to the sewer and go to the wastewater treatment plant), in the fertilizer product, or could accumulate on the adsorbent.

During technology development, systems-level analyses can be used to identify knowledge gaps that merit further study at the laboratory scale. We conducted an economic and environmental assessment of household nitrogen recovery using cation exchange, and found that manufacturing of sulfuric acid (used to regenerate the resin) was the major contributor to energy inputs and greenhouse gas emissions.<sup>48</sup> Thus, in the current study we compared alternative regenerants and several metrics of regeneration efficiency to assess whether these environmental impacts could be reduced.

The overall goal of this investigation was to characterize continuous-flow recovery of nutrients from urine using ion exchange. While phosphate recovery by anion exchange has been modeled and optimized, nitrogen recovery via cation exchange has not been extensively investigated. The specific objectives of this study were to: (i) demonstrate the feasibility of combined nutrient recovery, (ii) evaluate the effects of operating conditions (flow rate and concentration) on nitrogen adsorption and regeneration, (iii) compare recovery efficiencies of different regenerants, and (iv) determine the fate of indicator trace organic compounds during cation exchange. These results can guide design decisions for implementing ion exchange for nutrient recovery.



## 2. MATERIALS AND METHODS

### 2.1 Column setup

Columns were constructed from polyvinyl chloride (PVC) plastic (2.54 cm diameter, 16 cm length unless otherwise noted) and operated in continuous upflow mode for both adsorption (synthetic or real urine influent) and regeneration ( $\text{H}_2\text{SO}_4$ ,  $\text{HCl}$ ,  $\text{HNO}_3$ , or  $\text{NaCl}$  influent) experiments. The columns were packed with ion exchange adsorbent with sponges at the ends to retain media. Adsorbents were either Dowex Mac 3, a macroporous cation exchange resin, or LayneRT, an anion exchange resin modified with ferrous oxide nanoparticles (properties in Table B1). For every experiment, column effluent samples were collected regularly (approximately every 20 minutes) and analyzed for inorganic ions (e.g., ammonium, potassium, and phosphate) via ion chromatography, generating breakthrough curves.

### 2.2 Combined nutrient recovery

Three treatment trains were compared for combined nutrient recovery: (i) struvite precipitation followed by cation exchange, (ii) anion and cation exchange in series (separate columns), and (iii) simultaneous anion and cation exchange in a mixed bed column. Ammonium, phosphate, and potassium breakthrough curves were generated for each treatment scheme and compared in terms of bed volumes to 50% breakthrough, slope, and adsorption density. In all setups, real urine was pumped at  $4.5 \text{ mL min}^{-1}$ . Urine for nutrient recovery was collected from a household urine-diverting toilet in Richmond, California; urine for trace organic analysis was collected from adult volunteers in Berkeley, California and stored for several weeks to ensure urea hydrolysis (CPHS protocol 2016-10-9284).

To recover struvite from hydrolyzed urine,  $\text{MgCl}_2$  was added in a 1.1:1 molar ratio of added magnesium to phosphate in urine.<sup>32</sup> The solution was mixed for 10 minutes and settled for 10 minutes; then the supernatant was pumped into another bottle and subsequently into a cation exchange column. For anion and cation exchange in series, hydrolyzed urine was pumped through first the anion and then the cation exchange column. For the mixed bed, equal masses of LayneRT and Dowex Mac 3 were mixed dry and added to one 32-cm column to maintain the same bed volume as all other experiments with 16-cm columns.

In addition to the mixed bed column, columns with Dowex Mac 3 were pretreated with 1 M borate buffer; LayneRT columns were pretreated with pH 12 NaOH. The mixed bed was pretreated with pH 12 NaOH to avoid borate sorption to the anion exchange resin. Regeneration solutions were based on previous research, which demonstrated regeneration of Dowex Mac 3 and LayneRT resins with 0.122 M  $\text{H}_2\text{SO}_4$ <sup>98</sup> and 2% NaOH/2% NaCl (0.5 M NaOH/0.342 M NaCl),<sup>34</sup> respectively. Nitrogen and phosphorus recovery efficiencies were compared for these regenerants pumped at  $2 \text{ mL min}^{-1}$  through exhausted mixed bed columns for a total of 300 minutes in three setups: NaOH/NaCl only, 150 minutes of  $\text{H}_2\text{SO}_4$  followed by 150 minutes of NaOH/NaCl, and 150 minutes of NaOH/NaCl followed by 150 minutes of  $\text{H}_2\text{SO}_4$ .

Effects of operating and design parameters on phosphorus adsorption and elution have been well-characterized in previous studies. For example, phosphate adsorption with hybrid anion exchange resins such as LayneRT has been accurately modeled using a Freundlich isotherm and pseudo-second-order kinetic model;<sup>97</sup> batch adsorption densities have also been determined for influent streams with varying phosphate concentrations.<sup>33</sup> Regeneration of LayneRT has been optimized to 3.5 bed volumes with 2% NaOH/2% NaCl solution.<sup>35</sup> In comparison to phosphate, effects of operating and design parameters on cation exchange columns for urine treatment are not well understood and were investigated through additional experiments in this study.

### **2.3 Operating Conditions and Adsorption**

Effects of flow rate, influent concentration, and intermittent operation on nitrogen and potassium recovery were investigated through continuous adsorption experiments with synthetic urine and Dowex Mac 3. Synthetic urine was used because of its constant composition (Tables B2-B3), whereas real urine composition varies among individuals, times, and regions.<sup>102</sup> Based on potential variations in total ammonia concentration in real urine, three dilutions of synthetic urine were used: 8000 (undiluted), 5700, and 3600 mg N L<sup>-1</sup>. 3600 mg N L<sup>-1</sup> was indicative of total ammonia levels after dilution in NoMix source-separating flush toilets<sup>28</sup> and 5700 mg N L<sup>-1</sup> was chosen as an intermediate concentration. 4.5 mL min<sup>-1</sup> was the estimated average urine production rate for a five-person household; this flow rate was halved (2.2 mL min<sup>-1</sup>) to better represent U.S. conditions (2.5 people household<sup>-1</sup>),<sup>103</sup> and doubled (10 mL min<sup>-1</sup>) to simulate conditions in which the urine could be collected and then pumped faster than the average generation rate. Each flow rate and concentration condition was conducted in triplicate; flow rate variations were all conducted with undiluted synthetic urine and concentration experiments were performed at constant flow rate (4.5 mL min<sup>-1</sup>).

Intermittent flow was explored because it is more realistic than continuous operation, as toilet use is intermittent. Intermittently run column experiments can also be used to confirm the rate-limiting step of adsorption (e.g., external diffusion, intraparticle diffusion, surface reaction).<sup>104</sup> Triplicate experiments were performed with synthetic urine in which pumping (4.5 mL min<sup>-1</sup>) was stopped for 24 hours after 1, 2, 3, and 5 hours of cumulative operation.

For all column adsorption experiments, adsorption densities were calculated using numerical integration of breakthrough curves (Section B1.1, Equations B1-B2).

### **2.4 Operating Conditions and Regeneration**

Sulfuric acid has been validated as an effective regenerant (99% recovery efficiency) for ammonium in cation exchange columns.<sup>98</sup> Effects of flow rate and regenerant concentration on regeneration of Dowex Mac 3 were investigated through column experiments with exhausted resin from synthetic urine adsorption. Flow rate and sulfuric acid concentration were varied

independently and by the same factors (22.5, 10, and 2.25 lower) from the previously established 0.122 M H<sub>2</sub>SO<sub>4</sub> at 22.5 mL min<sup>-1</sup> to determine their effects on regeneration of Dowex Mac 3. Several equinormal regenerants (0.244 N H<sub>2</sub>SO<sub>4</sub>, HNO<sub>3</sub>, HCl, and NaCl) were compared. Nanopure water and tap water were also used as regenerants to determine the extent to which adsorbed ammonium would desorb during resin exposure to water.

Experimental conditions were compared in terms of bed volumes to 90% elution, stoichiometric efficiency, and recovery efficiency. Stoichiometric efficiency ( $\eta_{\text{stoich}}$ ) was defined as the proportion of supplied protons (based on commonly available stock concentrations, Table B4) that displaced an ammonium ion on Dowex Mac 3 (Equation 3.1).

$$\eta_{\text{stoich}} = \frac{q * W}{Q * t_{\text{elution}} * N * C_{\text{regen}}} \times 100\% \quad (\text{Equation 3.1})$$

In Equation 1,  $q$  is adsorption density (mmol N g resin<sup>-1</sup>= meq g resin<sup>-1</sup>),  $W$  is resin mass (g resin),  $Q$  is flow rate (mL min<sup>-1</sup>),  $t_{\text{elution}}$  is time to 90% elution (min, to 90% of total amount eluted),  $N$  is normality of regenerant (meq mmol regenerant<sup>-1</sup>), and  $C_{\text{regen}}$  is concentration of regenerant (mol regenerant L regenerant solution<sup>-1</sup>). Recovery efficiency was calculated by numerical integration (Equation B1, B3). The number of bed volumes to 90% elution was calculated based on cumulative and total areas under elution curves (Equation B4). An optimal regenerant would have few bed volumes to elution, high stoichiometric efficiency (~100%), and high regeneration efficiency (~100%). Higher concentrations and lower flow rates were also tested and were expected to decrease the number of bed volumes required for elution.

## 2.5 Trace organic contaminants

A suite of 10 trace organic compounds, including antibiotics, antivirals, and beta blockers, was added to real urine before adsorption (Table B5). Trace organic compounds were quantified with an Agilent 1200 series HPLC (high-performance liquid chromatography) system followed by an Agilent 6460 mass spectrometer (triple quadrupole tandem MS), according to previously published methods for wastewater.<sup>105</sup> Mass balances were conducted to compare adsorption and regeneration with 0.122 M sulfuric acid (22.5 mL min<sup>-1</sup>) to determine the fate of urine-relevant TrOCs during ion exchange. The lowest detectable regeneration efficiency was 2.8%.

## 2.6 Chemical Analysis

Ion concentrations (NH<sub>4</sub><sup>+</sup>, Na<sup>+</sup>, K<sup>+</sup>, Li<sup>+</sup>, Mg<sup>2+</sup>, Ca<sup>2+</sup> and SO<sub>4</sub><sup>2-</sup>, PO<sub>4</sub><sup>3-</sup>, Cl<sup>-</sup>, NO<sub>2</sub><sup>-</sup>, NO<sub>3</sub><sup>-</sup>, F<sup>-</sup>, C<sub>2</sub>H<sub>3</sub>O<sub>2</sub><sup>-</sup>, Br<sup>-</sup>) were measured via ion chromatography using a Dionex chromatograph (IonPac CS12 column for cations, IonPac AS23 column for anions), as reported previously.<sup>98</sup> Samples were acidified to measure total ammonia nitrogen (TAN) as NH<sub>4</sub><sup>+</sup>. pH was measured with a pH probe and meter (MP220, Mettler Toledo, Columbus, OH).

## 2.7 Modeling Breakthrough Curves

For every breakthrough curve generated, adsorption density was calculated by numerically integrating breakthrough curves and dividing by adsorbent mass (Equation B2). Breakthrough curves were compared using a two-parameter model that includes bed volumes to 50% breakthrough and slope of the breakthrough curve (Equation 2).<sup>106</sup>

$$\ln\left(\frac{\frac{C_t}{C_0}}{1-\frac{C_t}{C_0}}\right) = k'(b - \beta) \quad (2)$$

In this model,  $C_t$  is concentration at time  $t$ ,  $C_0$  is initial concentration, and  $b$  is the number of bed volumes at time  $t$ . The two model parameters are  $k'$ , the slope of the breakthrough curve, and  $\beta$ , the number of bed volumes to 50% breakthrough ( $C_t/C_0=0.5$ ). The original model was adapted from breakthrough curves that related absolute concentration and time to breakthrough curves in this study that related relative concentration and bed volumes.

## 2.8 Statistical Analysis

One-way ANOVA and paired t-tests were used to compare calculated adsorption densities and parameters in the two-parameter model for adsorption breakthrough curves for varying flow rate, influent concentration, and intermittency conditions. A two-tailed significance level of 1% ( $p<0.01$ ) was used. Parameters (slope  $k'$  and bed volumes to 50% breakthrough  $\beta$ ) for ammonium breakthrough curves for different combined nitrogen and phosphorus recovery schemes were also compared using one-way ANOVA and paired t-tests.

# 3. RESULTS AND DISCUSSION

## 3.1 Combined nitrogen and phosphorus recovery

### 3.1.1 Phosphorus Recovery

Phosphate was completely removed from hydrolyzed urine during struvite precipitation (Figure B1a). Based on the stoichiometry of nitrogen and phosphorus in struvite ( $MgNH_4PO_4 \cdot 6H_2O$ ), concentrations of both species were expected to decrease by the same amount (25.9 mM P removed from urine). However, ammonium concentrations only decreased by 84% of the phosphate decrease (Figure B1b), indicating precipitation of phosphate minerals with cations other than ammonium (e.g., hydroxyapatite,  $Ca_5(PO_4)_3OH$ ).

Phosphate breakthrough curves for all three treatment trains are shown in Figure 3.1a. For struvite, phosphate was not detected after precipitation due to complete recovery with  $MgCl_2$ . Although slopes of the mixed bed and in series breakthrough curves were not significantly different statistically, the steeper slope of the in series curve signaled faster adsorption kinetics (Table B6). Bed volumes to 50% breakthrough were significantly different (7.7 for mixed bed, 10.6 for in series), indicating a reduction in number of available phosphate adsorption sites or slower rate of filling them due to the presence of Dowex Mac 3. Phosphate adsorption densities for mixed bed and in series columns were 0.53 and 0.50 mmol g resin<sup>-1</sup>, respectively, and were

not significantly different (Table B6); both were higher than predicted based on expected adsorption densities from a Freundlich isotherm in hydrolyzed urine ( $0.255 \text{ mmol P g resin}^{-1}$ , Equations B5-B6).<sup>97</sup>

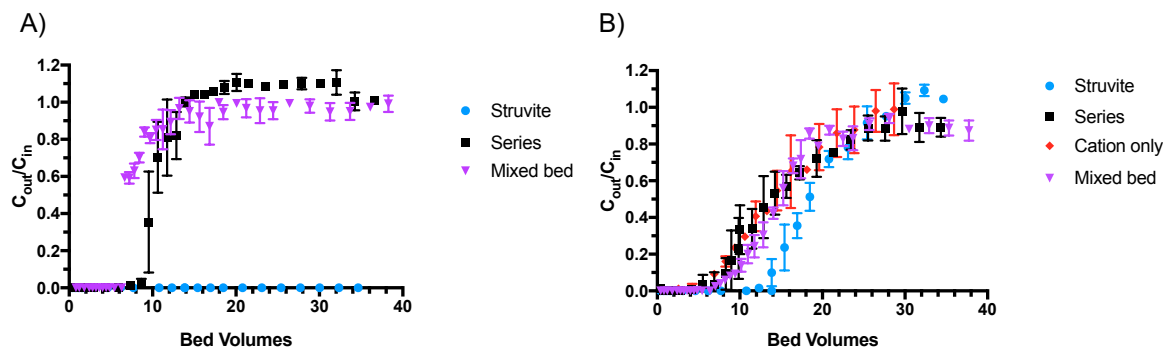


Figure 3.1 Breakthrough curves for varying treatment trains for (a) phosphorus as phosphate and (b) nitrogen as ammonium.

### 3.1.2 Nitrogen Recovery

Nitrogen breakthrough curves for struvite supernatant, mixed bed, separate columns, and cation exchange alone are presented in Figure 3.1b. Although struvite supernatant was characterized by more bed volumes to breakthrough and the lowest slope, the lack of statistically significant differences for number of bed volumes to 50% breakthrough and slope for all setups indicated similar ammonium adsorption rates (Table B7). Thus, the presence of LayneRT before cation exchange (in series) and in the same column as Dowex Mac 3 (mixed bed) did not significantly affect kinetics of ammonium adsorption. Ammonium breakthrough was observed latest (largest  $\beta$ ) for struvite supernatant due to the removal of approximately 9% of ammonium during struvite precipitation and lower influent urine ammonium concentrations. Similarly, adsorption density for struvite supernatant was lower than all other setups, although only significantly lower than the mixed bed column (Table B7).

### 3.1.3 Potassium Recovery

The molar adsorption density for potassium in synthetic urine ( $0.3\text{-}0.4 \text{ mmol K g resin}^{-1}$ ) was more than ten times lower than the nitrogen adsorption density ( $4.23 \text{ mmol K g resin}^{-1}$ ). Both the tenfold lower concentration of potassium in urine and the selectivity of Dowex Mac 3 for  $\text{NH}_4^+$  contributed to low potassium adsorption. Potassium also began to break through the column ( $C_{\text{out}}/C_{\text{in}} > 0$ ) at fewer bed volumes than nitrogen (Figure B2). Thus, to achieve higher potassium recovery, it should be removed in a separate column after N removal or with an adsorbent other than Dowex Mac 3. Potassium has not been a priority for nutrient recovery because it is less abundant in urine than nitrogen and has a lower specific value than phosphorus ( $1.5 \text{ USD kg P}^{-1}$ ,  $0.7\text{-}1 \text{ USD kg K}^{-1}$ ),<sup>47</sup> thus potassium recovery was not optimized in this study. Future work could optimize potassium recovery by potassium struvite precipitation or cation exchange after nitrogen recovery to enhance the value of combined nutrient fertilizers derived from urine.

### 3.1.4 Considerations for implementation

Molar nitrogen adsorption densities were up to an order of magnitude higher than phosphorus adsorption densities due to the lower adsorption capacity of LayneRT (phosphate) compared to Dowex Mac 3 (ammonium). Accounting for differences in adsorption density and concentration in urine, the treatment of 1 L of urine would require 106 g LayneRT and 50 g Dowex Mac 3. Thus, mixed bed columns should have roughly twice as much LayneRT as Dowex Mac 3, and for separate columns the cation exchange column could contain half the resin mass as the anion exchange column.

While separate regenerants can be used for each resin type for columns in series, regeneration of a mixed bed column exposes both anion and cation exchange resins to any regenerant used. For mixed bed regeneration, ammonium recovery efficiencies were higher than phosphate recovery efficiencies for all regenerants tested (50-60% for N and 20-30% for P, Figure B3). Desorption of ammonium happened faster than phosphate desorption due to the more tightly bound Lewis acid-base interactions between phosphate and the anion exchange resin.<sup>34</sup> Further decreasing flow rate (below 2 mL min<sup>-1</sup>, thus increasing hydraulic residence time) could enhance phosphate recovery efficiency. 2% NaOH/2% NaCl exhibited the highest regeneration efficiencies for both phosphorus and nitrogen (Figure B3). Compared to NaOH/NaCl, eluting with sulfuric acid first halved the phosphorus regeneration efficiency, and eluting with sodium chloride/hydroxide first reduced ammonium regeneration efficiency by 10%. Thus, exposing LayneRT to a pH far below its operating range (5.5-8.5) negatively affected phosphate desorption more than sodium affected ammonium desorption.

Future work could optimize serial regeneration for mixed bed columns to determine if nitrogen and phosphorus could be selectively recovered to facilitate tailored fertilizer production; for columns in series, nutrients are easily recovered separately. Phosphorus recovery could occur through struvite precipitation or anion exchange; anion exchange columns could be used before or after urea hydrolysis. Recovering phosphate via anion exchange in fresh urine reduces precipitation potential of phosphate minerals such as struvite and hydroxyapatite because of low total ammonia concentrations and the lower pH of fresh urine (6 vs. 9 in stored urine).<sup>33</sup> Urea hydrolysis could be accelerated by adding urease enzyme or optimizing conditions for microbial hydrolysis (e.g., fixed biofilm column, increasing temperature). For example, phosphorus recovery from fresh urine, urea hydrolysis in a fixed biofilm column, and ammonium adsorption in a cation exchange column could be an effective treatment scheme.

### 3.2 Effects of operating conditions on adsorption

The number of bed volumes to breakthrough varied inversely with total ammonia concentration in influent synthetic urine and was significantly different for each concentration (Figure 3.2a). This trend was expected given a fixed number of sites available per gram of resin, which would become occupied in fewer bed volumes when more ammonium ions were present (higher

concentration). The slope of the breakthrough curves was not significantly different for varying concentration conditions. Adsorption densities were not significantly different, which was expected based on the adsorption isotherm (Figure B4).

Variations in flow rate within the range tested did not have a significant impact on bed volumes to breakthrough nor slope of the breakthrough curve (Figure 3.2b). Adsorption densities for varying flow rates were not significantly different, but varied inversely with flow rate (Figure 3.2c). Because breakthrough curve slope was not affected by increasing flow rate from 2.2 to 10 mL min<sup>-1</sup> (and thus the rate at which ammonium is supplied) transport through the liquid film could be excluded as the rate-limiting step of the adsorption process within this range.

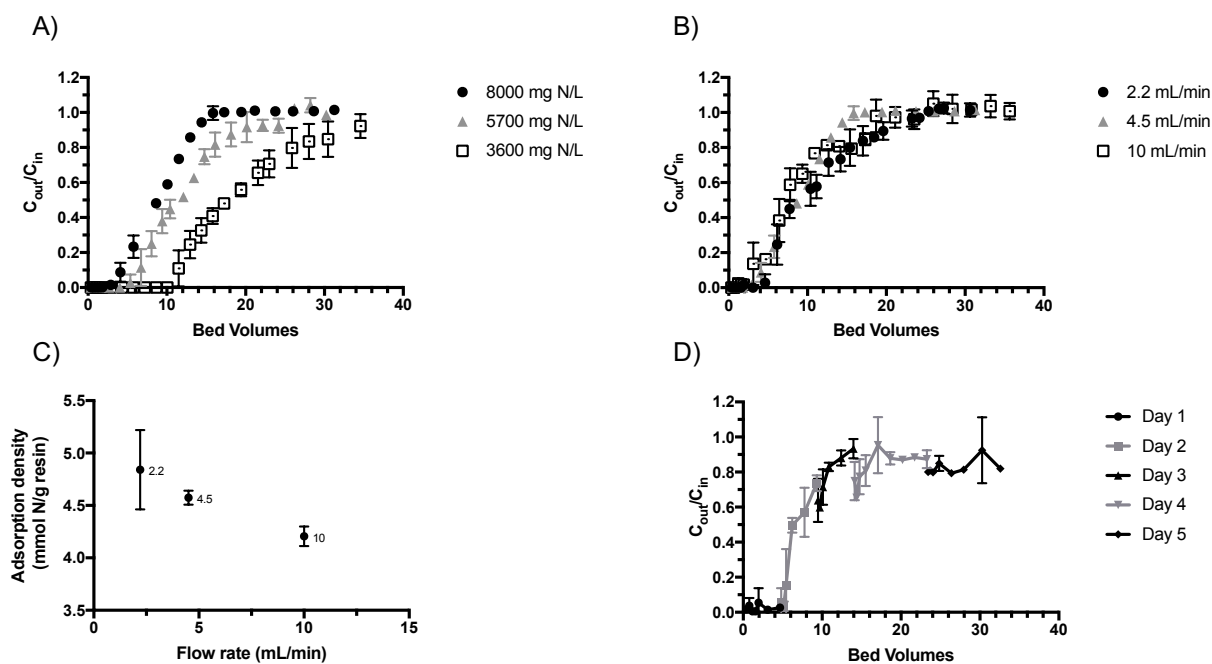


Figure 3.2 Ammonium breakthrough curves with synthetic urine influent for (a) varying influent TAN concentration and (b) varying flow rate. Panel (c) shows adsorption densities for varying flow rate with undiluted synthetic urine (8000 mg N/L), and point labels are flow rates. Panel (d) shows ammonium breakthrough for intermittent operation. Error bars represent  $\pm$  one standard deviation for experimental triplicates. Error bars not shown are smaller than symbol.

Intermittent flow of urine led to similar adsorption density as continuous flow (no significant difference). After each 24-hr rest period, effluent ammonium concentrations decreased (Figure 3.2d). This decrease could have been due to microbial oxidation or sorption. Based on low NO<sub>2</sub><sup>-</sup> and NO<sub>3</sub><sup>-</sup> concentrations in the column effluent (below detection limit of 1 mg L<sup>-1</sup>), additional ammonium adsorption was identified as the predominant mechanism. Gaseous products (e.g., N<sub>2</sub>, NO, N<sub>2</sub>O) could have been formed from microbial oxidation, but no bubbles were observed despite N<sub>2</sub>, NO, and N<sub>2</sub>O being water-insoluble gases ( $K_H \leq 2.5 \times 10^{-2} \text{ M atm}^{-1}$ ,<sup>107</sup> Table B8). Ammonium adsorption during quiescence demonstrated that intraparticle diffusion was the rate-

limiting step of ammonia removal via ion exchange.<sup>104</sup> Total ammonia concentrations no longer decreased once the resin was exhausted (i.e., between day 4 and day 5).

For potassium adsorption, the only significant differences were between the number of bed volumes to 50% breakthrough for the most diluted influent concentration and the other concentrations tested (Figure B2). Adsorption densities were not significantly different and no clear trend was observed (Figure B5). Potassium emerged from the column in fewer bed volumes than ammonium for all conditions tested.

### 3.3 Effects of operating conditions on regeneration

An optimal regenerant would have few bed volumes to elution, high stoichiometric efficiency (~100%), and high regeneration efficiency (~100%). The first two parameters minimize the volume of regenerant required for elution, as well as associated life-cycle costs, embedded energy, and greenhouse gas emissions.<sup>48</sup> The estimated number of bed volumes required for up-concentration from urine was 8 (Equation B9). Elution curves for varying flow rate and sulfuric acid concentration are shown in Figure B6; summary parameters are described below. Stoichiometric efficiency varied inversely with flow rate and sulfuric acid concentration (Figure 3.3). Nitrogen recovery efficiency was consistently above 90%, with the exception of the 5.42 mM sulfuric acid, the lowest concentration tested (Figure B7). Although increasing flow rate did not have a significant effect on bed volumes to 90% elution, increasing concentration drastically reduced bed volumes to elution (Figure 3.3a). Regenerant concentration had a larger effect (higher absolute value of slope) than flow rate on stoichiometric efficiency and bed volumes required for elution for both nitrogen (Figure 3.3) and potassium (Figure B8). Based on these results, proton concentration was the predominant operating parameter influencing the volume of acid required for elution. The lack of effect from flow rate on bed volumes to elution indicated that proton loading rates for the flow rates tested were sufficiently high to desorb ammonium. For potassium, most recovery efficiencies were above 90% (Figure B9).

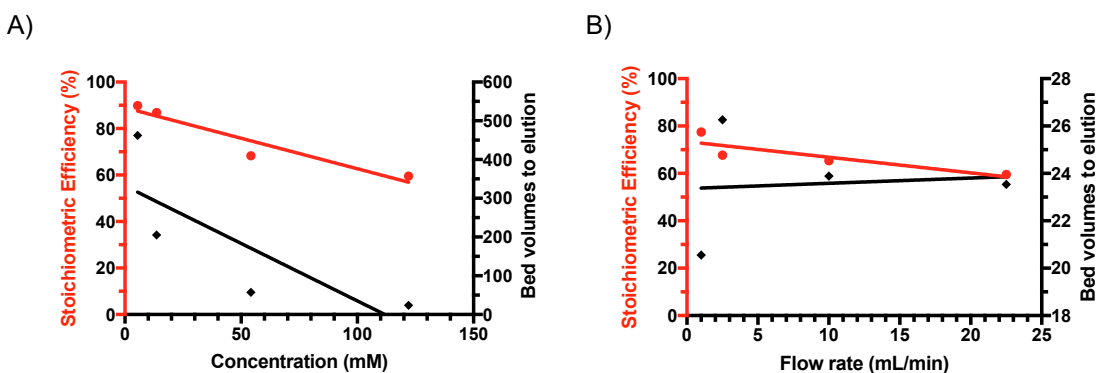


Figure 3.3 Sulfuric acid use efficiency compared to stoichiometric exchange for ammonium elution and column regeneration with (a) varying concentration (flow rate constant at 22.5 mL min<sup>-1</sup>) and (b) varying flow rate (concentration constant at 122 mM H<sub>2</sub>SO<sub>4</sub>). Linear regression lines show slope of each correlation. Resin was exhausted during adsorption with synthetic urine.



None of the conditions shown in Figure 3 produced an eluent solution that resulted in up-concentrating ammonium. Thus, higher sulfuric acid concentrations were tested (2, 3, and 6 M). Bed volumes to elution were minimized to 2.78 bed volumes at the highest sulfuric acid concentration; however, stoichiometric efficiency was only 19% (Figure B10, Table B9). Ammonium sulfate was produced at concentrations as high as 22 g N L<sup>-1</sup> (3 M H<sub>2</sub>SO<sub>4</sub> at 2 mL min<sup>-1</sup>), which is 25% of common (NH<sub>4</sub>)<sub>2</sub>SO<sub>4</sub> liquid fertilizers available on the market (Equations B7-B8).<sup>108,109</sup> While high product ammonium concentrations are desirable, more acid was required for up-concentration during elution, demonstrating that it was not possible to maximize both product concentration and stoichiometric efficiency. To mitigate this tradeoff, ammonium sulfate could be recycled through multiple regenerations to produce higher concentration product while reusing acid.

### 3.4 Comparing regenerants

Bed volumes to 90% elution, stoichiometric efficiency, and regeneration efficiency for equinormal HNO<sub>3</sub>, HCl, NaCl, and H<sub>2</sub>SO<sub>4</sub> are compared in Table 3.1 (elution curves in Figure B11). Of the regenerants tested, sulfuric acid exhibited the lowest number of bed volumes to elution and stoichiometric efficiency, indicating the most efficient use of regenerant. The only significant differences between performance metrics for different regenerants were the regeneration efficiency of NaCl (77%) with all other regenerants (all approximately 100%). NaCl had a lower regeneration efficiency because of the lower affinity of Dowex Mac 3 for sodium ions compared to protons and ammonium.<sup>98</sup> This low performance of NaCl regeneration may potentially be mitigated by using more concentrated NaCl regenerants. With NaCl, the Na<sup>+</sup> sorbed during column regeneration would desorb during subsequent urine treatment, increasing the salinity of the urine effluent. If this stream is disposed to the sewer, it could be a disadvantage for treatment plants that discharge to inland freshwater or if the water is reused; for ocean discharge, the additional salinity is likely not an issue.

Table 3.1 Recovery efficiencies, and stoichiometric efficiencies, and bed volumes to 90% elution for triplicate elution experiments with various regenerants. Resin was exhausted during adsorption with synthetic urine.

	Bed volumes to 90% elution	Stoichiometric Efficiency (%)	Recovery Efficiency (%)
HNO <sub>3</sub>	21.9 ± 1.76	95.3 ± 2.4	104 ± 1.8
HCl	23.2 ± 0.87	101 ± 3.4	102 ± 4.2
NaCl	28.9 ± 2.81	85.9 ± 10.7	77.4 ± 5.5
H <sub>2</sub> SO <sub>4</sub>	20.0 ± 2.19	107 ± 16.8	99.3 ± 0.3*

\*experimental duplicate

For potassium regeneration with Dowex Mac 3, no significant differences in elution metrics were observed. At most 8% of protons contributed to potassium desorption for all regenerants, which

was expected given the tenfold lower adsorption density of potassium compared to ammonium. Similar to nitrogen results, all three acid regenerants exhibited recovery efficiencies of at least 100% while NaCl was only 87%; sulfuric acid had the lowest number of bed volumes to 90% elution (Table B10).

To evaluate the potential for desorption if the column is exposed to water, nanopure water and tap water were used as regenerants on ammonium-loaded Dowex Mac 3 resin. Based on elution curves (Figure B12), only 6.9% (nanopure) and 8.9% (tap) of sorbed ammonium was desorbed during 2.7 L of water flow. The low proton concentration in these waters can explain the unfavorable desorption of ammonium. Low levels of elution with water indicate that desorption of ammonium due to exposure to very dilute urine streams, flush water, or water used for cleaning is not a major impediment.

### 3.5 Fate of indicator trace organics

Trace organics could adsorb to Dowex Mac 3 via electrostatic and van der Waals interactions. As expected, only trace organic contaminants that were positively charged at stored urine pH (~9.1) were adsorbed (Figure 3.4a), indicating electrostatic interactions as the primary mechanism. Neutral and negatively charged compounds of similar size to adsorbed compounds were not adsorbed to Dowex Mac 3, including sulfamethoxazole, acetaminophen, acyclovir, and emtricitabine. Compounds with published  $pK_a$  values below the pH of stored urine were assumed to be positively charged (Table B5), with a couple exceptions. Although abacavir has a published  $pK_a$  of 5.01, it is regarded as a monoacidic base because of delocalized positive charge in the heterocycle.<sup>110</sup> Similarly, trimethoprim has a  $pK_a$  of 7.4, which would indicate neutral charge at pH 9 in stored urine. However, trimethoprim has been particularly well-removed by synthetic macro porous resins and zeolites;<sup>111</sup> it has also been suggested to be positively charged when bound to enzymes like dihydrofolate reductases.<sup>112</sup> These enzymes are required for production of purines and some amino acids, and are thus ubiquitous in bacterial cells present in stored urine ( $\sim 5 \times 10^8$  cells  $mL^{-1}$ ).<sup>31</sup>

TrOC adsorption onto anion exchange resins has been measured and modeled for several non-steroidal anti-inflammatory drugs (e.g., diclofenac, naproxen).<sup>101</sup> Acetaminophen (also called paracetamol) was the only compound also monitored in this study, and did not appreciably adsorb to anion nor cation exchange resins due to only 40% being negatively ionized (60% neutral) at pH 9. For anion exchange resins, electrostatic interactions were responsible for TrOC adsorption densities while selectivity was a function of hydrophobicity.<sup>101</sup> Based on only positively charged organic compounds adsorbing to Dowex Mac 3, adsorption density and thus removal efficiency during adsorption were functions of electrostatic interactions. Given the similar polymeric backbones of anion and cation exchange resins, selectivity is also expected to be a function of hydrophobicity and van der Waals interactions for cation exchange resins. In

future work similar suites of prevalent trace organic compounds could be applied to both resin types.

Elution suited for nitrogen recovery was used with TrOC-loaded resin to determine TrOC concentrations in produced ammonium sulfate and elution efficiencies for trace organics. Only beta blockers (atenolol and metoprolol) were eluted (Figure 3.4b), and at less than 10% efficiencies. This finding indicates that the majority of atenolol and metoprolol, as well as compounds that were adsorbed but not eluted (carbamazepine, zidovudine, abacavir, and trimethoprim) will continue to accumulate on Dowex Mac 3 over multiple adsorption-regeneration cycles. Atenolol ( $0.046 \pm 0.013$  ng/L) and metoprolol ( $0.077 \pm 0.028$  ng/L) were also the only compounds at detectable levels in the ammonium sulfate product.

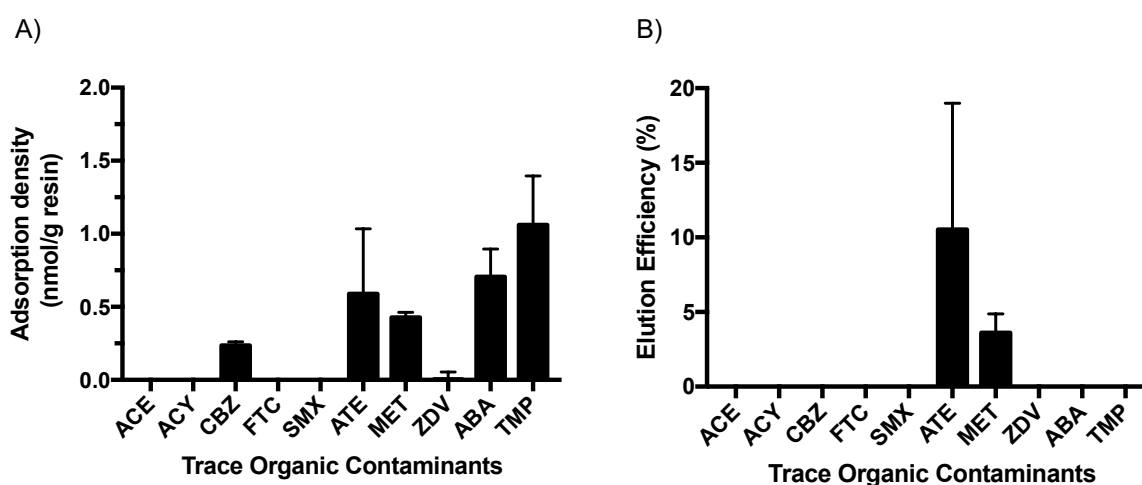


Figure 3.4 (a) Adsorption density and (b) elution efficiency of trace organic contaminants with cation exchange resin Dowex Mac 3. Compound abbreviations are in Table B5.

Many pharmaceuticals present in urine are contaminants of emerging concern that should be treated before discharge. Based on many TrOCs passing through cation exchange columns, pre-or post-treatment for TrOC removal in urine will be required. For the compounds that accumulate on Dowex Mac 3, regeneration may be required and has been demonstrated with 5% (m/m) NaCl with equal volumes of water and methanol.<sup>101</sup> Atenolol and metoprolol in the ammonium sulfate product should also be monitored for environmental impacts. When biosolids containing atenolol were applied to corn, carrot, and potato crops, atenolol was detected in the 0.5-1 ng/L range in the plants, which was not considered significant uptake.<sup>113</sup> Metoprolol may behave similarly, but has not been measured during field trials. While these data indicate that urine-derived ammonium sulfate concentrate does not contain biologically significant pharmaceutical levels, future work can more robustly answer this question for compounds outside of the ten tested in this study.

#### 4. CONCLUSIONS

In this study the effects of operating parameters of adsorption and regeneration on system performance were investigated for nutrient recovery via ion exchange. Based on previous life-

cycle analysis that indicated sulfuric acid manufacturing contributes significantly to energy use and greenhouse gas emissions, efficacies of alternative regenerants were compared. Removal of trace organics during cation exchange was determined, and treatment schemes for nitrogen and phosphorus recovery were compared. Overall, these findings contribute to an improved understanding of continuous-flow nitrogen recovery via ion exchange. The major implications of this work for implementation were:

- Ammonium recovery from urine can be performed intermittently and regenerated periodically to produce ammonium sulfate concentrate.
- Acidic regenerants performed better than sodium chloride and avoid brine generation.
- Trace organics that are positively charged at pH 9 were co-adsorbed with ammonium. Most adsorbed compounds were not eluted into the ammonium sulfate product, but may accumulate on resin over several adsorption-regeneration cycles.
- Phosphorus and nitrogen can be recovered from urine using anion and cation exchange without a loss of performance for nitrogen recovery.

Future work could more comprehensively analyze trace organic compound fate through non-target analysis and evaluate recovery at larger scale; in addition, optimizing nitrogen recovery in terms of product concentration and efficient regenerant use could advance the technology toward implementation. Based on a vision for selective nutrient recovery and production of fertilizers of any desired NPK (nitrogen: phosphorus: potassium) ratio, additional adsorbents for phosphate and potassium recovery could be further explored with additional adsorbents and integrated into a complete nutrient recovery treatment train from source-separated urine.

# **Chapter 4. Electrochemical stripping to recover nitrogen from source-separated urine**

The following chapter is adapted from the manuscript Tarpeh et al. (2017) Electrochemical stripping to recover nitrogen from source-separated urine. *Environmental Science & Technology* (in preparation) with permission from James M. Barazesh, Tzahi Y. Cath, and Kara L. Nelson.

## **1. INTRODUCTION**

Nitrogen in municipal wastewater effluent can lead to eutrophication, which affects over 70% of U.S. lakes and costs an estimated \$2.2 billion due to losses in recreation, livelihood, and remediation.<sup>9</sup> Recently, nitrogen removal has become a priority in regions where nitrogen limits algal growth in surface water, such as the Chesapeake Bay and the San Francisco Bay.<sup>53,114</sup> Urine is an ideal component to target in wastewater for nitrogen recovery because it is only 1% of wastewater volume but contributes 80% of wastewater nitrogen.<sup>14</sup> Current approaches to removing nitrogen from wastewater and producing nitrogen fertilizers can be cost and energy-intensive; they are also unlikely to be implemented in settings that are remote or lack formal sewer infrastructure. Recent advances have focused on recovering nutrients from urine as value-added products rather than removing it from wastewater as nitrogen gas via nitrification-denitrification processes. Several techniques (e.g., nitrification-distillation,<sup>37</sup> struvite precipitation,<sup>32</sup> cation exchange<sup>98</sup>) can be utilized for recovering nitrogen from concentrated waste streams such as urine or anaerobic digester centrate. Extracting nitrogen fertilizers (e.g., ammonium sulfate) from urine could reduce required energy and costs for wastewater treatment and produce a revenue stream.<sup>11-13</sup>

Ammonia stripping is an established, effective process that requires base addition to convert nitrogen as ammonium ( $\text{NH}_4^+$ ) into volatile ammonia ( $\text{NH}_3$ ); the basic solution is then passed through a stripping tower to facilitate liquid-gas exchange of ammonia. In addition to municipal wastewater, ammonia stripping has been applied to nitrogen-rich waste streams such as urine,<sup>39</sup> digestate,<sup>115</sup> landfill leachate,<sup>116</sup> and swine manure.<sup>117</sup> Ammonia can be recovered via stripping with an acid trap that converts volatile  $\text{NH}_3$  into stable  $\text{NH}_4^+$ .

Electrochemical stripping aims to improve upon conventional ammonia stripping in two ways: (1) pH increase without base addition and (2) internal ammonia stripping without a stripping tower. Electric current is used to generate hydroxide ions at the cathode, and a hydrophobic (e.g., polypropylene), gas-permeable membrane is used to strip ammonia from solution. By using electricity to drive base production, electrochemical stripping can be applied to decentralized and remote treatment systems if intermittent electricity or photovoltaic cells are available. In

electrochemical stripping, ammonia is recovered as a valuable product (e.g., ammonium sulfate, a common fertilizer) rather than simply removed from the influent. We investigated ammonia recovery in a three-chamber design comprised of anodic  $\text{NH}_4^+$  migration, cathodic conversion to  $\text{NH}_3$ , and reconversion to  $\text{NH}_4^+$  in a sulfuric acid trap to selectively recover nitrogen based on charge ( $\text{NH}_4^+$ ) and volatility ( $\text{NH}_3$ ).

Several other electrochemical approaches have been used to treat source-separated urine, including microbial electrochemical technologies, in which anodic bacteria oxidize organic matter and are net producers of energy.<sup>118,119</sup> In electrolysis cells (without bacteria), ammonia can be removed from urine by electrochemical oxidation to gaseous nitrogen species (77%), nitrate (21%), and nitrite (2%).<sup>120</sup> Electrodialysis has also been used to remove ions (including  $\text{NH}_4^+$ ) by migration from urine<sup>40,121</sup> and anaerobic digester effluent.<sup>122</sup> Recent theoretical studies suggested that the rate-limiting step for nitrogen migration during electrodialysis was the cathodic conversion of  $\text{NH}_4^+$  to  $\text{NH}_3$ .<sup>123</sup> Electrochemical stripping overcomes this barrier with an acid trap in which  $\text{NH}_3$  is converted to  $\text{NH}_4^+$ , effectively conserving the driving force for  $\text{NH}_3$  migration. While other studies have used external air stripping<sup>121</sup> or membrane stripping units,<sup>124,125</sup> this is the first study to describe electrodialysis and membrane stripping in one apparatus.

The goal of this study was to characterize electrochemical stripping of ammonia from urine in terms of nitrogen recovery mechanisms and efficiency, product and effluent characterization, and energy consumption. The parameters of real urine that impact nitrogen recovery efficiency were determined through experiments with synthetic and real urine solutions in batch and continuous-flow setups. We identified predominant reactions, including those facilitated by electrical current and reactions between electrochemical products. The fate of trace organic contaminants (TrOCs) was investigated and correlated with compound properties (e.g., structure, pKa). Overall, the validation and mechanistic understanding of nitrogen migration during electrochemical stripping is useful for evaluating, optimizing, and identifying applications for a novel nitrogen recovery unit process.

## 2. MATERIALS AND METHODS

### 2.1 Electrochemical Stripping Setup

A process schematic is shown in Figure 4.1. Experiments were performed in a three-chambered parallel plate reactor in which three square Perspex frames (internal dimensions:  $8 \times 8 \times 1.9$  cm) were bolted together between two larger square Perspex plates ( $10 \times 10 \times 1.9$  cm) to create the anode, cathode, and trap chambers (122 mL each). The anode and cathode chambers were separated by a cation exchange membrane (CMI-7000, Membranes International Inc., Ringwood, NJ); the cathode and trap chambers were separated by a microporous polypropylene membrane (3M, St. Paul, MN). More information on the membranes can be found in Table C1. The anode was Ti mesh coated with Ir mixed-metal oxide ( $64 \text{ cm}^2$ , Magneto Special Anodes, Netherlands)

and the cathode was stainless steel (known to reduce oxygen and water)<sup>126</sup>; both had a 64 cm<sup>2</sup> surface area. An Ag/AgCl reference electrode (+ 0.197 V vs. SHE, BASi, USA) and multichannel potentiostat (Gamry Instruments Inc., Warminster, PA) were used to measure and control applied potential.

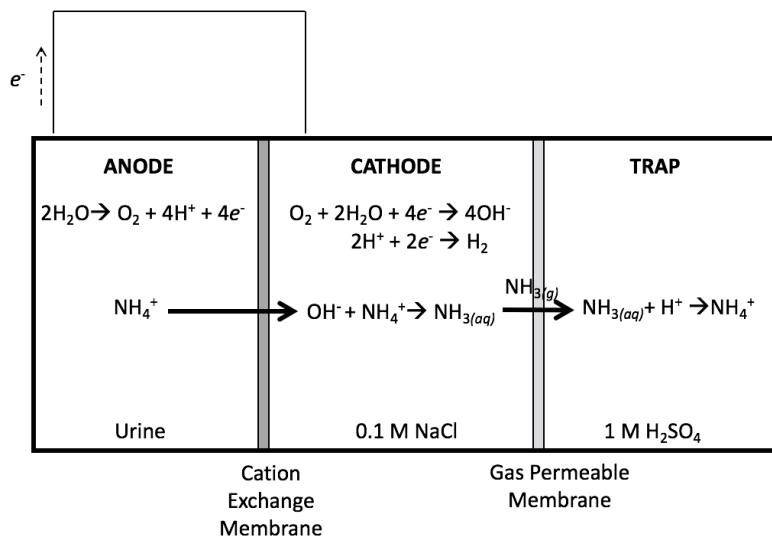


Figure 4.1 Schematic of the electrochemical stripping setup. For batch experiments, each solution was recirculated in separate 1-L bottles. For continuous experiments the anode was fed continuously and the cathode and trap were recirculated only.

## 2.2 Electrolysis Operation

Chronopotentiometric experiments were performed at a current density of 100 A m<sup>-2</sup>. Batch experiments were used to evaluate nitrogen recovery efficiency; measured potentials were approximately 2.2 V. Anolyte, catholyte, and trap solutions were recirculated separately at 75 mL min<sup>-1</sup> for 24 hours. Experiments were conducted in triplicate for real urine, synthetic urine, and ammonium sulfate (all ~4 g N L<sup>-1</sup>, see section 2.3; compositions in Table C2). Anion concentrations were measured to confirm that physical mixing between chambers did not occur. A mass balance was performed to track total ammonia nitrogen (TAN;  $\text{NH}_3 + \text{NH}_4^+$ ) in each chamber over time. Recovery efficiencies were calculated by dividing final trap chamber concentrations by initial anode chamber concentrations (Equation C1).

Continuous-flow experiments were performed to determine nitrogen fluxes and energy demand. Anolyte was supplied continuously; catholyte and trap solution were recirculated in batch mode. The anode feed rate was 1.7 mL min<sup>-1</sup> (2.4 L d<sup>-1</sup>, 1.22 hr hydraulic retention time, HRT); all chambers were recirculated at 100 mL min<sup>-1</sup> for mixing. To approximate steady-state conditions, samples were taken at 3, 4, and 5 HRTs and averaged (see section 2.5). Full cell potential was measured with a voltmeter (MAS830B, Commercial Electric, Cleveland, Ohio) connected to the anode and cathodic current collector. Based on full cell potential and pumping energy for all three cells, energy input per kg N recovered was calculated (Equation C2).

Cyclic voltammetry was used to identify predominant anodic reactions in three different solutions ((NH<sub>4</sub>)<sub>2</sub>SO<sub>4</sub>, synthetic urine, and real urine) and in nonaqueous dimethyl sulfoxide (DMSO) to inhibit water oxidation. To reduce mass transfer limitations and ohmic resistance, cyclic voltammetry was performed in a smaller, unseparated cell with 10 cm<sup>2</sup> electrodes and 200 mL of anolyte. Three cycles were run between 0 and 1.5 V at a scan rate of 10 mV s<sup>-1</sup>. Besides water, we expected chloride, acetate, and ammonia to be the major oxidizable species in urine; accordingly, single-salt solutions of LiCl (10 mM Cl<sup>-</sup>), NaC<sub>2</sub>H<sub>3</sub>O<sub>2</sub> (10 mM C<sub>2</sub>H<sub>3</sub>O<sub>2</sub><sup>-</sup>), and (NH<sub>4</sub>)<sub>2</sub>CO<sub>3</sub> (10 mM NH<sub>4</sub>-N) were prepared in DMSO and compared to pure DMSO and a solution with 10 mM of all three salts.

### 2.3 Electrolysis solutions

To examine the factors and mechanisms affecting electrochemical treatment of urine, three anolyte solutions were compared (Table C2): (i) (NH<sub>4</sub>)<sub>2</sub>SO<sub>4</sub> adjusted to pH 9 with NH<sub>4</sub>OH; (ii) synthetic stored urine (pH ~ 9); and (iii) real stored urine (pH ~ 9; influent compositions in Table C2). Synthetic solutions were diluted to match the total ammonia concentration of real urine (~4 g N L<sup>-1</sup>). (NH<sub>4</sub>)<sub>2</sub>SO<sub>4</sub> was used for the ideal solution because sulfate is inert at applied potentials used in this study ( $E^0$  of SO<sub>4</sub><sup>2-</sup>/S<sub>2</sub>O<sub>8</sub><sup>2-</sup>=2.1 V vs. standard hydrogen electrode, SHE). Synthetic urine and (NH<sub>4</sub>)<sub>2</sub>SO<sub>4</sub> were compared to elucidate the effect of competition from other cations, such as Na<sup>+</sup> and K<sup>+</sup>. We used an existing synthetic urine recipe based on the composition of real stored urine (Table C3); the heterogeneous mixture of organics in real urine was approximated as acetate.<sup>23</sup> Real urine for electrochemical experiments was collected from approximately 20 male and female adult volunteers in Berkeley, CA and stored for at least 4 weeks to hydrolyze urea (CPHS protocol 2016-10-9284). Aqueous magnesium and calcium concentrations were below detection limits due to spontaneous struvite and hydroxyapatite precipitation in collection containers.<sup>22</sup> To further elucidate the effects of solution composition on system performance, phenol (100 mM) was added to synthetic urine in one set of experiments to quench chlorine. All experiments were conducted at room temperature (23 ± 2 °C) with nanopure water and analytical grade chemicals. In all experiments, 0.1 M NaCl and 1 M H<sub>2</sub>SO<sub>4</sub> were used as catholyte and trap solution, respectively.

### 2.4 Chemical Analysis

Ion concentrations (NH<sub>4</sub><sup>+</sup>, Na<sup>+</sup>, K<sup>+</sup>, Li<sup>+</sup>, Mg<sup>2+</sup>, Ca<sup>2+</sup> and SO<sub>4</sub><sup>2-</sup>, PO<sub>4</sub><sup>3-</sup>, Cl<sup>-</sup>, NO<sub>2</sub><sup>-</sup>, NO<sub>3</sub><sup>-</sup>, F<sup>-</sup>, C<sub>2</sub>H<sub>3</sub>O<sub>2</sub><sup>-</sup>, Br<sup>-</sup>) were measured via cation and anion chromatography (Dionex 120, IonPac CS12 column for cations, IonPac AS23 column for anions), as described previously.<sup>98</sup> Acetate was analyzed with a separate calibration curve made with NaC<sub>2</sub>H<sub>3</sub>O<sub>2</sub> (1, 4, 8, 16, 24, 40 mg L<sup>-1</sup>). Free and combined chlorine were measured according to the standard *N,N*,diethyl-*p*-phenylenediamine (DPD) method<sup>127</sup> with a Shimadzu UV-2600 spectrophotometer at 515 nm.



pH was measured with a pH probe (MP220, Mettler Toledo, Columbus, OH). Metals were measured using an ICP-MS (Agilent 7700 series, Santa Clara, CA).

To determine the fate of trace organics in real urine, 11 trace organic contaminants (TrOCs), including antibiotics, antivirals, and beta blockers, were added to synthetic and real urine before electrochemical stripping (Table C4). TrOCs were added at 20 µg/L, a typical concentration in urine<sup>128</sup> but 100 to 10,000 times higher than concentrations found in influent combined wastewater.<sup>100,129</sup> In batch experiments, TrOCs were measured in the anode, cathode, and trap chamber at each time point. Trace organics were also measured in three different sources of urine: (1) untreated, stored urine collected from ~20 adult volunteers in Berkeley, CA; (2) NoMix toilets in Zurich, Switzerland (>100 users); and (3) a container-based sanitation system in Nairobi, Kenya (>1000 users). TrOCs were quantified by high-performance liquid chromatography–tandem mass spectrometry (HPLC–MS/MS) in the multiple reaction monitoring (MRM) mode using an Agilent 1200 series HPLC system with a Hydro-RP column (150 × 3 mm, 4µM; Phenomenex, Aschaffenburg, Germany) coupled to a 6460 triple quadrupole tandem mass spectrometer, as described previously.<sup>105</sup>

## 2.5 Statistical Analysis

Batch nitrogen recovery efficiencies for each influent (including synthetic urine with phenol) were compared using a one-way ANOVA and paired t-tests. In continuous-flow experiments, nitrogen fluxes and energy demands were also compared using a one-way ANOVA and paired t-tests.

## 3. RESULTS AND DISCUSSION

### 3.1 Nitrogen recovery from real urine in batch experiments

Batch experiments with real urine demonstrated that nitrogen was efficiently and selectively recovered via electrochemical stripping. More than 90% ( $92.7 \pm 4.12\%$ ) of total ammonia in real urine was recovered in the trap chamber at 24 h (Figure 4.2). Competitor cations (e.g.,  $\text{Na}^+$ ,  $\text{K}^+$ ) present in urine accumulated in the cathode but were not detected in the ammonium sulfate trap solution, indicating selective ammonia recovery (Figure C1); anions present in urine (e.g., acetate, phosphate) were not detected in the cathode or trap chambers, demonstrating limiting mixing between chambers. Using the same operating parameters (e.g., current, recirculation rate, reactor geometry) as in batch experiments, the optimal HRT for continuous electrochemical stripping appears to be between 12 and 24 hours. For comparison, a previous study using electrodialysis for ammonium migration required 6 hours HRT but also an additional treatment step to separate ammonium from other cations.<sup>121</sup> For electrodialysis, increased hydraulic residence time led to higher removal efficiencies but lower fluxes for ammonium, particularly at high current densities ( $\geq 50 \text{ A m}^{-2}$ ).<sup>121</sup> For electrochemical stripping, changes to HRT by changing reactor geometry or flow rate could optimize ammonium recovery efficiency and flux.

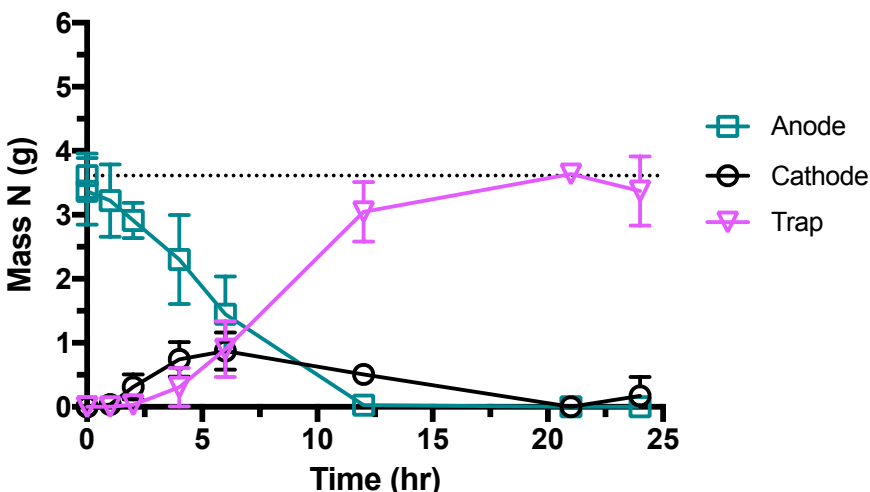


Figure 4.2 Mass of total ammonia nitrogen in each chamber over time in batch experiment. Dotted horizontal line is initial mass of TAN in anode. Error bars represent  $\pm$  one standard deviation. Bars not shown are smaller than symbol, except for 21 hours (n=1).

### 3.2 Continuous electrochemical stripping with real urine

Continuous-flow experiments were used to further characterize electrochemical stripping in terms of transmembrane fluxes, recovery efficiencies, and energy demand. With an influent concentration of  $7490 \text{ mg N L}^{-1}$ , average concentrations after 3-5 HRTs were  $2960 \text{ mg N L}^{-1}$  (anode),  $1950 \text{ mg N L}^{-1}$  (cathode), and  $2250 \text{ mg N L}^{-1}$  (trap). Nitrogen flux across the cation exchange membrane ( $1710 \text{ g N m}^{-2} \text{ d}^{-1}$ ) was higher than the flux across the hydrophobic gas permeable membrane ( $1010 \text{ g N m}^{-2} \text{ d}^{-1}$ , Figure C2, Equations C3-C4), indicating that the latter is the rate-limiting step of the electrochemical stripping process and a high priority for future work. For example, an asymmetric cathode chamber could be used to create a larger membrane surface area for the gas permeable membrane than the cation exchange membrane. Other gas permeable membranes could also be tested to optimize ammonia flux to the trap chamber. Based on open circuit experiments (no current), only 9% of flux across the cation exchange membrane was attributed to diffusion; electro-migration accounted for the balance. This finding was similar to electrodialysis in urine, in which diffusion accounted for 4-11% of ammonium flux and the contribution of diffusion to flux was larger for longer HRTs.<sup>121</sup> Flux across the cation exchange membrane measured in this study was significantly higher than reported electrodialysis values due to the addition of a gas permeable membrane (to reduce accumulation of aqueous  $\text{NH}_3$  in the cathode) and operation at a higher current density ( $100 \text{ A m}^{-2}$  in this study, maximum  $50 \text{ A m}^{-2}$  in literature, Table C5).

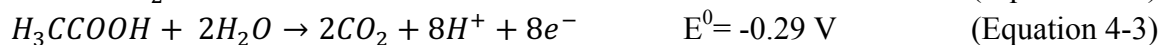
Overall, 61% of influent nitrogen was removed from the anode (Equation C5); increasing anodic HRT could increase removal efficiency. Nitrogen removal efficiencies (across cation exchange membrane, 60.6%, Equation C5) were higher than nitrogen recovery efficiencies (across gas permeable membrane, 49.6%, Equation C6, Figure C2). Based on 26% of TAN remaining in the

cathode at steady state, increasing cathodic HRT (currently 1.22 hr) could increase recovery efficiencies for both the gas permeable membrane and the overall electrochemical stripping process. Significant ammonia removal was observed at a continuous-flow HRT much shorter than the time needed in batch experiments (Figure 4.2) because of a smaller effective chamber volume in continuous flow (122 mL for continuous, 1000 mL for batch). Longer HRTs have been demonstrated to reduce flux but increase removal efficiency.<sup>121</sup> Lower influent TAN concentrations are expected to decrease flux (Equation C3); the degree of this effect is expected to vary based on the relative contribution of diffusion, which depends on a concentration gradient and varies directly with HRT. Transmembrane nitrogen recovery efficiencies for electrochemical stripping were higher than electrodialysis and microbial fuel cells, but lower than electrodialysis with external ammonia stripping (Table C6).

Electrochemical stripping with real urine required 29.5 MJ kg N<sup>-1</sup> for supply of electric current, the lowest energy input reported for physicochemical electrochemical treatment of urine to date (Table C7, all studies exclude pumping energy). The energy demand for electrochemical stripping was 5% less than conventional ammonia stripping but still 30% higher than nitrification-denitrification (Figure C3). Current efficiency (mol N (mol e<sup>-</sup>)<sup>-1</sup>, Equation C7) for ammonium in real urine was greater than that previously reported for electrodialysis (61%)<sup>121</sup> and even surpassed 100%, indicating contributions from diffusion (Figure C4). The higher current efficiency is likely due to the addition of the gas permeable membrane, which increased flux across the cation exchange membrane. Lower current efficiencies were observed in synthetic urine solutions due to differences in electrical conductivity and competing oxidation reactions (section 3.3).

### 3.3 Electrochemical oxidation reactions

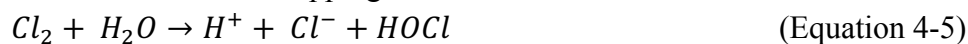
Several electrochemical oxidation reactions could potentially take place at the anode during electrochemical stripping (standard reduction potentials also shown), including



Cyclic voltammetry and measurements of anticipated products were used to elucidate the contributions of each potential oxidation reaction. Acetate is an organic compound abundant in urine that could be oxidized (complete mineralization shown in Equation 3); ammonia could be oxidized to several nitrogen species, including nitrite (Equation 4).

Voltammograms performed in aqueous electrolytes confirmed that water oxidation was the primary anodic reaction (Figure C5). In cyclic voltammetry performed in DMSO, an aprotic solvent, voltammograms in LiCl were similar to those with a combined solution (LiCl, NaC<sub>2</sub>H<sub>3</sub>O<sub>2</sub>, (NH<sub>4</sub>)<sub>2</sub>CO<sub>3</sub>), demonstrating that chloride oxidation was the second most predominant

reaction (Figure C6). Chloride oxidation leads to disproportionation of  $\text{Cl}_2$  to hypochlorous acid (Equation 5), which was detected in the anode chamber in both synthetic and real urine treated via electrochemical stripping.



Acetate and ammonia oxidation were confirmed to be insignificant based on constant anodic acetate concentrations and <2% of influent nitrogen detected as nitrate or nitrite. While gaseous nitrogen oxidation products (e.g., NO,  $\text{N}_2\text{O}$ ,  $\text{N}_2$ ) were not measured, the similarity of voltammograms of  $(\text{NH}_4)_2\text{CO}_3$  in DMSO and pure DMSO demonstrated limited ammonia oxidation (Figure C6). Current efficiency for chloride oxidation was 0.052% (Figure C7, Equation C8), which puts an upper bound on acetate and ammonia oxidation. Although current efficiency was low for chloride oxidation, because reactive chlorine species react with urine constituents (e.g., ammonia, organic compounds), they influenced the fate of nitrogen in the anode chamber, as discussed in the next section.

### 3.4 Mechanisms of ammonia transformation

Mechanisms of ammonia transformation were determined by comparing electrochemical stripping results from real urine with synthetic urine and ammonium sulfate. As shown in Figure 4.3a, the nitrogen recovery efficiencies in ammonium sulfate ( $100.0 \pm 1.19\%$ , Figure C8a) and real urine ( $92.7 \pm 4.12\%$ ) were significantly higher than in synthetic urine ( $82.4 \pm 1.30\%$ ,  $p < 0.05$ ). Recovery efficiencies in real urine and ammonium sulfate were not significantly different, indicating that the effects of competition from  $\text{Na}^+$  and  $\text{K}^+$  in real urine were negligible or were overcome during the 24 h batch experiment.

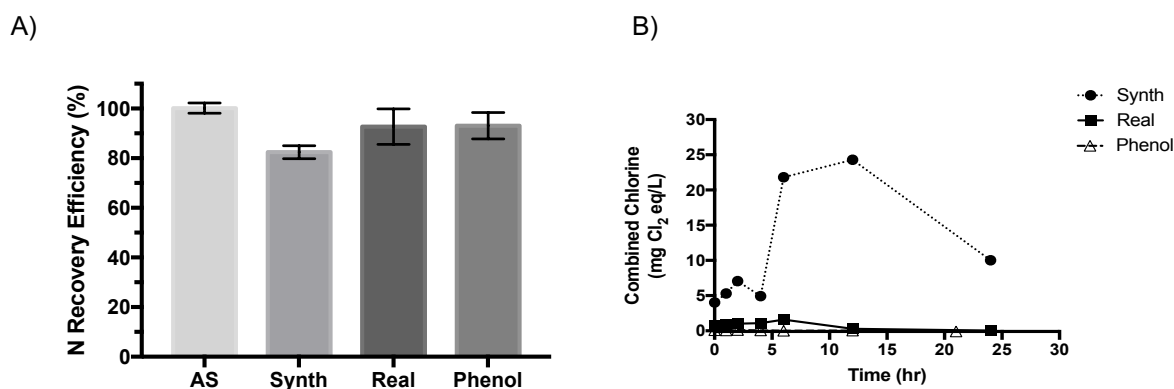


Figure 4.3. Results for varied influents from 24 hr batch experiments: (a) Nitrogen recovery efficiency measured. Error bars indicate  $\pm$  one standard deviation. AS= ammonium sulfate, phenol = synthetic urine with phenol addition. (b) Combined chlorine measured in synthetic urine, synthetic urine with phenol addition (10 mM), and real urine.

The lower nitrogen recovery efficiency observed in synthetic urine was investigated through additional experiments. While 99% of TAN present at 24 hours was in the trap, 17% of initial

TAN had been lost from the system (Figure C8b). Electrochemically produced free chlorine could form chloramine species (e.g., Equation 6; formation of monochloramine).<sup>130</sup>



Combined chlorine concentrations in the anode chamber were higher for synthetic urine than real urine (Figure 4.3b), confirming that ammonia loss by chloramination occurred to a greater extent in synthetic urine than real urine. Chloramine species are neutrally charged and remained in the anode, as confirmed by combined chlorine measurements below the detection limit (0.5 mg Cl<sub>2</sub> equivalents L<sup>-1</sup>) for all time points in the cathode and trap chambers.

Differential production of combined chlorine in synthetic and real urine was primarily due to heterogeneous organics in real urine that were approximated as acetate in synthetic urine. Acetate reacts much more slowly than primary organic urine constituents with free chlorine (Table C8). The addition of phenol to synthetic urine in batch experiments resulted in a nitrogen recovery efficiency of 93.1 ± 3.06% (Figure 4.3a, p>0.05 compared to real urine) and a 98% reduction of combined chlorine concentrations compared to synthetic urine (Figure 4.3b); neither nitrogen recovery efficiency nor chloramine concentration was significantly different between real urine and synthetic urine with phenol (p>0.05). Over 24 hours, both TAN and anodic pH (Figure C9) decreased, affecting the kinetics of chlorination of ammonia and organics. In synthetic urine, ammonia chlorination was always faster than acetate chlorination; in synthetic urine with phenol, ammonia chlorination was slower than phenol chlorination for the majority of the experimental period (Figure C10). Chlorination of phenol preserved ammonia for migration and led to a higher nitrogen recovery in synthetic urine with phenol compared to synthetic urine alone. Thus, adding phenol to synthetic urine made it a more accurate model solution for studying the electrochemical treatment of real urine.

### 3.5 Fate of trace organic contaminants

Trace organic contaminants have been detected at significant concentrations in urine, especially because 64% of pharmaceuticals are excreted in urine.<sup>128</sup> Most organics in urine are hydrophilic (e.g., phenolic, deprotonated amine functional groups) because lipophilic compounds tend to partition into feces.<sup>131</sup> We measured a suite of trace organics, including beta blockers, antibiotics, and antivirals, in urine from Berkeley, California, USA; Nairobi, Kenya; and Zurich, Switzerland. Compounds with notably high concentrations included sulfamethoxazole (up to 10 mg L<sup>-1</sup>), abacavir (up to 1 mg L<sup>-1</sup>), atenolol (up to 200 ug L<sup>-1</sup>), and carbamazepine (up to 10 ug L<sup>-1</sup>; Figure 4.4a). Most concentrations were highest in Nairobi urine, with acetaminophen in Berkeley and carbamazepine in Zurich being notable exceptions.

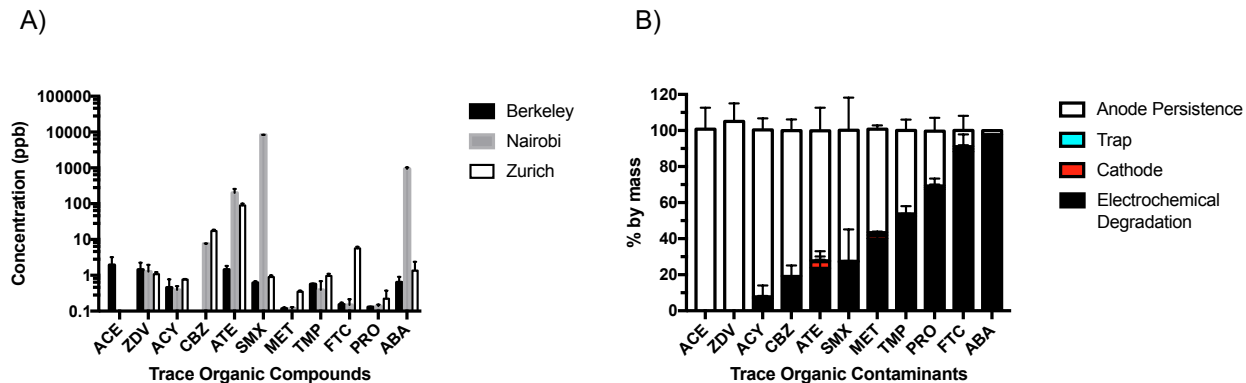


Figure 4.4. (a) Concentrations of 11 trace organic contaminants (TrOCs) in urine from Berkeley, Nairobi, and Zurich. (b) Fate of TrOCs in batch experiments with real urine. Error bars represent  $\pm$  one standard deviation. See Table C4 for abbreviations and compound names.

Four primary fates of trace organics were evaluated: reaction with electro-generated oxidants in the anode chamber, electro-migration to cathode and trap chambers, transformation in the cathode chamber, and transformation in the trap chamber. The latter two fates were neglected based on no observed transformation in control experiments, with the exceptions of cathodic removal of emitricitabine and propranolol (Figure C11). Based on a mass balance that neglected cathodic and trap transformation, the fate of each compound in real urine is presented in Figure 4.4b. Most importantly, TrOCs were not detected in the ammonium sulfate product (trap chamber). Two compounds were noticeably transported through the cation exchange membrane: atenolol (4% in cathode, pKa 9.6) and metoprolol (2% in cathode, pKa 9.5). Anodic transformation of parent compounds correlated roughly with electron-rich moieties, which was expected due to predominant mechanisms of electrochemical oxidation and reactions with electrophilic chlorine species (e.g., HOCl and chloramines).<sup>132</sup> Key exceptions included zidovudine and acyclovir, which may have back-diffused from the cathode to the anode due to their hydrophilicity ( $\log K_{ow} < 0$ , Table C4) and positive charge at stored urine pH (pKa values  $\sim 9$ , Table C4). In particular, 30% of zidovudine diffused from the cathode to the anode when trace organics were spiked into the cathode (Figure C11). Although propranolol also has a pKa of approximately 9, it sorbs to mixed metal anodes due to its high hydrophobicity (Table C4), which contributed to its higher level of removal from anolyte.<sup>132</sup> Similarly, emitricitabine is hydrophobic but is neutrally charged at pH 9, preventing transport through the cation exchange membrane.

Anodic degradation was significantly higher in synthetic urine than real urine (all compounds  $>94\%$  degraded in synthetic urine, Figure C12). For all compounds, observed anodic degradation first order rate constants were higher in synthetic urine than in real urine (Figure C13). This difference was further evidence of less chlorine quenching in synthetic urine due to the presence of heterogeneous organics in real urine instead of acetate. Higher residual concentrations of free and combined chlorine in the anode with synthetic urine led to higher observed rate constants for

trace organics and lower nitrogen recovery efficiencies. While nitrogen recovery remains the primary goal of electrochemical stripping, further investigations into the mechanisms contributing to anodic degradation of TrOCs in urine could enhance understanding of effluent treatment required after electrochemical stripping.

### 3.6 Implications for urine treatment

The required energy input was calculated for each influent in continuous experiments. Based on only full cell potential, real urine required 29.5 MJ kg N<sup>-1</sup>, which was 55% less energy than ammonium sulfate, 26% less energy than synthetic urine, and 8% less energy than conventional ammonia stripping (Figure C2). Pumping energy required an additional 1.13 MJ kg N<sup>-1</sup> for all three chambers. The high conductivity of real urine lowers ohmic resistance for charge transport through the anode, explaining the higher energy efficiency compared to ammonium sulfate (Figure C14). Additionally, higher nitrogen recovery efficiency in real urine over synthetic urine was responsible for higher energy efficiency in real urine. More generally, real urine composition varies, and conductivity could be an indicator for nitrogen recovery efficiency by electrochemical stripping (Figure C14).

In addition to nitrogen, potassium could also be recovered by electrochemical stripping. Potassium was effectively recovered in the cathode chamber (Figure C1); no measurable amount was detected in the anode nor in the trap after batch experiments. In most regions potassium is an inexpensive fertilizer (between 0.50 and 1 USD kg<sup>-1</sup>);<sup>47,133</sup> however, recovering it could enhance the value of urine-derived fertilizers. Recovering potassium and ammonium separately, along with phosphorus recovery before electrochemical stripping, could allow for production of fertilizers with customized macronutrient ratios.

Urine-derived products should be safe for use, especially in the case of fertilizers. Processes for nitrogen recovery benefit from selective concentration of ammonium relative to other urine constituents, including other cations, TrOCs, and metals. Besides ammonium and sulfate, no other ions were observed at measurable concentrations in the ammonium concentrate product (detection limits and compounds in Table C9). Similarly, TrOCs were not detected in the trap chamber (see section 3.5). Trace elements were not detected in the ammonium sulfate product above 30 ppb. Measured elements with maximum contaminant limits (MCLs, highest concentration allowed in drinking water)<sup>134</sup> were all detected below their respective MCLs in produced ammonium sulfate (Figure C15a, Table C10).

The major effluent produced from electrochemical stripping is electrolyzed urine from the anode chamber. Disinfectant residuals were at most 1.6 mg Cl<sub>2</sub> equivalents L<sup>-1</sup> for combined chlorine (Figure 4.3b) and 0.89 mg Cl<sub>2</sub> equivalents L<sup>-1</sup> for free chlorine. If treated urine goes to a wastewater treatment plant, the disinfectant residual will be consumed quickly when mixed with sewage. If treated urine is discharged to the environment, free chlorine will likely be consumed

by ammonia in surface waters; however, combined chlorine at 1-2 mg L<sup>-1</sup> could negatively impact aquatic life.<sup>135</sup> Disinfection byproducts (DBPs) were not measured in this study; future work could lead to further characterization of DBPs in fertilizer and effluent produced from urine by electrochemical stripping. Anode material strongly influences production of DBPs (e.g., trihalomethanes, ClO<sub>3</sub><sup>-</sup>, and ClO<sub>4</sub><sup>-</sup>) during electrochemical oxidation of ammonia; stripping and oxidation are significant pathways for DBP transformation.<sup>130</sup> While DBPs may be of concern, a potential benefit of the electrochemically produced chlorine is inactivation of pathogens in urine at the anode, which is particularly attractive in decentralized settings in which there is no wastewater treatment facility to receive electrolyzed urine effluent. Trace metal concentrations were below MCLs for urine treated via electrochemical stripping; arsenic was one exception (Figure C15a).

If catholyte is not recirculated and reused, it could also be a process effluent. Catholyte concentrations of TrOCs were less than 0.4 ppb, with the exception of atenolol (0.74 ppb) and acetaminophen (1.24 ppb). Trace elements were not detected above 20 ppb in catholyte (Figure C15b). Further optimization (e.g., of HRT, operating potential, temperature) could be investigated for trace organic and metal removal from effluent urine and catholyte.



# **Chapter 5. Evaluating ion exchange for nitrogen recovery from source-separated urine in Nairobi, Kenya**

The following chapter is adapted from the co-authored manuscript Tarpeh et al. (2017) Evaluating ion exchange for nitrogen recovery from source-separated urine in Nairobi, Kenya. *Development Engineering Journal* (in preparation) with permission from Ileana Wald, Michael Otieno Omollo, Timothy Egan, and Kara L. Nelson.

## **1. INTRODUCTION**

The majority of people in the developing world live with untreated feces and urine in their communities.<sup>10</sup> Urban centers in developing countries are expected to experience a disproportionately large share of population growth that is likely to continue to outpace provision of services such as water supply and sanitation.<sup>136</sup> The proportion of urban residents who live in slums has remained constant at 72% in sub-Saharan Africa;<sup>136</sup> residents of these high-density, unplanned settlements are particularly vulnerable to water and excreta-related diseases. Excreta collection and treatment can improve human health and environmental quality by reducing the transmission of these diseases and avoiding nutrient discharges that irreversibly alter aquatic environments.<sup>137</sup> Globally, estimated costs to society from inadequate sanitation are \$260 billion per year due to associated health care, premature deaths, and productivity losses.<sup>138</sup>

With only 10% of sub-Saharan Africans connected to sewer systems and less than 50% expected by 2050,<sup>15,139</sup> universal coverage with conventional sewers and centralized wastewater treatment is an unrealistic proximate goal. Decentralized collection and treatment may be less costly and require less energy while providing opportunities for revenue generation through resource recovery from waste.<sup>140</sup> An approach in which sanitation providers aim to improve public health, environmental quality, and profit may accelerate and sustain sanitation access. Valuable nutrients (e.g., nitrogen, phosphorus, potassium) can be extracted from human excreta. They are especially valuable near Nairobi, Kenya, where agricultural soil nutrient levels are low due to over-farming, population density, and poor water quality.<sup>141</sup> These constraints create high demand for manufactured fertilizers, which the Kenyan government has subsidized since 2009.<sup>142,143</sup> Despite these subsidies, fertilizers are often underutilized by the average Kenyan farmer because of high import and transport costs,<sup>144</sup> limited fertilizer supply,<sup>145</sup> distance to fertilizer distribution channels,<sup>146</sup> and cumulative soil degradation.<sup>147</sup>

Separate collection of urine facilitates nutrient recovery and fertilizer production because urine contains the majority of excreted macronutrients but is typically only 1% of wastewater

volume.<sup>14</sup> Phosphorus is an increasingly scarce fertilizer component that can be recovered from urine through precipitation of struvite (magnesium ammonium phosphate,  $\text{MgNH}_4\text{PO}_4$ ).<sup>148</sup> Nitrogen can be recovered from urine using several techniques, including urea stabilization,<sup>42</sup> nitrification-distillation,<sup>149</sup> and ion exchange.<sup>98</sup> During urine storage, nitrogen in the form of urea is hydrolyzed to ammonium ( $\text{NH}_4^+$ ),<sup>73</sup> which is retained on the ion exchange adsorbent's negatively charged sites. Once loaded with  $\text{NH}_4^+$ , cation exchange adsorbents could be applied as solid fertilizers (if naturally derived) or regenerated to produce liquid fertilizer and reusable adsorbent. In this study, ammonium sulfate fertilizer was produced; other options include ammonium nitrate and ammonium chloride, which can be generated by varying the compound used to elute the adsorption columns. Ion exchange can be applied at various scales, from individual toilets or households to centralized urine collection depots. A previous comparison of adsorbents showed that Dowex Mac 3, a cation exchange resin, has high adsorption density and regeneration efficiency that make it well-suited for ammonium recovery from urine.<sup>98</sup>

The goal of this investigation was to determine if producing ammonium sulfate from urine via ion exchange is a viable business model for container-based, source-separated excreta collection and treatment services. Our objectives were to: (i) demonstrate proof-of-concept and measurement methods in the field, (ii) evaluate the implications of urine composition, process indicators, and scalability for urine collection and treatment, and (iii) compare the cost of nitrogen recovery via ion exchange to current excreta management and fertilizer production practices in the study region.

## 2. MATERIALS AND METHODS

### 2.1 Description of Field Site

The field site for the research was Nairobi, Kenya, where the social enterprise Sanergy operates more than 700 dry, source-separating, toilets in several slums.<sup>150</sup> The toilets, branded as Fresh Life Toilets (FLT), are primarily owned and operated by local entrepreneurs via a franchise business model. These toilets are used over 33,000 times a day and revenues from user payments go to franchisees.<sup>150</sup> While most toilets are open to the public, some are located at schools and multi-family units. Sanergy charges toilet operators for daily collection of the waste and generates revenue from the sale of excreta-derived products.<sup>17</sup> Urine and feces containers (25 L urine, 30 L feces) are collected and replaced daily by Sanergy employees. The containers are taken to a central transfer station where urine and feces are processed separately. The fecal waste is transported 30 km by truck to a processing facility where it is converted into several value-added products: soil conditioner branded as *Evergrow* through a co-composting process, biogas through an anaerobic digestion process, and a black soldier fly animal feed. Urine from the toilets is stored in 1,000-L tanks at the transfer station, which are emptied every 2-3 days and the urine is trucked 20 km to a wastewater treatment facility.

## 2.2 Synthetic and Real Urine Composition

Synthetic stored urine was used to validate column operation because its composition was known and constant between locations (Table D1). Real urine from different locations (Nairobi, Kenya; Dubendorf, Switzerland; Berkeley, California, USA) and collection systems was compared to determine the effects of varying urine composition and collection methods on urine treatment. In Berkeley, urine from participants was collected, homogenized in sterile containers, and stored in closed containers for one month. In Nairobi, source-separated urine from eight urine-diverting dry toilets and centralized collection tanks was analyzed. In Dubendorf, multiple waterless urinals and urine-diverting flush toilets in a building drained to a single collection tank, from which samples were drawn. Urea hydrolysis to total ammonia ( $\text{NH}_3/\text{NH}_4^+$ ) proceeded spontaneously in collection systems (Dubendorf and Nairobi); jack bean urease was added to Berkeley urine to accelerate the process (Sigma Aldrich, St Louis, MO). Magnesium and calcium concentrations were negligible (i.e.,  $<0.05$  mg/L) in stored urine due to struvite and hydroxyapatite precipitation.<sup>73</sup>

## 2.3 Column experiments

Upflow continuous adsorption experiments were performed in plastic columns (2.54-cm diameter, 16-cm length, PVC plastic) packed with Dowex Mac 3, a cation exchange resin. After pretreatment with 1 M borate buffer, either synthetic or real urine (from closed tanks at transfer station) was pumped at 4.5 mL/min (6.5 L/d, 0.0148 cm/s) through each column for 6 hours, and 1.5-mL effluent samples were collected every 20 minutes and analyzed for ammonium. Adsorption densities were calculated by numerically integrating breakthrough curves to determine the total mass of ammonium retained by the columns, and dividing by resin mass (Equations D1-D2). The hydraulic performance of columns was verified in experiments with synthetic urine and measurement of chloride as a conservative tracer.

Regeneration experiments were performed using 0.1 M (0.65%)  $\text{H}_2\text{SO}_4$ , pumped at 22.5 mL/min for 2 hours, to elute the ammonium from the columns after they were saturated. The total volume of eluent was larger than the volume of urine treated; while this approach is impractical for implementation, it was useful for our goal of identifying the maximum amount of nitrogen that could be recovered. Effluent was combined over the course of the experiment and ammonium concentration was measured in the composite sample. Regeneration efficiencies were calculated by dividing the mass of ammonium eluted (product of composite concentration and effluent volume) by the mass of ammonium adsorbed in the previous cycle (Equation D3).

Ten adsorption-regeneration cycles were conducted in triplicate to evaluate regeneration lifetimes with real urine collected from FLT's. For each cycle, adsorption densities and regeneration efficiencies were calculated using the methods above.

Performance at larger scale (scaling factor of 10) was investigated with larger columns (5.08-cm diameter, 40-cm length) and flow rates (65 L/d), with the same laboratory set-up and analysis methods as for the 2.54-cm diameter columns. Larger columns were constructed in Mukuru from locally available PVC plastic. The objective of these experiments was to validate the ammonium recovery process at larger scales that may be more relevant to centralized nitrogen recovery in the Sanergy container-based system.

Column experiments were also conducted with anaerobic digester effluent for comparison to real urine. Digestate is produced during anaerobic digestion of feces and has high total ammonia concentrations (Table 1), making it another potential liquid stream for nitrogen recovery via ion exchange.

Table 5.1 Digestate and urine composition (closed tank). All concentrations in mg/L except for pH and EC (mS/cm). SEM values in parentheses.

	Digestate	Urine
pH	8.45	8.98
EC	23.5	35.9
COD	5790 (1070)	8640 (61.1)
Na <sup>+</sup>	628 (3.11)	2520 (104)
NH <sub>4</sub> <sup>+</sup> -N	3030 (9.60)	6420 (138)
K <sup>+</sup>	1530 (9.74)	2750 (76.9)
Cl <sup>-</sup>	786 (18.7)	4840 (154)
PO <sub>4</sub> <sup>3-</sup> -P	616 (14.1)	1040 (21.8)

## 2.4 Chemical Analysis

In Berkeley, total ammonia nitrogen (TAN; NH<sub>3</sub> + NH<sub>4</sub><sup>+</sup>), sodium, and potassium were measured via cation chromatography (Dionex, IonPac CS12 column, 30 mM methanesulfonic acid eluent, 1.0 mL/min, 40 °C) for column experiments conducted in Berkeley and influent urine samples from Nairobi. In Nairobi, Hach kits were used to measure total ammonia nitrogen (salicylate method 10031). Chloride, phosphate, and sulfate were measured in Berkeley by anion chromatography (Dionex, IonPac AS23 column, 4.5 mM NaHCO<sub>3</sub>/0.8 mM Na<sub>2</sub>CO<sub>3</sub>, 1.0 mL/min, 30 °C). In Nairobi, Hach kits were also used to measure potassium (method 8049), chemical oxygen demand (COD, method 8000), and phosphate (method 8190). Samples from column experiments performed in Nairobi were measured in Nairobi. pH and electrical conductivity (EC) were measured with a pH/EC/ORP meter (H12211 meter, Hanna Instruments, Padova, Italy).

## 2.5 Statistical analysis

One-way ANOVA and paired t-tests were used to compare the slope of breakthrough curves and time to breakthrough. Two-tailed analyses were used with a significance level of  $p=0.05$ . For urine composition, the standard error of the mean was calculated for triplicate measurements.

## 3. RESULTS AND DISCUSSION

### 3.1 Comparing lab and field nitrogen recovery

Synthetic urine was used to compare ammonium breakthrough curves measured with cation chromatography (Berkeley) and Hach methods (Nairobi). There was no significant difference between calculated adsorption densities nor slopes of breakthrough curves (Figure 5.1a), indicating that column setups and ammonium measurement methods were similar in Berkeley and Nairobi.

For real urine, breakthrough was observed in fewer bed volumes with Nairobi urine than Berkeley urine (Figure 5.1b). Because the ammonium measurement methods were not statistically different, the differences between breakthrough curves in Berkeley and Nairobi were attributed to variation in urine composition. The fewer bed volumes to breakthrough observed in Nairobi urine can be explained by higher total ammonia concentrations (see section 3.4.1), which leads to adsorption sites filling faster.<sup>106</sup> Nairobi urine was likely more concentrated due to a less hydrated population and the collection method. Berkeley urine was collected in one day and stored for one month; in Nairobi, each day's urine was added to a larger volume of already hydrolyzed urine. Urease-containing bacteria were likely present at higher concentrations in Nairobi containers due to multiple uses; in addition, urease is not consumed during urea hydrolysis, meaning that hydrolyzed urine contains urease that could rapidly hydrolyze the fresh urine added each day in Nairobi.

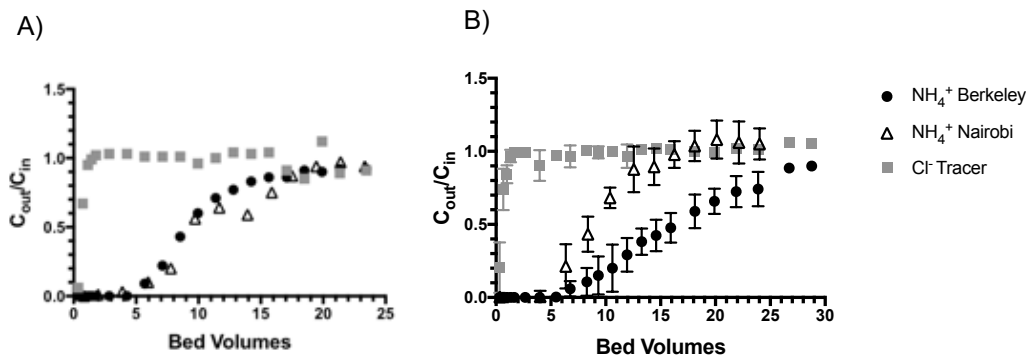


Figure 5.1 Adsorption breakthrough curves for (a) synthetic urine and (b) real urine in Berkeley and Nairobi. Chloride curves are from Berkeley experiments. Figure a is for one experimental replicate; Figure b reports results from triplicate columns ( $\pm 1$  standard deviation; some error bars too small to see).

### 3.2 Repeated adsorption and regeneration

There was no significant decrease in adsorption density over ten adsorption-elution cycles (Figure 5.2), indicating Dowex Mac 3 resin could be regenerated at least ten times. The average adsorption density for all cycles and columns was 4.02 mmol N/g resin, which was not significantly different from the repeat adsorption density measured in Berkeley of 4.14 mmol N/g resin (calculated from Berkeley  $\text{NH}_4^+$  curve in Figure 1b). During cycle 6, flow through all columns slowed to below 1 mL/min, likely due to a pressure increase from resin swelling.<sup>69</sup> To restore flow, approximately 12 g resin was removed from each column; resin mass was adjusted in adsorption density calculations for subsequent cycles. Given its exceptionally low flow rate, cycle 6 was not included in average adsorption density calculations. With the exception of cycles 5 and 6, all experiments reached greater than 90% breakthrough ( $C_{\text{out}}/C_{\text{in}} > 0.9$ ). The majority of regeneration efficiencies were above 90%, indicating successful elution of ammonium from the resin to create ammonium sulfate (Figure D1). Lower regeneration efficiencies (e.g., cycles 1, 6, 7) were not significantly different than the mean for all other cycles and were more likely a result of measurement error than residual ammonium. If ammonium remained after a given regeneration experiment, we would expect a decrease in the next adsorption cycle, but this phenomenon was not observed (Figure 5.2).

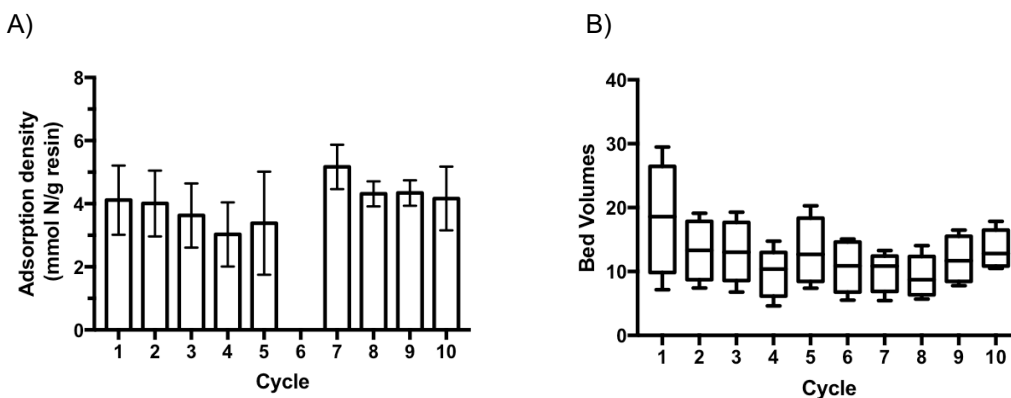


Figure 5.2 a) Average adsorption density vs. cycle for triplicate columns. Error bars indicate +/- standard deviation. (b) Average number of bed volumes for 10%, 25%, 50%, 75%, and 90% breakthrough for each cycle.

### 3.3 Scalability

Nitrogen recovery via ion exchange could be implemented at individual toilets, a centralized collection center, or at semi-centralized transfer centers. This modularity makes ion exchange an attractive option for container-based sanitation services. The average Sanergy toilet collects 6.4 L of urine per day (Equation D4), very close to the lab-scale flowrate (6.5 L/d) in this investigation. The adsorption-elution process was also performed at a scale ten times larger (flow rate and resin mass) to mimic conditions relevant for a transfer or collection center. The adsorption density (4.21 mmol N/g resin) and regeneration efficiency (110%) for columns scaled up by a factor of ten were not significantly different from those observed at small scale (4.02

mmol N/g resin; 99% regeneration efficiency), indicating similar performance at both scales. Adsorption densities at both scales were within 5% of predicted adsorption density based on a three-solute Jain-Snoeyink isotherm (4.20 mmol N/g resin, Equations D5-D10),<sup>98</sup> which was interpreted as efficient use of resin in the columns. Sanergy currently collects 5000 liters of urine per day, which could be treated by 50 parallel columns that each treat 100 L/d. A smaller number of larger-volume columns could also be used. Results from experiments at different scales inform implementation tradeoffs such as column dimensions, number of columns, and degree of centralization that can be evaluated in future research.

### 3.4 Implementation considerations

#### 3.4.1 Urine composition

Urine can vary in salt concentrations, pH, and color. To determine the effects of urine variation on implementation of nitrogen recovery, we compared urine composition in several Sanergy toilets, throughout the Sanergy collection system (collection containers and depot storage tanks), and in three unique collection schemes (Nairobi, Dubendorf, Berkeley).

Table 5.1 Characteristics of urine in individual toilets, \*Ammonium sample number, n = 7 not 8. All measured on IC in Berkeley.

Urine Source	Chloride mg/L Cl	Phosphorus mg P/L	Sulfate mg SO <sub>4</sub> /L	Sodium mg Na/L	Ammonium* mg N/L	Potassium mg K/L
KR 16	4660	1270	1420	3320	7040	2750
VW 72	3950	1100	1300	2660	5480	2130
KB38	4360	1480	1740	3760	n.a.	3430
KR94	3320	1210	1430	2670	6560	1840
KR21	5460	971	1380	3890	6260	2480
VW64	6670	1130	1440	4140	6110	2710
KM39	4880	1110	1600	3070	7890	2610
MK15	5470	1050	1370	3980	6600	2850
<b>Mean (SEM, n=8)</b>	<b>4840 (366)</b>	<b>1170 (55.2)</b>	<b>1460 (50.4)</b>	<b>3440 (209)</b>	<b>6560(287)</b>	<b>2600 (169)</b>

Table 5.2 provides an overview of the ionic composition of urine from eight individual FLTs (containers were labeled KR16, VW72, KB38, KR94, KR21, VW64, KM39, MK15). The containers were sampled on the day of collection (<24 hours storage). The average pH was 9.00 ± 0.06. The average total ammonia concentration was 6560 mg/L NH<sub>4</sub>-N (range of 5480-7888 mg/L NH<sub>4</sub>-N, SEM=287) and average phosphate was 1170 mg/L PO<sub>4</sub>-P (range of 971-1480 mg/L PO<sub>4</sub>-P, SEM=55.2). The high ammonium concentrations indicated that most of the urea present in the freshly excreted urine was hydrolyzed by bacteria to NH<sub>3</sub>/NH<sub>4</sub><sup>+</sup> in the approximately 24 hours between urine collections. Rapid hydrolysis of urea to ammonia is likely due to the presence of urease from bacteria in urine (commonly 5 x 10<sup>8</sup> cells/mL)<sup>31</sup> and from fecal cross-contamination.<sup>151</sup> Total ammonia measurements by Hach methods and ion

chromatography conducted on FLT samples showed less than 10% variation (data not shown), further validating Hach field methods. Average chloride, sodium and potassium concentrations had a larger variation than phosphate, sulfate and ammonium. Measured ion concentrations were similar to those reported in previous studies.<sup>23</sup>

Urine composition was also compared between individual toilets (average of the eight toilets reported above) and the large collection tanks at the current centralized urine depot. TAN, COD, electrical conductivity, and pH were higher at individual toilets than collection tanks; the same parameters were higher for closed tanks than those left open (Figure 5.3). These trends primarily result from volatilization of NH<sub>3</sub>, carbon dioxide (CO<sub>2</sub>), and volatile organic compounds, which are common problems that alter urine composition and cause odor in urine collection systems (see Section D1.4, Equations D11-12).<sup>152</sup> pH is expected to decrease due to NH<sub>3</sub>, a base, leaving the aqueous phase. Electrical conductivity decreases were likely due to CO<sub>2</sub> volatilization, which decrease electrical conductivity by two moles for every mole CO<sub>2</sub> volatilized (Equation D12). COD likely decreased due to volatilization of CO<sub>2</sub> and organic compounds (e.g., trimethylamine),<sup>153</sup> as well as microbial assimilation and metabolism. The difference in TAN, COD, pH, and EC between toilets and closed tanks was smaller than the difference between closed and open tanks. Urine storage is usually required for urea hydrolysis; however, high total ammonia concentrations in individual toilet samples indicate that the majority of urea was hydrolyzed in the 24-h period between container collections. Residual biofilms may form in containers or on squat plates, including bacteria that contain urease and hydrolyze urea quickly. Urine containers for each toilet are washed with soap and water before reuse; however, 1,000-L urine storage tanks are not washed and thus foster growth of biofilms and bacteria in sediments.

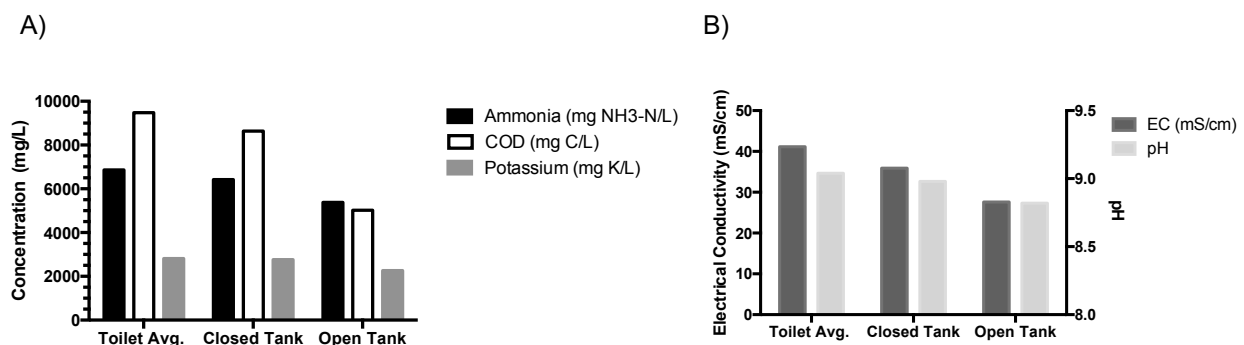


Figure 5.3 Comparison of urine composition from average of individual toilets, closed storage tank, and open storage tank.

These compositional differences in urine within the Sanergy collection system are important to consider for the ion exchange process because loss of ammonia translates to a loss of revenue, which could impact the business model for a fertilizer product. While ammonia is lost in collection and storage, the effect of open storage containers (1,000 L) is larger than the effect of open collection containers (25 L). To reduce ammonia losses, storage containers should remain closed as much as possible at the centralized treatment station.



We compared total ammonia concentrations in urine collected for laboratory experiments in Berkeley, California, USA; urine from waterless urinals and low-flush urine-diverting toilets in Dubendorf, Switzerland; and urine collected in a waterless, container-based system in Nairobi, Kenya (Figure D2). For the samples from Nairobi, closed storage tank values are shown. Nairobi samples were more concentrated than urine from Berkeley and Dubendorf. Dilution by flush water is one reason for the lower concentrations observed in Dubendorf; incomplete urea hydrolysis may explain those in Berkeley. Samples taken later from stored Berkeley urine showed higher concentrations (7000 mg N/L vs. 4000 mg N/L), further supporting incomplete urea hydrolysis as the source of lower ammonium concentrations. Urine composition data are useful for predicting adsorption density and breakthrough times for planning ion exchange columns in different regions and urine collection systems.

#### *3.4.2 Process indicators*

Measuring ammonia can be time-consuming and requires laboratory equipment and expertise. Process indicators that might be easier or less expensive to measure, including electrical conductivity, pH, and absorbance (color), were also explored. These benefits may be especially significant in decentralized recovery schemes and resource-constrained communities. In particular, the current approach to creating breakthrough curves requires measuring total ammonia nitrogen for several regularly spaced samples; on-line monitoring of a process indicator could provide a more robust, automated solution.

Color and electrical conductivity differ between stored urine and pretreatment solution (1 M borate buffer), making them potentially useful indicator parameters. Effluent absorbance at 585 nm was a useful indicator for urine because stored urine was brown while the borate buffer used to pre-treat the columns was clear. In three different adsorption experiments, absorbance increased around one bed volume (Figure 5.4a). Thus, measuring absorbance is an alternative to measuring chloride as a conservative tracer in cation exchange columns. Effluent electrical conductivity was a better indicator for ammonium breakthrough (Figure 5.4b). Electrical conductivity showed two increases: the first around one bed volume, and the second mirrored ammonium breakthrough. The first increase was due to constituents in urine, which was more conductive than pretreatment solution. Because ammonium was retained on the resin, this effluent had a slightly lower electrical conductivity than influent synthetic urine; the second increase accounts for the difference once the resin was exhausted. pH was not indicative of ammonium breakthrough because the pretreatment solution had a similar pH to synthetic urine (both 8.5-9, Figure D3). Based on these results, we concluded that effluent absorbance at 585 nm was a conservative tracer for urine and electrical conductivity could be measured to monitor ammonium breakthrough.

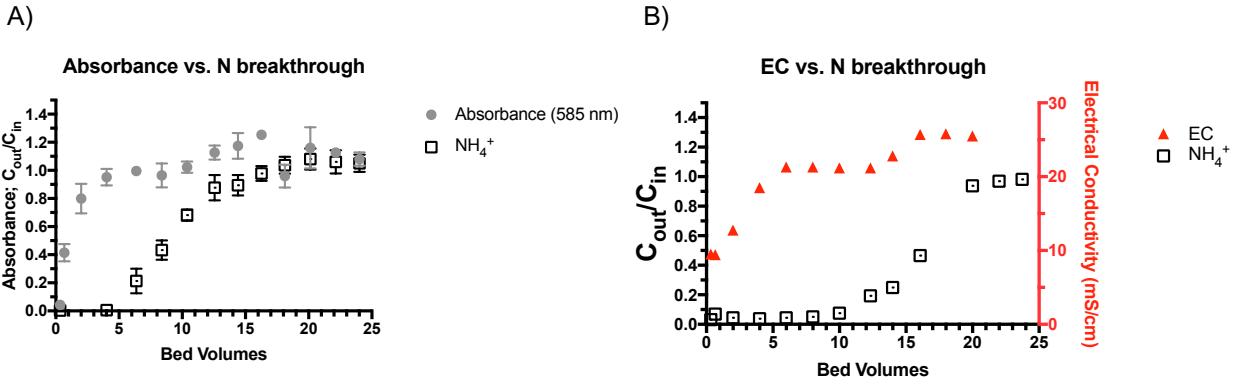


Figure 5.4 (a) Absorbance at 585 nm and (b) electrical conductivity vs. ammonium breakthrough curves. Error bars indicate one standard deviation above and below for figure A; some error bars are too small to be shown. For Figure 4b, only one replicate measured and shown.

### 3.5 Business Model Evaluation

Three potential value propositions exist for recovering nitrogen from urine with Sanergy: (1) reducing urine exhaustion volume and cost, (2) supplementing solid organic fertilizer with nitrogen, and (3) creating a separate nitrogen fertilizer product.

Resin and regenerant are the primary contributors to cost for the ion exchange process because they require continuous, long-distance supply chains. Other elements, including plastic housing and pumping, are available locally and are inexpensive by comparison. Transporting urine from toilets to a treatment facility also affects cost; however, daily collection of urine and feces containers already occurs in the Sanergy business model. While resin costs are constant whether ion exchange occurs at individual toilets or the transfer station, collecting nitrogen in a concentrated form (on resin) reduces transport costs compared to collecting untreated urine from each toilet because of the high water content (96%<sup>29</sup>) of urine.

In principle, removing nitrogen and phosphorus from urine could replace trucking urine to wastewater treatment plants with discharge to water bodies or leaching to soil. Costs of urine exhaustion, ion exchange, and fertilizer are shown in Figure 5.5.

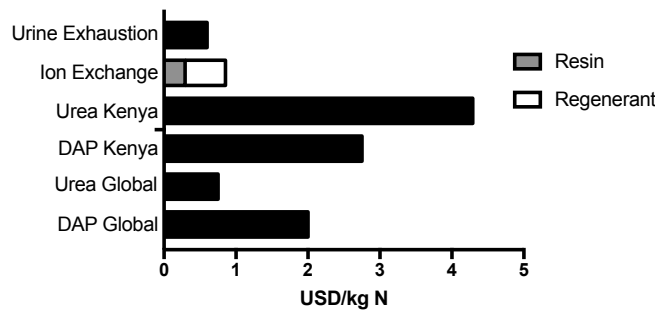


Figure 5.5 Costs (USD/kg N) for urine exhaustion to wastewater treatment plant, ion exchange (resin and regenerant costs), and nitrogen fertilizer prices (in Kenya and globally).

Urine exhaustion currently costs 450 KES/m<sup>3</sup> (~4.45 USD/m<sup>3</sup> or 0.60 USD/kg N, Equation D16). Dowex Mac 3 resin costs decrease with number of uses from 22 (10 uses) to 2.20 USD/m<sup>3</sup> urine (100 uses, Equation D14). Constant performance was observed for ten adsorption-regeneration cycles (see section 3.2) and calculated for 100 cycles for comparison; the resin has not yet been validated for 100 cycles. Sulfuric acid for regeneration costs an additional 4.20 USD/m<sup>3</sup> urine (Equation D15); thus, Dowex Mac 3 resin and regeneration costs total 6.40 USD/m<sup>3</sup> urine (0.85 USD/kg N). Based on the cost of urine exhaustion alone, ion exchange is the same order of magnitude but not yet competitive with urine exhaustion when both resin and regeneration costs are included. Other regenerants (such as NaCl) could improve the cost effectiveness of ion exchange. Loading urine containers at individual toilets with ion exchange resin and leaching the effluent could reduce collection frequency and thus collection costs, which are 30% of Sanergy's expenditures.

Ammonium sulfate produced from urine could be sold as a liquid fertilizer or added to solid fertilizer to make a premium Evergrow product. The additional revenue generated from selling fertilizer could make nitrogen recovery from urine profitable. While demand for organic fertilizers in Kenya is high (\$178 million, growing at 7% annually), supply is low because domestic production is minimal.<sup>142</sup> Urine-derived fertilizers are locally produced, avoiding large import transport costs that contribute as much as 40% markup for conventional fertilizers.<sup>143</sup> Producing ammonium sulfate from urine (\$0.85/kg N for Dowex Mac 3, 100 uses) is less expensive than government-subsidized prices for commercial fertilizers like diammonium phosphate (\$2.75/kg N, see Section D1.7) and urea (\$4.29/kg N, see Section D1.4). Resin and regenerant costs are lower than the global price of DAP but 13% higher than global urea prices (Figure 5, Section D1.7). Note that the costs of transporting urine from toilets was not included in these cost estimates, as this activity is already part of Sanergy's operations; however, it would need to be included for settings without existing excreta collection.

Other costs to consider for nitrogen recovery include facility space for regeneration and fertilizer production, as well as transport of ammonium sulfate to farmers. Partnerships with farm supply distributors could facilitate introduction of urine-derived fertilizers into existing distribution channels. Several sub-Saharan African countries have higher fertilizer prices than Kenya (e.g., landlocked countries with higher transportation markups),<sup>142</sup> indicating even higher potential margins for urine-derived fertilizers. The volatility of synthetic fertilizer prices and their intermittent supply could make urine-derived fertilizers even more cost competitive. Fertigation may be a potential market segment for ammonium sulfate produced from urine because liquid fertilizers are easily incorporated into irrigation systems. Combining the value propositions of treating urine to meet discharge limits and produce fertilizer could improve the profitability for nitrogen recovery via ion exchange. Other high-value products, including industrial inputs (e.g.,

$\text{NH}_4\text{Cl}$ ,  $\text{NH}_4\text{OH}$ , microbially produced proteins<sup>154</sup>), could also be extracted from urine to improve financial viability.

### **3.6 Anaerobic digester effluent**

Anaerobic digester effluent (digestate) is another underexploited waste stream from which ammonium could be recovered. Separately collected feces could be fed into an anaerobic digester, which produces an ammonia-rich liquid effluent (Table 1). In addition to producing ammonium sulfate fertilizer, removing ammonium from digestate reduces ammonium inhibition during microbial digestion of feces.<sup>122</sup> Similar to urine, the anaerobic digester effluent would need to be disposed of or treated before discharge. Recovering nitrogen from digestate could generate fertilizer products and reduce costs of digestate exhaustion. Ion exchange could be used to recover ammonium from digestate at various scales. In digestate, later breakthrough (~10 bed volumes) and a 25% lower adsorption density than urine were observed. The lower ammonium concentration in digestate compared to urine explains both later breakthrough and lower adsorption density. The slopes of normalized breakthrough curves in digestate and urine only differed by 2.5% (Figure D4), indicating that longer run times or more resin would result in similar performance for digestate and urine.

## **4. CONCLUSIONS**

In this study we evaluated the technical and financial feasibility of producing ammonium sulfate from urine using ion exchange. Ammonium breakthrough curves were reliably measured in Nairobi with Hach methods as an alternative to ion chromatography. Ten adsorption-regeneration cycles were performed without a decrease in performance, indicating Dowex Mac 3 could be used at least ten times before replacement. Adsorption density and regeneration efficiency were maintained at 65 L/d, a ten times larger setup than the 6.5 L/d representative of individual toilets. Based on urine composition, some nitrogen as ammonia was lost during the collection process; keeping storage tanks closed can reduce associated revenue losses. For implementation, process indicators such as effluent absorbance and electrical conductivity can be easily and cheaply measured. Based on resin and regenerant costs, ion exchange is not currently cost-competitive with current urine exhaustion, but is less expensive than commercial fertilizers in Nairobi. Future work includes evaluation and optimization of ion exchange for additional scales, geographical settings, and sanitation service provision schemes.

## **CHAPTER 6. Conclusion**

The overall goal of this dissertation was to design and evaluate two unit processes for recovering nitrogen from urine: ion exchange and electrochemical stripping. For each approach, we demonstrated high nitrogen recovery efficiency, determined the effect of urine parameters on recovery efficiency, and evaluated real-world parameters such as energy demand and cost.

In Chapters 2 and 3, ion exchange was characterized by comparing four adsorbents in batch studies and evaluating the effects of continuous-flow operating parameters on nitrogen recovery. Adsorbents were characterized in terms of adsorption models, adsorption densities, regeneration efficiencies, and treatment costs. Chapter 4 detailed the novel electrochemical stripping process by comparing real and synthetic urine solutions. Chlorine production was identified as a major reaction that could consume ammonia through chloramine production. Chapter 5 described the application of ion exchange in a container-based sanitation system in Nairobi, Kenya, which produced fertilizer at lower cost than commercially available fertilizers. This conclusion chapter summarizes key results and offers future research opportunities.

### **6.1 ION EXCHANGE**

#### **6.1.1 Main Findings**

Comparison of four cation exchange adsorbents (clinoptilolite, biochar, Dowex 50, and Dowex Mac 3) showed that Dowex Mac 3 had the highest adsorption density and regeneration efficiency. Based on calculated adsorption densities, Dowex Mac 3 also required the smallest volume to capture nitrogen for one week from a four-person household. Although Dowex Mac 3 had the highest adsorption capacity, material costs (\$/g N removed) were lower for clinoptilolite and biochar because of their substantially lower unit cost. The low regeneration efficiency and cost of natural adsorbents makes them suitable for application directly as fertilizer once loaded with ammonium, assuming pathogen concerns are addressed. Alternatively, a concentrated ammonium solution can be produced by eluting ammonium from synthetic cation exchange resins with sulfuric acid. Competition from sodium and potassium present in real urine did not significantly decrease ammonium adsorption. Several models for predicting adsorption density based on real urine composition, with the three-solute Jain-Snoeyink model showing the lowest error between measured and modeled results.

The effects of operating parameters on adsorption and regeneration with Dowex Mac 3 were further evaluated. Higher influent concentration led to earlier breakthrough but did not significantly affect adsorption kinetics (as measured by breakthrough curve slope); changing flow rate did not affect kinetics nor time to breakthrough. During regeneration, regenerant concentration had a larger effect on amount of acid used and bed volumes required for elution

than did flow rate. Ammonium sulfate was produced at 22 g/L, or 25% of commonly available fertilizer concentrations. Intraparticle diffusion was determined to be the rate-limiting step of cation exchange through intermittent operation. Columns operated with intermittent flow exhibited statistically similar adsorption density as continuous operation. Nitrogen and phosphorus were simultaneously recovered from urine through combinations of either struvite or anion exchange resin with cation exchange resin; the different treatment trains did not significantly affect ammonium adsorption kinetics. Based on regeneration results, separate columns for nitrogen and phosphorus recovery are most promising. Of four regenerants tested on Dowex Mac 3, acidic solutions all showed >99% recovery efficiency, NaCl was 77%. Of ten pharmaceuticals measured during adsorption and regeneration, only atenolol and metoprolol were measured in the ammonium sulfate product, both at <0.1 ng L<sup>-1</sup>.

### 6.1.2 Future Research

While effects of pH and cation competitors (e.g., Na<sup>+</sup>, K<sup>+</sup>) on nitrogen recovery via cation exchange were determined, the effect of organics in urine on adsorption would benefit from further study. Preliminary results indicated that organic compounds such as acetate may decrease surface tension and increase accessibility to previously inaccessible adsorption sites; conversely, other organic compounds present in real urine may compete with ammonium for negatively charged sites. The effects of these compounds on phosphorus recovery has also not yet been determined, and could play a role in full treatment trains for nutrient recovery from urine. The fate of trace organic compounds could also be better characterized through non-target analysis to supplement the targeted analysis of the ten pharmaceuticals studied in this dissertation.

In terms of practical implementation, several key questions remain. Regeneration of anion exchange resins and mixed bed columns in continuous-flow could be optimized. Evaluation of ion exchange at different scales of implementation is also necessary for determining optimal scale. Ion exchange adsorbents could be employed in on-site or centralized wastewater treatment. A decentralized scheme might involve a service provider that regularly collects and replaces household cartridges and transports them to a centralized regeneration facility. Alternatively, cation exchange adsorbents could be used and regenerated on-site at a central facility to which source-separated urine is transported (by manual transport, such as in high-density slums, or via dedicated pipes in a large buildings and neighborhoods). While this optimization will be context-specific, benefits such as energy savings and cost reduction need to be expressly quantified for implemented systems. Additional post-treatment, such as pharmaceutical removal from the eluent or eluate, or converting liquid fertilizer to solid, may be desirable and will affect process costs. Characterizing and potentially accelerating urea hydrolysis in urine collection systems is a necessary pretreatment step for recovering nitrogen as ammonium. Practical challenges, including toilet maintenance, designing automated flushing and pumping systems, and monitoring columns for ammonium breakthrough will be need to be solved. Because source

separation has not yet been widely adopted, resource recovery technologies like ion exchange can potentially influence the design and scale of source separation systems.

Beyond urine, ion exchange has been characterized in drinking water and wastewater for nitrogen removal. The three-solute Jain-Snoeyink model could be used to predict adsorption density based on waste stream composition, which could be particularly useful for investigating other nitrogen-rich waste streams (e.g., digestate, piggery slurry) as targets of nitrogen recovery via ion exchange. As new adsorbents are identified, the process modeling conducted in this dissertation can be used to specify adsorption capacities and regeneration lifetimes required for newly developed adsorbents to be cost effective for nitrogen recovery from urine.

## **6.2 ELECTROCHEMICAL STRIPPING**

### **6.2.1 Main Findings**

Electrochemical stripping was established as a novel unit process for recovering nitrogen from urine based on charge ( $\text{NH}_4^+$ ) and volatility ( $\text{NH}_3$ ) using electricity, a cation exchange membrane, and a gas permeable membrane. Nitrogen was selectively recovered compared to competitor cations in urine (e.g.  $\text{Na}^+$ ,  $\text{K}^+$ ) in batch and continuous setups. Chlorine production was identified as a predominant electrolytic reaction that can lower nitrogen recovery efficiency through chloramination, especially if organics such as phenol are not present to quench chlorine. Although urine contains several trace organic contaminants, ammonium sulfate produced by electrochemical stripping did not contain measurable concentrations of trace organics nor metals measured in this study. Trace organic contaminants were generally limited to the anode, where they were oxidized directly by electrolysis or indirectly by chlorine; the extent to which these reactions occurred varied with the prevalence of electron-rich functional groups. Unoptimized electrochemical stripping from real urine required 30.6 MJ/kg N, which is less than conventional ammonia stripping but more than nitrification-denitrification.

### **6.2.2 Future Work**

Based on the finding that nitrogen flux across the cation exchange membrane was 70% higher than flux across the gas permeable membrane, a transport or transformation process between the two membranes is the rate-limiting step of the electrochemical stripping process and a high priority for future work to accelerate nitrogen recovery from urine. In future work, the rate-limiting step could be more explicitly identified among cathodic hydroxide production, volatilization of ammonia, or transport of volatile ammonia through the gas permeable membrane. At the process level, mitigation options and process models based on the slowest step could be proposed to optimize nitrogen recovery while minimizing process inputs (e.g. cost, energy).

Nitrogen recovery could also be maximized through optimization of operating parameters, such as hydraulic residence time and operating potential. These parameters have been demonstrated to affect trace organic and metal removal, which in particular affects the quality of the effluent urine and catholyte produced from electrochemical stripping. While disinfection byproducts were not studied in this dissertation, future work could lead to their characterization in the ammonium sulfate product and effluents produced from treating urine with electrochemical stripping. Similarly, the fate of pathogens needs to be understood; inactivation in bulk solutions may occur due to extreme pH values (2 in anode, 11 in cathode, 1 in trap), whereas pathogens sorbed to the cation exchange membrane could be released during cleaning. Membrane fouling is also another area of research to consider before long-term implementation.

In addition to nitrogen, potassium could also be recovered by electrochemical stripping. Potassium was effectively recovered in the cathode chamber. Recovering potassium and ammonium separately, along with phosphorus recovery before electrochemical stripping, could allow for production of urine-derived fertilizers with customized macronutrient ratios.

Beyond the molecular and process scales, electrochemical stripping should also be evaluated in real-world settings, including centralized wastewater treatment and decentralized urine collection in unsewered communities. Like ion exchange, the electrochemical stripping process could also be applied to liquid streams with high nitrogen concentrations, such as sidestream treatment at wastewater treatment plants.

## **6.3 NITROGEN RECOVERY AND DEVELOPMENT ENGINEERING**

### **6.3.1 Main Findings**

Ion exchange was demonstrated to efficiently recover nitrogen from urine and up-concentrate it to ammonium sulfate fertilizer in a dry toilet system in Nairobi, Kenya. Adsorption density and regeneration efficiency of Dowex Mac 3 resin did not decrease during ten adsorption-regeneration cycles, the longest-term performance studied yet. In the container-based collection system studied, total ammonia concentrations decreased during storage more than during collection, suggesting that keeping storage tanks closed could prevent losses in ammonium and associated revenues. Given the limited resources available for increasing sanitation access in Nairobi, on-line parameters that were cheaper and easier to measure than ammonium concentration were investigated, which could decrease the overall cost of implementing ion exchange. Effluent absorbance was an indicator of urine breakthrough and electrical conductivity could be used to predict column saturation with ammonium. Urine-derived fertilizers produced by ion exchange were produced below market costs of synthetic fertilizers, but were more expensive than trucking urine to municipal waste treatment facilities.



### 6.3.2 Future Work

Treatment systems ten times larger than lab scale (65 L/d vs. 6.5 L/d) were constructed from locally available materials in Nairobi, and performed similarly to lab scale columns. Future work includes evaluation of ion exchange at additional scales and further optimization to reduce costs. Based on previous work estimating cost, greenhouse gas emissions, and energy required for household ion exchange in sewered settings,<sup>48</sup> similar metrics could be calculated for container-based systems such as the one studied outside of Nairobi. Comparing results for different contexts, including public vs. private sanitation service providers, will help determine the major contributors to each metric and ultimately future research or implementation priorities with considerable impact. The ion exchange system could be optimized further to reduce costs.

Business models for settings like Nairobi are already being developed for nitrogen recovery from urine. For example, a major value proposition is locally-produced fertilizer that avoids transportation and import costs associated with imported fertilizers. Market studies with potential customers are a logical next step toward implementation in developing communities. Similar to many development engineering approaches, lessons learned in resource-constrained settings can be applied to industrialized settings. Studying resource recovery from urine in a large-scale sanitation system in Nairobi with Sanergy provides key lessons for designing a pilot scale system in the U.S. For example, pilot-scale implementation allows for observation of long-term performance, maintenance issues, and user concerns such as odor.

## 6.4 CHARACTERIZING SOURCE SEPARATION AND RESOURCE RECOVERY

This dissertation has been focused primarily on nitrogen recovery from urine. While novel processes have been developed to optimize nitrogen recovery, urine also contains other nutrients (e.g., phosphorus, potassium) and contaminants, such as trace organic compounds and pathogens. The ammonium recovery processes in this research could be combined with unit processes for recovering phosphorus and potassium to separately recover macronutrients and then combine them for tailored fertilizer production from urine.

In terms of contaminants, urine has been reported to contain potentially pathogenic viruses (rotavirus, norovirus) and bacteria (*Clostridium perfringens*, *Shigella spp.*) due to cross-contamination from feces.<sup>30</sup> Trace organics are also common in urine because 67% of pharmaceuticals are excreted in urine.<sup>128</sup> Any urine-derived product should have acceptably low concentrations of trace organics and pathogens. In addition to targeted studies of key compounds known to occur in urine, non-target analysis can be used to identify more compounds and their fate during urine treatment by ion exchange. Determining the fate of pathogens and trace organics in nitrogen recovery process technologies is a vital step toward evaluation and potential implementation of urine separation and resource recovery from urine. Results from this work can

be used to determine what classes of trace organic contaminants and pathogens still need to be removed after ion exchange and electrochemical stripping, allowing for comparison with other nitrogen recovery technologies. They will also inform monitoring practices because steps with high contaminant concentrations can be optimal locations for on-line sensing.

The major contribution of this dissertation is characterizing nitrogen recovery from urine at molecular, process, and system scales. Simultaneous research at all three scales is necessary to better characterize the source separation and resource recovery paradigm. Understanding the benefits of recovering nitrogen from urine, including reduced treatment cost and energy, allows for further research and preliminary implementation of treatment technologies. Molecular-scale investigations have been used to characterize mechanisms of nitrogen transport and transformation during ion exchange and electrochemical stripping. Process engineering has been performed to further develop two unit processes for recovering nitrogen from urine, and can be applied to other nitrogen-rich waste streams (e.g., anaerobic digestate) and improved with novel materials (e.g., membranes, resins). Systems-level questions have been researched through business models in Nairobi, Kenya, and life-cycle assessment of decentralized nitrogen recovery compared to existing nitrogen management processes. Connecting findings from systems, process, and molecular scales will lead to informed implementation and more fundamental, mechanistic questions that can improve process efficiencies and elucidate the fate of non-target species, such as pathogens and organic contaminants. Urine separation is a promising alternative to conventional waste management that has the potential to create valuable products through targeted resource recovery. Although it may not displace existing fertilizer production and nitrogen removal processes globally, there may be scales and regions for which the benefits of urine separation and resource recovery are especially significant. Separately collecting and treating urine should be considered among the suite of 21<sup>st</sup> century approaches for sustainability managing wastewater.

## **REFERENCES**

- (1) Stillwell, A. S.; Hoppock, D. C.; Webber, M. E. Energy Recovery from Wastewater Treatment Plants in the United States: A Case Study of the Energy-Water Nexus. *Sustainability* **2010**, *2* (4), 945–962.
- (2) Rodriguez, C.; Van Buynder, P.; Lugg, R.; Blair, P.; Devine, B.; Cook, A.; Weinstein, P. Indirect Potable Reuse: A Sustainable Water Supply Alternative. *Int. J. Environ. Res. Public Health* **2009**, *6* (3), 1174–1203.
- (3) Le Corre, K. S.; Valsami-Jones, E.; Hobbs, P.; Parsons, S. A. Phosphorus recovery from wastewater by struvite crystallization: A review. *Crit. Rev. Environ. Sci. Technol.* **2009**, *39* (6), 433–477.
- (4) Heimersson, S.; Svanström, M.; Laera, G.; Peters, G. Life cycle inventory practices for major nitrogen, phosphorus and carbon flows in wastewater and sludge management systems. *Int. J. Life Cycle Assess.* **2016**, *21* (8), 1197–1212.
- (5) Westerhoff, P.; Lee, S.; Yang, Y.; Gordon, G. W.; Hristovski, K.; Halden, R. U.; Herckes, P. Characterization, Recovery Opportunities, and Valuation of Metals in Municipal Sludges from U.S. Wastewater Treatment Plants Nationwide. *Environ. Sci. Technol.* **2015**, *49* (16), 9479–9488.
- (6) Shen, Y.; Linville, J. L.; Urgun-Demirtas, M.; Mintz, M. M.; Snyder, S. W. An overview of biogas production and utilization at full-scale wastewater treatment plants (WWTPs) in the United States: Challenges and opportunities towards energy-neutral WWTPs. *Renew. Sustain. Energy Rev.* **2015**, *50*, 346–362.
- (7) Bellona, C.; Drewes, J. E. Viability of a low-pressure nanofilter in treating recycled water for water reuse applications: A pilot-scale study. *Water Res.* **2007**, *41* (17), 3948–3958.
- (8) Leverenz, H. L.; Tchobanoglous, G.; Asano, T. Direct potable reuse: a future imperative. *J. Water Reuse Desalination* **2011**, *1* (1), 2–10.
- (9) Dodds, W. K.; Bouska, W. W.; Eitzmann, J. L.; Pilger, T. J.; Pitts, K. L.; Riley, A. J.; Schloesser, J. T.; Thornbrugh, D. J. Eutrophication of U.S. Freshwaters: Analysis of Potential Economic Damages. *Environ. Sci. Technol.* **2009**, *43* (1), 12–19.
- (10) Baum, R.; Luh, J.; Bartram, J. Sanitation: A Global Estimate of Sewerage Connections without Treatment and the Resulting Impact on MDG Progress. *Environ. Sci. Technol.* **2013**, *47* (4), 1994–2000.
- (11) Ma, X. (Cissy); Xue, X.; González-Mejía, A.; Garland, J.; Cashdollar, J. Sustainable Water Systems for the City of Tomorrow—A Conceptual Framework. *Sustainability* **2015**, *7* (9), 12071–12105.
- (12) Tervahauta, T.; Hoang, T.; Hernández, L.; Zeeman, G.; Buisman, C. Prospects of Source-Separation-Based Sanitation Concepts: A Model-Based Study. *Water* **2013**, *5* (3), 1006–1035.
- (13) Wood, A.; Blackhurst, M.; Hawkins, T.; Xue, X.; Ashbolt, N.; Garland, J. Cost-effectiveness of nitrogen mitigation by alternative household wastewater management technologies. *J. Environ. Manage.* **2015**, *150*, 344–354.
- (14) Friedler, E.; Butler, D.; Alfiya, Y. Wastewater Composition. In *Source Separation and Decentralization for Wastewater Management*; IWA Publishing: London, 2013; pp 241–257.
- (15) Larsen, T. A.; Hoffmann, S.; Lüthi, C.; Truffer, B.; Maurer, M. Emerging solutions to the water challenges of an urbanizing world. *Science* **2016**, *352* (6288), 928–933.

- (16) Jonsson, H.; Baky, A. *Composition of urine, faeces, greywater and biowaste for utilisation in the URWARE model*; 2005:6; The Mistra Programme Urban Water.
- (17) O’Keefe, M.; Lüthi, C.; Tumwebaze, I. K.; Tobias, R. Opportunities and limits to market-driven sanitation services: evidence from urban informal settlements in East Africa. *Environ. Urban.* **2015**, *27* (2), 421–440.
- (18) Dodane, P.-H.; Mbeguere, M.; Sow, O.; Strande, L. Capital and Operating Costs of Full-Scale Fecal Sludge Management and Wastewater Treatment Systems in Dakar, Senegal. *Environ. Sci. Technol.* **2012**, *46* (7), 3705–3711.
- (19) Foote, A. M.; Woods, E.; Fredes, F.; Leon, J. S. Rendering fecal waste safe for reuse via a cost-effective solar concentrator. *J. Water Sanit. Hyg. Dev.* **2017**, washdev2017112.
- (20) Muspratt, A. M.; Nakato, T.; Niwagaba, C.; Dione, H.; Kang, J.; Stupin, L.; Regulinski, J.; Mbéguéré, M.; Strande, L. Fuel potential of faecal sludge: calorific value results from Uganda, Ghana and Senegal. *J. Water Sanit. Hyg. Dev.* **2014**, *4* (2), 223–230.
- (21) Udert, K. M.; Larsen, T. A.; Gujer, W. Biologically induced precipitation in urine-collecting systems. *Water Sci. Technol. Water Supply* **2003**, *3* (3), 71–78.
- (22) Udert, K. M.; Larsen, T. A.; Biebow, M.; Gujer, W. Urea hydrolysis and precipitation dynamics in a urine-collecting system. *Water Res.* **2003**, *37* (11), 2571–2582.
- (23) Udert, K.; Larsen, T.; Gujer, W. Fate of major compounds in source-separated urine. *Water Sci. Technol.* **2006**, *54* (11–12), 413–420.
- (24) Bond, T.; Roma, E.; Foxon, K. M.; Templeton, M. R.; Buckley, C. A. Ancient water and sanitation systems - applicability for the contemporary urban developing world. *Water Sci. Technol. J. Int. Assoc. Water Pollut. Res.* **2013**, *67* (5), 935–941.
- (25) Guzha, E.; Nhapi, I.; Rockstrom, J. An assessment of the effect of human faeces and urine on maize production and water productivity. *Phys. Chem. Earth* **2005**, *30*, 840–845.
- (26) Pradhan, S. K.; Nerg, A.-M.; Sjöblom, A.; Holopainen, J. K.; Heinonen-Tanski, H. Use of Human Urine Fertilizer in Cultivation of Cabbage (*Brassica oleracea*)—Impacts on Chemical, Microbial, and Flavor Quality. *J. Agric. Food Chem.* **2007**, *55* (21), 8657–8663.
- (27) Berndtsson, J. C. Experiences from the implementation of a urine separation system: Goals, planning, reality. *Build. Environ.* **2006**, *41* (4), 427–437.
- (28) Rossi, L.; Lienert, J.; Larsen, T. A. Real-life efficiency of urine source separation. *J. Environ. Manage.* **2009**, *90* (5), 1909–1917.
- (29) Drangert, J.-O. Urine blindness and the use of nutrients from human excreta in urban agriculture. *GeoJournal* **1998**, *45* (3), 201–208.
- (30) Bischel, H. N.; Özel Duygan, B. D.; Strande, L.; McArdell, C. S.; Udert, K. M.; Kohn, T. Pathogens and pharmaceuticals in source-separated urine in eThekweni, South Africa. *Water Res.* **2015**, *85*, 57–65.
- (31) Lahr, R. H.; Goetsch, H. E.; Haig, S. J.; Noe-Hays, A.; Love, N. G.; Aga, D. S.; Bott, C. B.; Foxman, B.; Jimenez, J.; Luo, T.; et al. Urine Bacterial Community Convergence through Fertilizer Production: Storage, Pasteurization, and Struvite Precipitation. *Environ. Sci. Technol.* **2016**, *50* (21), 11619–11626.
- (32) Etter, Tilley, E.; Khadka, R.; Udert, K. M. Low-cost struvite production using source-separated urine in Nepal. *Water Res.* **2011**, *45* (2), 852–862.
- (33) O’Neal, J. A.; Boyer, T. H. Phosphate recovery using hybrid anion exchange: Applications to source-separated urine and combined wastewater streams. *Water Res.* **2013**, *47* (14), 5003–5017.

- (34) Blaney, L. M.; Cinar, S.; SenGupta, A. K. Hybrid anion exchanger for trace phosphate removal from water and wastewater. *Water Res.* **2007**, *41* (7), 1603–1613.
- (35) Williams, A. T.; Zitomer, D. H.; Mayer, B. K. Ion exchange-precipitation for nutrient recovery from dilute wastewater. *Environ. Sci. Water Res. Technol.* **2015**, *1* (6), 832–838.
- (36) Maurer, M.; Pronk, W.; Larsen, T. A. Treatment processes for source-separated urine. *Water Res.* **2006**, *40* (17), 3151–3166.
- (37) Udert, K. M.; Wächter, M. Complete nutrient recovery from source-separated urine by nitrification and distillation. *Water Res.* **2012**, *46* (2), 453–464.
- (38) N. Bischel, H.; Schertenleib, A.; Fumasoli, A.; M. Udert, K.; Kohn, T. Inactivation kinetics and mechanisms of viral and bacterial pathogen surrogates during urine nitrification. *Environ. Sci. Water Res. Technol.* **2015**, *1* (1), 65–76.
- (39) Başakçılardan-Kabakci, S.; İpekoğlu, A. N.; Talinli, I. Recovery of Ammonia from Human Urine by Stripping and Absorption. *Environ. Eng. Sci.* **2007**, *24* (5), 615–624.
- (40) Pronk, W.; Biebow, M.; Boller, M. Treatment of source-separated urine by a combination of bipolar electrodialysis and a gas transfer membrane. *Water Sci. Technol. J. Int. Assoc. Water Pollut. Res.* **2006**, *53* (3), 139–146.
- (41) Boncz, M. A. Methods for stabilising and concentrating human urine for use as a fertilizer; Athens, Greece, 2016.
- (42) Randall, D. G.; Krähenbühl, M.; Köpping, I.; Larsen, T. A.; Udert, K. M. A novel approach for stabilizing fresh urine by calcium hydroxide addition. *Water Res.* **2016**, *95*, 361–369.
- (43) Ahn, Y.-H. Sustainable nitrogen elimination biotechnologies: A review. *Process Biochem.* **2006**, *41* (8), 1709–1721.
- (44) Galloway, J. N.; Winiwarer, W.; Leip, A.; Leach, A. M.; Bleeker, A.; Erisman, J. W. Nitrogen footprints: past, present and future. *Environ. Res. Lett.* **2014**, *9* (11), 115003.
- (45) Oakley, S. M.; Gold, A. J.; Oczkowski, A. J. Nitrogen control through decentralized wastewater treatment: Process performance and alternative management strategies. *Ecol. Eng.* **2010**, *36* (11), 1520–1531.
- (46) McCray, J. E.; Kirkland, S. L.; Siegrist, R. L.; Thyne, G. D. Model Parameters for Simulating Fate and Transport of On-Site Wastewater Nutrients. *Ground Water* **2005**, *43* (4), 628–639.
- (47) *Source Separation and Decentralization for Wastewater Management*, 1st ed.; Larsen, T. A., Udert, K. M., Lienert, J., Eds.; IWA Publishing, 2013.
- (48) Kavvada, O.; Tarpeh, W.; Horvath, A.; Nelson, K. L. Life cycle cost and environmental assessment of decentralized nitrogen recovery from source-separated urine through spatial modeling. *Environ. Sci. Technol.* **2017**.
- (49) Galloway, J. N.; Dentener, F. J.; Capone, D. G.; Boyer, E. W.; Howarth, R. W.; Seitzinger, S. P.; Asner, G. P.; Cleveland, C. C.; Green, P. A.; Holland, E. A.; et al. Nitrogen Cycles: Past, Present, and Future. *Biogeochemistry* **2004**, *70* (2), 153–226.
- (50) Nordin, A.; Nyberg, K.; Vinnerås, B. Inactivation of *Ascaris* Eggs in Source-Separated Urine and Feces by Ammonia at Ambient Temperatures. *Appl. Environ. Microbiol.* **2009**, *75* (3), 662–667.
- (51) Fumasoli, A.; Etter, B.; Sterkele, B.; Morgenroth, E.; Udert, K. M. Operating a pilot-scale nitrification/distillation plant for complete nutrient recovery from urine. *Water Sci. Technol.* **2016**, *73* (1), 215–222.

- (52) Jimenez, J.; Bott, C.; Love, N.; Bratby, J. Source Separation of Urine as an Alternative Solution to Nutrient Management in Biological Nutrient Removal Treatment Plants. *Water Environ. Res.* **2015**, *87* (12), 2120–2129.
- (53) *The Pulse of the Bay: The State of Bay Water Quality, 2015 and 2065*; SFEI Contribution #759; San Francisco Estuary Institute: Richmond, CA, 2015.
- (54) Aissa-Grouz, N.; Garnier, J.; Billen, G.; Mercier, B.; Martinez, A. The response of river nitrification to changes in wastewater treatment (The case of the lower Seine River downstream from Paris). *Ann. Limnol. - Int. J. Limnol.* **2015**, *51* (4), 351–364.
- (55) Harris-Lovett, Sasha. Water Infrastructure in the Face of Uncertainty: An Integrative Approach to Nitrogen Management in the San Francisco Bay Estuary. Masters of Science, University of California at Berkeley, 2013.
- (56) O’Keefe, M.; Lüthi, C.; Tumwebaze, I. K.; Tobias, R. Opportunities and limits to market-driven sanitation services: evidence from urban informal settlements in East Africa. *Environ. Urban.* **2015**, *27* (2), 421–440.
- (57) Etter, B.; Udert, K. M.; Gounden, T. *Valorisation of Urine Nutrients (VUNA) Final Report*; Swiss Federal Institute of Aquatic Science and Technology (Eawag): Dübendorf, Switzerland, 2015.
- (58) Karadag, D.; Koc, Y.; Turan, M.; Armagan, B. Removal of ammonium ion from aqueous solution using natural Turkish clinoptilolite. *J. Hazard. Mater.* **2006**, *136* (3), 604–609.
- (59) Beler-Baykal, B.; Cinar-Engin, S. Ion exchange with clinoptilolite to control ammonium in drinking water. *J. Water Supply Res. Technol.* **2007**, *56* (8), 541.
- (60) Karadag, D.; Tok, S.; Akgul, E.; Turan, M.; Ozturk, M.; Demir, A. Ammonium removal from sanitary landfill leachate using natural Gördes clinoptilolite. *J. Hazard. Mater.* **2008**, *153* (1–2), 60–66.
- (61) Beler Baykal, B.; Kocaturk, N. P.; Allar, A. D.; Sari, B. The effect of initial loading on the removal of ammonium and potassium from source-separated human urine via clinoptilolite. *Water Sci. Technol.* **2009**, *60* (10), 2515.
- (62) Landry, K. A.; Boyer, T. H. Diclofenac removal in urine using strong-base anion exchange polymer resins. *Water Res.* **2013**, *47* (17), 6432–6444.
- (63) Boyer, T. H.; Landry, K.; Sendrowski, A.; O’Neal, J. Nutrient Recovery from Urine using Selective Ion Exchange. *Proc. Water Environ. Fed.* **2012**, *2012* (15), 1942–1943.
- (64) Wang, S.; Peng, Y. Natural zeolites as effective adsorbents in water and wastewater treatment. *Chem. Eng. J.* **2010**, *156* (1), 11–24.
- (65) Jorgensen, T. ; Weatherley, L. . Ammonia removal from wastewater by ion exchange in the presence of organic contaminants. *Water Res.* **2003**, *37* (8), 1723–1728.
- (66) Beler-Baykal, B.; Allar, A. D.; Bayram, S. Nitrogen recovery from source-separated human urine using clinoptilolite and preliminary results of its use as fertilizer. *Water Sci. Technol. J. Int. Assoc. Water Pollut. Res.* **2011**, *63* (4), 811–817.
- (67) Ding, Y.; Liu, Y.-X.; Wu, W.-X.; Shi, D.-Z.; Yang, M.; Zhong, Z.-K. Evaluation of Biochar Effects on Nitrogen Retention and Leaching in Multi-Layered Soil Columns. *Water. Air. Soil Pollut.* **2010**, *213* (1–4), 47–55.
- (68) Kizito, S.; Wu, S.; Kipkemoi Kirui, W.; Lei, M.; Lu, Q.; Bah, H.; Dong, R. Evaluation of slow pyrolyzed wood and rice husks biochar for adsorption of ammonium nitrogen from piggery manure anaerobic digestate slurry. *Sci. Total Environ.* **2015**, *505*, 102–112.
- (69) *DOWEX MAC-3 Engineering Information*; 177-01560–703; Dow Chemical Company, Dow Liquid Separations: Midland, MI, 2003.

- (70) Lehmann, J.; Joseph, S. *Biochar for Environmental Management: Science and Technology*; Routledge, 2012.
- (71) *DOWEX Fine Mesh Spherical Ion Exchange Resins For Fine Chemical and Pharmaceutical Column Separations*; 177-01509-904; Dow Chemical Company, Dow Water Solutions: Midland, MI.
- (72) Perrin, D.D. *Ionization Constants of Inorganic Acids and Bases in Aqueous Solution, Second Edition*; Pergamon: Oxford, 1982.
- (73) Udert, K. M.; Larsen, T. A.; Biebow, M.; Gujer, W. Urea hydrolysis and precipitation dynamics in a urine-collecting system. *Water Res.* **2003**, *37* (11), 2571–2582.
- (74) Parkhurst, D. L.; Appelo, C. A. J. Description of input and examples for PHREEQC version 3—A computer program for speciation, batch-reaction, one-dimensional transport, and inverse geochemical calculations. In *U.S. Geological Survey Techniques and Methods, book 6*; 2013; Vol. 6, p 497.
- (75) Pecton, B. M.; Nelson, K. L. Inactivation of *Ascaris suum* eggs by ammonia. *Environ. Sci. Technol.* **2005**, *39* (20), 7909–7914.
- (76) *Water Quality Engineering: Physical / Chemical Treatment Processes*, 1 edition.; Wiley: Hoboken, N.J, 2013.
- (77) Foo, K. Y.; Hameed, B. H. Insights into the modeling of adsorption isotherm systems. *Chem. Eng. J.* **2010**, *156* (1), 2–10.
- (78) Dochain, D.; Vanrolleghem, P. *Dynamical Modelling and Estimation in Wastewater Treatment Processes*; IWA Publishing, 2001.
- (79) Matott, L. S.; Rabideau, A. J. ISOFIT – A program for fitting sorption isotherms to experimental data. *Environ. Model. Softw.* **2008**, *23* (5), 670–676.
- (80) Jain, J. S.; Snoeyink, V. L. Adsorption from Bissolute Systems on Active Carbon. *J. Water Pollut. Control Fed.* **1973**, *45* (12), 2463–2479.
- (81) Xiong, C.; Han, X.; Yao, C. Sorption Behavior of In(III) Ions onto Cation-Exchange Carboxylic Resin in Aqueous Solutions: Batch and Column Studies. *Sep. Sci. Technol.* **2010**, *45* (16), 2368–2375.
- (82) Kithome, M.; Paul, J. W.; Lavkulich, L. M.; Bomke, A. A. Effect of pH on ammonium adsorption by natural Zeolite clinoptilolite. *Commun. Soil Sci. Plant Anal.* **1999**, *30* (9–10), 1417–1430.
- (83) Tobin, J. M.; Cooper, D. G.; Neufeld, R. J. Uptake of Metal Ions by *Rhizopus arrhizus* Biomass. *Appl. Environ. Microbiol.* **1984**, *47* (4), 821–824.
- (84) Nightingale, E. R. Phenomenological Theory of Ion Solvation. Effective Radii of Hydrated Ions. *J. Phys. Chem.* **1959**, *63* (9), 1381–1387.
- (85) Naidu, R.; Bolan, N. s.; Kookana, R. S.; Tiller, K. g. Ionic-strength and pH effects on the sorption of cadmium and the surface charge of soils. *Eur. J. Soil Sci.* **1994**, *45* (4), 419–429.
- (86) Doula, M. K.; Ioannou, A. The effect of electrolyte anion on Cu adsorption–desorption by clinoptilolite. *Microporous Mesoporous Mater.* **2003**, *58* (2), 115–130.
- (87) Bull, H. B.; Breese, K. Surface tension of amino acid solutions: A hydrophobicity scale of the amino acid residues. *Arch. Biochem. Biophys.* **1974**, *161* (2), 665–670.
- (88) Álvarez, E.; Vázquez, G.; Sánchez-Vilas, M.; Sanjurjo, B.; Navaza, J. M. Surface Tension of Organic Acids + Water Binary Mixtures from 20 °C to 50 °C. *J. Chem. Eng. Data* **1997**, *42* (5), 957–960.

- (89) Falk, M. W.; Reardon, D. J.; Neethling, J. B.; Clark, D. L.; Pramanik, A. Striking the Balance between Nutrient Removal, Greenhouse Gas Emissions, Receiving Water Quality, and Costs. *Water Environ. Res.* **2013**, *85* (12), 2307–2316.
- (90) Allar, A. D.; Baykal, B. B. An investigation into the potential use of nutrients recovered from urine diversion on a summer housing site: self-sufficiency based on nitrogen balance. *Water Sci. Technol.* **2016**, *73* (3), 576–581.
- (91) Güereña, D.; Lehmann, J.; Hanley, K.; Enders, A.; Hyland, C.; Riha, S. Nitrogen dynamics following field application of biochar in a temperate North American maize-based production system. *Plant Soil* **2012**, *365* (1–2), 239–254.
- (92) Landry, K. A.; Boyer, T. H. Life cycle assessment and costing of urine source separation: Focus on nonsteroidal anti-inflammatory drug removal. *Water Res.* **2016**, *105*, 487–495.
- (93) Larsen, T. A.; Gujer, W. Separate management of anthropogenic nutrient solutions (human urine). *Water Sci. Technol.* **1996**, *34* (3), 87–94.
- (94) Decrey, L.; Udert, K. M.; Tilley, E.; Pecson, B. M.; Kohn, T. Fate of the pathogen indicators phage ΦX174 and *Ascaris suum* eggs during the production of struvite fertilizer from source-separated urine. *Water Res.* **2011**, *45* (16), 4960–4972.
- (95) Hug, A.; Udert, K. M. Struvite precipitation from urine with electrochemical magnesium dosage. *Water Res.* **2013**, *47* (1), 289–299.
- (96) Triger, A.; Pic, J.-S.; Cabassud, C. Determination of struvite crystallization mechanisms in urine using turbidity measurement. *Water Res.* **2012**, *46* (18), 6084–6094.
- (97) Sendrowski, A.; Boyer, T. H. Phosphate removal from urine using hybrid anion exchange resin. *Desalination* **2013**, *322*, 104–112.
- (98) Tarpeh, W. A.; Udert, K. M.; Nelson, K. L. Comparing Ion Exchange Adsorbents for Nitrogen Recovery from Source-Separated Urine. *Environ. Sci. Technol.* **2017**, *51* (4), 2373–2381.
- (99) Udert, K. M.; Larsen, T. A.; Gujer, W. Estimating the precipitation potential in urine-collecting systems. *Water Res.* **2003**, *37* (11), 2667–2677.
- (100) Zhang, R.; Sun, P.; Boyer, T. H.; Zhao, L.; Huang, C.-H. Degradation of Pharmaceuticals and Metabolite in Synthetic Human Urine by UV, UV/H<sub>2</sub>O<sub>2</sub>, and UV/PDS. *Environ. Sci. Technol.* **2015**, *49* (5), 3056–3066.
- (101) Landry, K. A.; Sun, P.; Huang, C.-H.; Boyer, T. H. Ion-exchange selectivity of diclofenac, ibuprofen, ketoprofen, and naproxen in ureolyzed human urine. *Water Res.* **2015**, *68*, 510–521.
- (102) Rose, C.; Parker, A.; Jefferson, B.; Cartmell, E. The Characterization of Feces and Urine: A Review of the Literature to Inform Advanced Treatment Technology. *Crit. Rev. Environ. Sci. Technol.* **2015**, *45* (17), 1827–1879.
- (103) *Families and Living Arrangements*; U.S. Census Bureau.
- (104) Li, P.; SenGupta, A. K. Intraparticle diffusion during selective ion exchange with a macroporous exchanger. *React. Funct. Polym.* **2000**, *44* (3), 273–287.
- (105) Jasper, J. T.; Jones, Z. L.; Sharp, J. O.; Sedlak, D. L. Biotransformation of trace organic contaminants in open-water unit process treatment wetlands. *Environ. Sci. Technol.* **2014**, *48* (9), 5136–5144.
- (106) Onyango, M. S.; Leswifi, T. Y.; Ochieng, A.; Kuchar, D.; Otieno, F. O.; Matsuda, H. Breakthrough Analysis for Water Defluoridation Using Surface-Tailored Zeolite in a Fixed Bed Column. *Ind. Eng. Chem. Res.* **2009**, *48* (2), 931–937.



- (107) Sander, R. Compilation of Henry's law constants (version 4.0) for water as solvent. *Atmos Chem Phys* **2015**, *15* (8), 4399–4981.
- (108) Vargas, O. L.; Bryla, D. R. Growth and Fruit Production of Highbush Blueberry Fertilized with Ammonium Sulfate and Urea Applied by Fertigation or as Granular Fertilizer. *HortScience* **2015**, *50* (3), 479–485.
- (109) *Liquid Fertilizer Formulation Guide*; AdvanSix Inc., 2016.
- (110) Goizman, M. S.; Balayants, T. É.; Kamalova, A. A.; Popova, A. O.; Korlyukov, A. A.; Suponitskii, K. Y.; Trifilenkov, A. S.; Papikyan, S. K.; Shimanovskii, N. L.; Zaitsev, S. A.; et al. Physicochemical, Terminological, and Ethical Aspects of the Patenting of Substances and Medicinal Formulations of Abacavir Sulfate. *Pharm. Chem. J.* **2015**, *49* (1), 65–72.
- (111) Knappe, D. R. U.; Rossner, A.; Snyder, S. A.; Strickland, C. *Alternative Adsorbents for the Removal of Polar Organic Contaminants*; American Water Works Association, 2007.
- (112) Roberts, G.; Feeney, J.; Burgen, A.; Daluge, S. The Charge State of Trimethoprim Bound to Lactobacillus Casei Dihydrofolate Reductase. **1981**, *131* (1).
- (113) Sabourin, L.; Duenk, P.; Bonte-Gelok, S.; Payne, M.; Lapen, D. R.; Topp, E. Uptake of pharmaceuticals, hormones and parabens into vegetables grown in soil fertilized with municipal biosolids. *Sci. Total Environ.* **2012**, *431*, 233–236.
- (114) Kemp, W. M.; Boynton, W. R.; Adolf, J. E.; Boesch, D. F.; Boicourt, W. C.; Brush, G.; Cornwell, J. C.; Fisher, T. R.; Glibert, P. M.; Hagy, J. D.; et al. Eutrophication of Chesapeake Bay: historical trends and ecological interactions. *Mar. Ecol. Prog. Ser.* **2005**, *303*, 1–29.
- (115) Gustin, S.; Marinsek-Logar, R. Effect of pH, temperature and air flow rate on the continuous ammonia stripping of the anaerobic digestion effluent. *Process Saf. Environ. Prot.* **2011**, *89* (1), 61–66.
- (116) Kabdashlı, I.; Tünay, O.; Öztürk, İ.; Yılmaz, S.; Arıkan, O. Ammonia removal from young landfill leachate by magnesium ammonium phosphate precipitation and air stripping. *Water Sci. Technol.* **2000**, *41* (1), 237–240.
- (117) Liao, P. H.; Chen, A.; Lo, K. V. Removal of nitrogen from swine manure wastewaters by ammonia stripping. *Bioresour. Technol.* **1995**, *54* (1), 17–20.
- (118) Kuntke, P.; Sleutels, T. H. J. A.; Saakes, M.; Buisman, C. J. N. Hydrogen production and ammonium recovery from urine by a Microbial Electrolysis Cell. *Int. J. Hydrog. Energy* **2014**, *39* (10), 4771–4778.
- (119) Feng, Y.; Yang, L.; Liu, J.; E. Logan, B. Electrochemical technologies for wastewater treatment and resource reclamation. *Environ. Sci. Water Res. Technol.* **2016**, *2* (5), 800–831.
- (120) Zöllig, H.; Fritzsche, C.; Morgenroth, E.; Udert, K. M. Direct electrochemical oxidation of ammonia on graphite as a treatment option for stored source-separated urine. *Water Res.* **2015**, *69*, 284–294.
- (121) Luther, A. K.; Desloover, J.; Fennell, D. E.; Rabaey, K. Electrochemically driven extraction and recovery of ammonia from human urine. *Water Res.* **2015**, *87*, 367–377.
- (122) Desloover, J.; Woldeyohannis, A. A.; Verstraete, W.; Boon, N.; Rabaey, K. Electrochemical resource recovery from digestate to prevent ammonia toxicity during anaerobic digestion. *Environ. Sci. Technol.* **2012**, *46* (21), 12209–12216.

- (123) Dykstra, J. E.; Biesheuvel, P. M.; Bruning, H.; Ter Heijne, A. Theory of ion transport with fast acid-base equilibrations in bioelectrochemical systems. *Phys. Rev. E* **2014**, *90* (1), 13302.
- (124) Rodríguez Arredondo, M.; Kuntke, P.; ter Heijne, A.; Hamelers, H. V. M.; Buisman, C. J. N. Load ratio determines the ammonia recovery and energy input of an electrochemical system. *Water Res.* **2017**, *111*, 330–337.
- (125) Kuntke, P.; Zamora, P.; Saakes, M.; Buisman, C. J. N.; Hamelers, H. V. M. Gas-permeable hydrophobic tubular membranes for ammonia recovery in bio-electrochemical systems. *Env. Sci Water Res Technol* **2016**, *2* (2), 261–265.
- (126) Olivares-Ramírez, J. M.; Campos-Cornelio, M. L.; Uribe Godínez, J.; Borja-Arco, E.; Castellanos, R. H. Studies on the hydrogen evolution reaction on different stainless steels. *Int. J. Hydrog. Energy* **2007**, *32* (15), 3170–3173.
- (127) Greenberg, A. E. *Standard Methods: For the Examination of Water and Wastewater, 18th Edition*, 18 r.e. edition.; Amer Public Health Assn: Washington, DC, 1992.
- (128) Lienert, J.; Bürki, T.; Escher, B. I. Reducing micropollutants with source control: substance flow analysis of 212 pharmaceuticals in faeces and urine. *Water Sci. Technol.* **2007**, *56* (5), 87–96.
- (129) Luo, Y.; Guo, W.; Ngo, H. H.; Nghiem, L. D.; Hai, F. I.; Zhang, J.; Liang, S.; Wang, X. C. A review on the occurrence of micropollutants in the aquatic environment and their fate and removal during wastewater treatment. *Sci. Total Environ.* **2014**, *473–474*, 619–641.
- (130) Zöllig, H.; Remmele, A.; Fritzsche, C.; Morgenroth, E.; Udert, K. M. Formation of Chlorination Byproducts and Their Emission Pathways in Chlorine Mediated Electro-Oxidation of Urine on Active and Nonactive Type Anodes. *Environ. Sci. Technol.* **2015**, *49* (18), 11062–11069.
- (131) Bouatra, S.; Aziat, F.; Mandal, R.; Guo, A. C.; Wilson, M. R.; Knox, C.; Bjorndahl, T. C.; Krishnamurthy, R.; Saleem, F.; Liu, P.; et al. The Human Urine Metabolome. *PLOS ONE* **2013**, *8* (9), e73076.
- (132) Jasper, J. T.; Shafaat, O. S.; Hoffmann, M. R. Electrochemical Transformation of Trace Organic Contaminants in Latrine Wastewater. *Environ. Sci. Technol.* **2016**, *50* (18), 10198–10208.
- (133) Ott, H. *Fertilizer markets and their interplay with commodity and food prices*; European Commission Joint Research Centre, Institute for Prospective Technological Studies: Luxembourg, 2012.
- (134) *National Primary Drinking Water Regulations*; 2010; Vol. 40 CFR 141.
- (135) Brungs, W. A. Effects of Residual Chlorine on Aquatic Life. *J. Water Pollut. Control Fed.* **1973**, *45* (10), 2180–2193.
- (136) Jacobsen, M.; Webster, M.; Vairavamoorthy, K. *The Future of Water in African Cities: Why Waste Water?*; World Bank Publications, 2012.
- (137) Nelson, K. L.; Murray, A. Sanitation for Unserved Populations: Technologies, Implementation Challenges, and Opportunities. *Annu. Rev. Environ. Resour.* **2008**, *33* (1), 119–151.
- (138) Hutton, G. *Global costs and benefits of drinking-water supply and sanitation interventions to reach the MDG target and universal coverage*; World Health Organization, 2012.
- (139) Morella, E.; Foster, V.; Banerjee, Sudeshna Ghosh. *Climbing the Ladder: The State of Sanitation in Sub-Saharan Africa*; Africa's Infrastructure: A time for Transformation; 13; The International Bank for Reconstruction and Development/ The World Bank, 2008.

- (140) Nansubuga, I.; Banadda, N.; Verstraete, W.; Rabaey, K. A review of sustainable sanitation systems in Africa. *Rev. Environ. Sci. Biotechnol.* **2016**, *15* (3), 465–478.
- (141) Stoorvogel, J. J.; Smaling, E. A.; Janssen, B. H. Calculating soil nutrient balances in Africa at different scales. *Fertil. Res.* **1993**, *35* (3), 227–235.
- (142) Shimeles, A.; Gurara, D. Z.; Tessema, B.; Dawit. *Market Distortions and Political Rent: The Case of Fertilizer Price Divergence in Africa*; SSRN Scholarly Paper ID 2598938; Social Science Research Network: Rochester, NY, 2015.
- (143) *Kenya Fertilizer Assessment*; IFDC: Nairobi, Kenya, 2012.
- (144) Van den Bosch, H.; Gitari, J. N.; Ogaro, V. N.; Maobe, S.; Vlaming, J. Monitoring nutrient flows and economic performance in African farming systems (NUTMON).: III. Monitoring nutrient flows and balances in three districts in Kenya. *Agric. Ecosyst. Environ.* **1998**, *71* (1–3), 63–80.
- (145) Ochola, R. O.; Fengying, N. I. E. Evaluating the effects of fertilizer subsidy programmes on vulnerable farmers in Kenya. *J. Agric. Ext. Rural Dev.* **2015**, *7* (6), 192–201.
- (146) Jayne, T. S.; Govereh, J.; Wanzala, M.; Demeke, M. Fertilizer market development: a comparative analysis of Ethiopia, Kenya, and Zambia. *Food Policy* **2003**, *28* (4), 293–316.
- (147) Marenja, P. P.; Barrett, C. B. Soil quality and fertilizer use rates among smallholder farmers in western Kenya. *Agric. Econ.* **2009**, *40* (5), 561–572.
- (148) Etter, B.; Tilley, E.; Khadka, R.; Udert, K. M. Low-cost struvite production using source-separated urine in Nepal. *Water Res.* **2011**, *45* (2), 852–862.
- (149) Udert, K. M.; Wächter, M. Complete nutrient recovery from source-separated urine by nitrification and distillation. *Water Res.* **2012**, *46* (2), 453–464.
- (150) Auerbach, D. Sustainable Sanitation Provision in Urban Slums – The Sanergy Case Study. In *Broken Pumps and Promises*; Thomas, E. A., Ed.; Springer International Publishing, 2016; pp 211–216.
- (151) Schönning, C.; Leeming, R.; Stenström, T. A. Faecal contamination of source-separated human urine based on the content of faecal sterols. *Water Res.* **2002**, *36* (8), 1965–1972.
- (152) Zhang, J.; Giannis, A.; Chang, V. W. C.; Ng, B. J. H.; Wang, J.-Y. Adaptation of urine source separation in tropical cities: Process optimization and odor mitigation. *J. Air Waste Manag. Assoc.* **2013**, *63* (4), 472–481.
- (153) Troccaz, M.; Niclass, Y.; Anziani, P.; Starkenmann, C. The influence of thermal reaction and microbial transformation on the odour of human urine. *Flavour Fragr. J.* **2013**, *28* (4), 200–211.
- (154) Pikaar, I.; Matassa, S.; Rabaey, K.; Bodirsky, B. L.; Popp, A.; Herrero, M.; Verstraete, W. Microbes and the Next Nitrogen Revolution. *Environ. Sci. Technol.* **2017**.
- (155) Jorgensen, T. .; Weatherley, L. . Ammonia removal from wastewater by ion exchange in the presence of organic contaminants. *Water Res.* **2003**, *37* (8), 1723–1728.
- (156) Kowalczyk, P.; Sprynskyy, M.; Terzyk, A. P.; Lebedynets, M.; Namieśnik, J.; Buszewski, B. Porous structure of natural and modified clinoptilolites. *J. Colloid Interface Sci.* **2006**, *297* (1), 77–85.
- (157) Daković, A.; Kragović, M.; Rottinghaus, G. E.; Sekulić, Ž.; Milićević, S.; Milonjić, S. K.; Zarić, S. Influence of natural zeolitic tuff and organozeolites surface charge on sorption of ionizable fumonisin B1. *Colloids Surf. B Biointerfaces* **2010**, *76* (1), 272–278.
- (158) Ok, Y. S.; Uchimiya, S. M.; Chang, S. X.; Bolan, N. *Biochar: Production, Characterization, and Applications*; CRC Press, 2015.

- (159) Hendricks, D. W. *Water Treatment Unit Processes: Physical and Chemical*; CRC Press, 2006.
- (160) Brewer, C. E.; Chuang, V. J.; Masiello, C. A.; Gonnermann, H.; Gao, X.; Dugan, B.; Driver, L. E.; Panzacchi, P.; Zygourakis, K.; Davies, C. A. New approaches to measuring biochar density and porosity. *Biomass Bioenergy* **2014**, *66*, 176–185.
- (161) Inglezakis, V. J.; Zorpas, A. A. *Handbook of Natural Zeolites*; Bentham Science Publishers, 2012.
- (162) Ithaka Institute: Ayent, Switzerland, 2015.
- (163) Sigma-Aldrich: St. Louis, Missouri, USA, 2015.
- (164) *CRC Handbook of Chemistry and Physics, 97th Edition, 97 edition.*; Haynes, W. M., Ed.; CRC Press, 2016.
- (165) Shawahna, R.; Rahman, N. Evaluation of the use of partition coefficients and molecular surface properties as predictors of drug absorption: a provisional biopharmaceutical classification of the list of national essential medicines of Pakistan. *DARU J. Fac. Pharm. Tehran Univ. Med. Sci.* **2011**, *19* (2), 83–99.
- (166) Mohsen-Nia, M.; Ebrahimabadi, A. H.; Niknahad, B. Partition coefficient n-octanol/water of propranolol and atenolol at different temperatures: Experimental and theoretical studies. *J. Chem. Thermodyn.* **2012**, *54*, 393–397.
- (167) Giménez, B. G.; Santos, M. S.; Ferrarini, M.; Fernandes, J. P. S.; Fernandes, J. P. S. Evaluation of blockbuster drugs under the Rule-of-five. *Pharm. - Int. J. Pharm. Sci.* **2010**, *65* (2), 148–152.
- (168) Deborde, M.; von Gunten, U. Reactions of chlorine with inorganic and organic compounds during water treatment—Kinetics and mechanisms: A critical review. *Water Res.* **2008**, *42* (1–2), 13–51.
- (169) Barazesh, J. M.; Prasse, C.; Sedlak, D. L. Electrochemical Transformation of Trace Organic Contaminants in the Presence of Halide and Carbonate Ions. *Environ. Sci. Technol.* **2016**, *50* (18), 10143–10152.
- (170) Desloover, J.; De Vrieze, J.; de Vijver, M. V.; Mortelmans, J.; Rozendal, R.; Rabaey, K. Electrochemical Nutrient Recovery Enables Ammonia Toxicity Control and Biogas Desulfurization in Anaerobic Digestion. *Environ. Sci. Technol.* **2015**, *49* (2), 948–955.
- (171) Kuntke, P.; Smiech, K. M.; Bruning, H.; Zeeman, G.; Saakes, M.; Sleutels, T. H. J. A.; Hamelers, H. V. M.; Buisman, C. J. N. Ammonium recovery and energy production from urine by a microbial fuel cell. *Water Res.* **2012**, *46* (8), 2627–2636.
- (172) Ledezma, P.; Jermakka, J.; Keller, J.; Freguia, S. Recovering Nitrogen as a Solid without Chemical Dosing: Bio-Electroconcentration for Recovery of Nutrients from Urine. *Environ. Sci. Technol. Lett.* **2017**, *4* (3), 119–124.
- (173) Maurer, M.; Schwegler, P.; Larsen, T. A. Nutrients in urine: energetic aspects of removal and recovery. *Water Sci. Technol.* **2003**, *48* (1), 37–46.
- (174) Alibaba.com. Products.
- (175) Sheahan, M.; Ariga, J.; Jayne, T. S. Modeling the Effects of Input Market Reforms on Fertiliser Demand and Maize Production: A Case Study from Kenya. *J. Agric. Econ.* **2016**, *67* (2), 420–447.
- (176) Nyambati, R. O.; Opala, P. A. An agronomic and economic evaluation of integrated use of *Calliandra calothyrsus* and maize stover with urea in western Kenya. *Am. J. Exp. Agric.* **2014**, *4* (1), 80.

- (177) *World fertilizer trends and outlook to 2018*; Food and Agriculture Organization of the United Nations, 2015.
- (178) Camberato, J.; Nielsen, R. *Nitrogen management guidelines for corn in Indiana*; Applied Crop Research Update; Purdue University Department of Agronomy, 2017.
- (179) Calculations Used to Determine the Amount of Fertilizer Needed to Treat Turf (Center for Turfgrass Science)  
<http://plantscience.psu.edu/research/centers/turf/extension/factsheets/calculations-turfgrass-fertilization> (accessed Jun 15, 2017).
- (180) Resources, U. of C. A. and N. Fertilizing Vegetables  
[http://sfp.ucdavis.edu/pubs/Family\\_Farm\\_Series/Veg/Fertilizing/vegetables](http://sfp.ucdavis.edu/pubs/Family_Farm_Series/Veg/Fertilizing/vegetables) (accessed Jun 15, 2017).
- (181) Abdul-Baki, A. A.; Teasdale, J. R.; Korcak, R. F. Nitrogen Requirements of Fresh-market Tomatoes on Hairy Vetch and Black Polyethylene Mulch. *HortScience* **1997**, *32* (2), 217–221.
- (182) Coolong, T.; Boyhan, G. *Commercial Tomato Production Handbook*; B 1312; University of Georgia Extension.
- (183) Olson, S. M.; Simonne, E. H.; Stall, W. M.; Vallad, G. E.; Webb, S. E.; McAvoy, E. J.; Smith, S. A. Pepper production in Florida. *Veg. Prod. Handb. Fla.* **2010**, *2011*, 213–215.
- (184) Mylavarapu, R. S.; Zinati, G. M. Improvement of soil properties using compost for optimum parsley production in sandy soils. *Sci. Hortic.* **2009**, *120* (3), 426–430.
- (185) Sullivan, D.; Brown, B.; Shock, C.; Horneck, D.; Stevens, R.; Pelter, G.; Feibert, E. *Nutrient management for onions in the Pacific Northwest*; PNW 546; Pacific Northwest Extension, 2001.
- (186) *Fertilization Requirements for Onions*; Dixondale Farms, 2017.
- (187) Brown, B.; Westermann, D. *Soil fertility and bean production*; University of Idaho Extension, 2009.
- (188) Clough, G.; Bratsch, A. *Nitrogen Fertilization Rate and Plant Population Affect Yield and Quality of Drip-Irrigated Bell Pepper*; HAREC Research Report 95-1; Oregon State University Hermiston Agricultural Research & Extension Center.
- (189) Hartz, T. K.; LeStrange, M.; May, D. M. Nitrogen Requirements of Drip-irrigated Peppers. *HortScience* **1993**, *28* (11), 1097–1099.
- (190) Welch, N. C.; Tyler, K. B.; Ririe, D.; others. Cabbage yield and nutrient uptake. *Calif. Agric.* **1985**, *39* (7), 30–31.
- (191) Doerge, T.; Roth, R.; Gardner, B. *Nitrogen fertilizer management in Arizona*; 191025; College of Agriculture, University of Arizona: Tuscon, Arizona, 1991.

# APPENDICES

## A. COMPARING ION EXCHANGE ADSORBENTS FOR NITROGEN RECOVERY FROM SOURCE-SEPARATED URINE.

### A1. EQUATIONS

#### A1.1 Competitive adsorption curve fitting

Three multicomponent isotherms were fit to synthetic urine adsorption data: (1) competitive Langmuir, (2) Jain-Snoeyink, (3) and competitive Langmuir-Freundlich. These equations are written as equations 2.6-2.8 in Chapter 2. The three-solute Jain-Snoeyink model used in this study was expanded from the original Snoeyink two-solute model.<sup>80</sup> This model uses Langmuir isotherms but allows for different maximum adsorption densities for different cations. The interaction between solutes is competitive until the lower adsorption density is surpassed, and above this value adsorption is assumed to be non-competitive. The resulting equation for the adsorption density of each cation has a slightly different form (Equations A1-3).  $q_{\max}$  and  $K_{\text{ads}}$  for each cation were from the single-cation adsorption experiments, and numerical subscripts denote each cation from lowest (1) to highest (3) maximum adsorption density. Based on  $q_{\max}$  values from single-solute experiments (Table A4), ammonium was either predicted by Equation A1 (biochar, Dowex 50) or by Equation A2 (clinoptilolite, Dowex Mac 3).

$$q_{f,3} = \frac{q_{\max,1}K_{\text{ads},3}\{A_3\}}{1+K_{\text{ads},1}\{A_1\}+K_{\text{ads},2}\{A_2\}+K_{\text{ads},3}\{A_3\}} + \frac{(q_{\max,2}-q_{\max,1})K_{\text{ads},3}\{A_3\}}{1+K_{\text{ads},2}\{A_2\}+K_{\text{ads},3}\{A_3\}} + \frac{(q_{\max,3}-q_{\max,2})K_{\text{ads},3}\{A_3\}}{1+K_{\text{ads},3}\{A_3\}} \quad (\text{A1})$$

$$q_{f,2} = \frac{q_{\max,1}K_{\text{ads},2}\{A_2\}}{1+K_{\text{ads},1}\{A_1\}+K_{\text{ads},2}\{A_2\}+K_{\text{ads},3}\{A_3\}} + \frac{(q_{\max,2}-q_{\max,1})K_{\text{ads},2}\{A_2\}}{1+K_{\text{ads},2}\{A_2\}+K_{\text{ads},3}\{A_3\}} \quad (\text{A2})$$

$$q_{f,1} = \frac{q_{\max,1}K_{\text{ads},1}\{A_1\}}{1+K_{\text{ads},1}\{A_1\}+K_{\text{ads},2}\{A_2\}+K_{\text{ads},3}\{A_3\}} \quad (\text{A3})$$

Affinity constants and maximum adsorption densities from single-solute experiments were used as inputs for the competitive Langmuir and Jain-Snoeyink models. Affinity constants were also used as inputs to the competitive Langmuir-Freundlich, but  $q_{\max}$  and  $n$  were determined by nonlinear regression using the synthetic urine data. An important difference to note between the models is that the competitive Langmuir and Jain-Snoeyink models use individual  $q_{\max}$  values for each cation; in contrast, the Langmuir-Freundlich uses a single maximum adsorption density for all three cations.

To predict batch adsorption in undiluted real urine, we used initial cation activities and model parameters to solve a system of six equations containing model predictions for each cation and mass balances on each cation. For example, the following six equations were solved for the competitive Langmuir model:

$$q_{f,K} = \frac{K_{ads,K}q_{max,K}\{A_K\}}{1+K_{ads,K}\{A_K\}+K_{ads,Na}\{A_{Na}\}+K_{ads,N}\{A_N\}} \quad (A4)$$

$$q_{f,Na} = \frac{K_{ads,Na}q_{max,Na}\{A_{Na}\}}{1+K_{ads,K}\{A_K\}+K_{ads,Na}\{A_{Na}\}+K_{ads,N}\{A_N\}} \quad (A5)$$

$$q_{f,N} = \frac{K_{ads,N}q_{max,N}\{A_N\}}{1+K_{ads,K}\{A_K\}+K_{ads,Na}\{A_{Na}\}+K_{ads,N}\{A_N\}} \quad (A6)$$

$$q_{f,K} = \frac{V_L}{W} (C_{0,K} - C_{f,K}) \quad (A7)$$

$$q_{f,Na} = \frac{V_L}{W} (C_{0,Na} - C_{f,Na}) \quad (A8)$$

$$q_{f,N} = \frac{V_L}{W} (C_{0,N} - C_{f,N}) \quad (A9)$$

where  $V_L$  is solution volume (L),  $C_0$  is initial concentration of adsorbate (mg  $\text{NH}_4^+$ -N,  $\text{Na}^+$ , or  $\text{K}^+$ /L),  $C_f$  is adsorbate concentration at equilibrium (mg  $\text{NH}_4^+$ -N,  $\text{Na}^+$ , or  $\text{K}^+$ /L),  $W$  is adsorbent mass (g), and  $q_0$  is the initial adsorption density (mg  $\text{NH}_4^+$ -N,  $\text{Na}^+$ , or  $\text{K}^+$ /g adsorbent). The same process was used for Jain-Snoeyink and Langmuir-Freundlich, with the appropriate model equations instead of equations A4-A6. Pitzer coefficients were used to convert concentration to activity (Equation 2.4). The six unknowns were the equilibrium adsorption density and concentrations of each cation.

The sum of squared errors (SSE, Equation A10) and average relative error (ARE, Equation A11) were used to compare the fit of each model to experimental data; lower SSE and ARE indicate a better fit (Table A6).<sup>33</sup>

$$SSE = \sum_1^n (q_{f,experimental} - q_{f,model})_i^2 \quad (A10)$$

$$ARE = \frac{100}{n} \sum_1^n \left| \frac{q_{f,experimental} - q_{f,model}}{q_{f,experimental}} \right|_i \quad (A11)$$

In equations A1 and A2,  $n$  is the number of experimental data points and  $q_f$  is equilibrium adsorption density (mmol N/g adsorbent).

## A1.2 Dubinin-Radushkevich Isotherm

Mean free energy of adsorption was determined using the Dubinin-Radushkevich isotherm for each adsorbent (Equations A12 and A13):

$$q_e = q_0 \exp \left[ -\left(\frac{\varepsilon}{\sqrt{2E}}\right)^2 \right] \quad (\text{A12})$$

$$\varepsilon = RT \ln \left( 1 + \frac{1}{C_e} \right) \quad (\text{A13})$$

Where  $q$  is initial ( $q_0$ ) and equilibrium ( $q_e$ ) adsorption density (mmol N/g adsorbent);  $\varepsilon$  is the Dubinin-Radushkevich isotherm constant, and  $E$  is mean free energy (kJ/mol).  $R$  is the universal gas constant,  $T$  is temperature in Kelvins, and  $C_e$  is equilibrium concentration in mg N/L.<sup>77</sup>

### A1.3 Continuous Experiments

Breakthrough curves and elution curves were generated from continuous adsorption and regeneration experiments, respectively. Integration of both curves allowed for calculation of the mass of ammonium adsorbed or eluted. Numerical integration was performed using the trapezoid rule:

$$\int C(t)dt \approx \sum_1^n \{ (BV_n - BV_{n-1}) * \frac{1}{2} * [C(BV_n) - C(BV_{n-1})] \} \quad (\text{A14})$$

Where  $n$  is the number of data points,  $BV$  is number of bed volumes, and  $C(BV)$  is the concentration at a given number ( $BV$ ) of bed volumes. For adsorption experiments, the mass of ammonium adsorbed was proportional to the area above the ammonium breakthrough curve and below the chloride tracer curve. For regeneration, the mass of ammonium eluted is proportional to the area below the elution curve. The equations for adsorption density (Equation A15) and regeneration efficiency (Equation A16) are:

$$q = \frac{\int [C_{Cl,ads}(t) - C_{N,ads}(t)] dt}{PV * W * MW_N} \quad (\text{A15})$$

$$\eta_{regen} = \frac{\int C_{N,elution}(t) dt}{\int [C_{Cl,ads}(t) - C_{N,ads}(t)] dt} \quad (\text{A16})$$

Where  $PV$  is pore volume (L/bed volume), the volume of liquid retained by a column full of resin,  $W$  is adsorbent mass (g adsorbent),  $q$  is adsorption density (mmol N/g adsorbent), and the subscripts on concentration  $C(t)$  denote adsorption or elution. Pore volume was calculated by subtracting the mass of a column full of dry resin from the same column filled with resin and distilled water.

### A1.4 Calculation of cost of conventional nitrogen removal

We used Falk et al. 2013<sup>89</sup> to determine the cost of installing conventional nitrogen removal at a 10 MGD activated sludge wastewater treatment plant. Costs are likely to be higher for smaller



treatment plants. The net present value calculated in that study was \$40 million (\$150 million for installing basic biological nutrient removal, \$110 million for base case activated sludge). This annualized cost was divided by the 10 MGD flow rate and the 27 mg N removed/L wastewater (influent 35 mg N/L, effluent 8 mg N/L). Other assumptions made by Falk et al. include: \$0.10/kWh for operational energy use, 20 year life span, discount rate = 5.0%, and escalation rates for capital, energy and non-energy inflation rates = 3.5%.

$$\frac{\$40 \cdot 10^6}{\text{yr}} * \frac{1 \text{ day}}{10^7 \text{ gal}} * \frac{1 \text{ gal}}{3.78 \text{ L}} * \frac{1 \text{ yr}}{365.25 \text{ days}} * \frac{1 \text{ L ww}}{27 \text{ mg N}} * \frac{1000 \text{ mg N}}{1 \text{ g N}} = \frac{\$0.107}{\text{g N}} \quad (\text{A17})$$

## A2. TABLES

**Table A1.** Adsorbent characteristics.

Adsorbent	Particle size (mm)	Pore structure <sup>a</sup>	Functional Group	pKa or pHpZc <sup>b</sup>	Highest Reported NH <sub>4</sub> <sup>+</sup> Adsorption Density (mmol N/g)
Clinoptilolite	0.42	Macroporous <sup>c155,156</sup>	Aluminosilicate	3.35 <sup>157</sup>	2.19 <sup>64</sup>
Biochar <sup>d</sup>	0.25-1.25	Macroporous <sup>158</sup>	Carboxylate	4-5	3.19 <sup>68</sup>
Dowex 50	0.15-0.3 <sup>159</sup>	Microporous <sup>155</sup>	Sulfonate	-2	1.7 <sup>71</sup>
Dowex Mac 3	0.3-1.2 <sup>69</sup>	Macroporous <sup>69</sup>	Carboxylate	5 <sup>69</sup>	3.8 <sup>69</sup>

<sup>a</sup>The cut-off between macropores and micropores is 2 nm.<sup>158</sup>

<sup>b</sup>pHpZc is the pH of point of zero charge, another common metric for surface charge in zeolite and soil literature.

<sup>c</sup>Clinoptilolite pore sizes vary for grains (25-100 nm is typical) and for aggregates (500 nm is typical).<sup>156</sup>

<sup>d</sup>Given its heterogeneity, biochar has been documented to vary widely in particle size, pore structure, and adsorption density.<sup>160</sup>

**Table A2.** Synthetic Urine Recipe in 1 L nanopure water. Assumes urea completely hydrolyzed, struvite and hydroxyapatite precipitated, no volatilization, and no citrate/oxalate complexation.<sup>23</sup>

Substance	Amount	
	[g]	[ml]
Na <sub>2</sub> SO <sub>4</sub> anhydrous	2.30	
NaH <sub>2</sub> PO <sub>4</sub> anhydrous	2.10	
NaCl	3.60	
KCl	4.20	
NH <sub>4</sub> Ac	9.60	
NH <sub>4</sub> OH solution (25% NH <sub>3</sub> )		13.0
NH <sub>4</sub> HCO <sub>3</sub>	21.40	

**Table A3.** Composition of synthetic and real urine. Synthetic urine parameters based on recipe; real urine measured from samples used in these experiments.

	Synthetic Urine	Real Urine
<b>pH</b>	8.87	8.99
<b>Total Ammonia Nitrogen (mg N/L)</b>	7950	3820
<b>Sodium (mg Na/L)</b>	2560	1620
<b>Potassium (mg Na/L)</b>	2200	1470
<b>Chloride (mg Cl/L)</b>	4180	3060
<b>Total Phosphate (mg P/L)</b>	542	169
<b>Total Sulfate (mg SO<sub>4</sub>/L)</b>	472	1680
<b>Total Inorganic Carbon (mg C/L)</b>	3250	1860
<b>COD (mg O<sub>2</sub>/L)</b>	8000	3460

**Table A4.** Summary of Langmuir best fit parameters and correlation coefficients for pure salt solutions (no pH adjustment). These data were used to construct the Langmuir best fit lines in Figure 1 and the competitive Langmuir adsorption model in Figure 2a.

Adsorbent	<b>q<sub>max</sub> (mmol/g sorbent)</b>			<b>K<sub>ads</sub> (L/mmol) x 10<sup>-2</sup></b>			<b>R<sup>2</sup></b>		
	NH <sub>4</sub> <sup>+</sup>	Na <sup>+</sup>	K <sup>+</sup>	NH <sub>4</sub> <sup>+</sup>	Na <sup>+</sup>	K <sup>+</sup>	NH <sub>4</sub> <sup>+</sup>	Na <sup>+</sup>	K <sup>+</sup>
Clinoptilolite	3.56	2.97 <sup>a</sup>	2.56	1.86	1.89 <sup>a</sup>	5.05	0.887	0.896	0.772
Biochar	4.83	5.39	3.25	0.643	2.83	2.33	0.936	0.892	0.933
Dowex 50	4.98	5.71	2.87	7.60	2.43	80.2	0.922	0.988	0.887
Dowex Mac 3	9.14	9.04	3.41	0.316	0.260	0.810	0.807	0.915	0.933

<sup>a</sup>Two combinations of q<sub>max</sub> and K<sub>ads</sub> were determined from the ISOFIT model; the other was q<sub>max</sub>= 15.1 mmol/g adsorbent and K<sub>ads</sub>=0.208 x 10<sup>-2</sup>. The tabulated combination was chosen because of its proximity to the values for the other cations.

**Table A5.** Values used for modeling financial feasibility. Adsorption densities are the highest values measured in undiluted real urine adsorption experiments.

Adsorbent	Cost (USD/kg sorbent)	Adsorption Density (mmol N/g sorbent)	Bulk Density (kg/L)
Clinoptilolite	0.24 <sup>161</sup>	2.32	0.726
Biochar	0.684 <sup>162</sup>	2.54	0.314
Dowex 50	260 <sup>163</sup>	3.20	0.803
Dowex Mac 3	32 <sup>163</sup>	4.07	0.75

**Table A6.** Summary of single-solute Langmuir best fit parameters and correlation coefficients for ammonium in pure salt solutions (pH 9), synthetic urine, and real urine. These data were used to compare isotherms for different solutions. pH 4 pure salt solutions are in the  $\text{NH}_4^+$  column in Table A4.

Adsorbent	$q_{\max}$ (mmol/g sorbent)			$K_{\text{ads}}$ (L/mmol) x $10^{-2}$			$R^2$		
	pH 9	Synthetic	Real	pH 9	Synthetic	Real	pH 9	Synthetic	Real
Clinoptilolite	4.70	4.97	3.41	0.314	2.01	8.3	0.655	0.971	0.882
Biochar	3.64	5.22	4.00	0.339	0.578	5.25	0.938	0.920	0.917
Dowex 50	6.61	5.90	4.78	2.23	13.2	29.1	0.897	0.898	0.900
Dowex Mac 3	9.14	9.09	8.22	0.514	1.12	5.3	0.955	0.938	0.976

**Table A7.** Sum of squared errors (SSE) and average relative error (ARE) between multicomponent models and synthetic urine adsorption densities from batch experiments.

Adsorbent	Competitive Langmuir		Langmuir-Freundlich		Jain-Snoeyink	
	SSE (mmol/g) <sup>2</sup>	ARE (%)	SSE (mmol/g) <sup>2</sup>	ARE (%)	SSE (mmol/g) <sup>2</sup>	ARE (%)
Clinoptilolite	33.7	37.8	14.1	66.9	35.6	41.0
Biochar	11.5	85.9	36.0	473	15.6	92.0
Dowex 50	49.8	34.5	24.8	85.9	43.0	31.1
Dowex Mac 3	89.8	61.9	6.01	27.2	86.0	61.7

**Table A8.** Comparison of models to triplicate undiluted real urine adsorption. “Measured” is average ( $\pm$  SEM) of batch adsorption with undiluted urine. All adsorption densities in mmol N/g adsorbent. CL= competitive Langmuir, LF=Langmuir Freundlich, JS= Jain-Snoeyink.

Adsorbent	Measured	Predicted Value (% Error)		
		CL	LF	JS
Clinoptilolite	2.21 $\pm$ 0.09	2.16 (-2.26)	1.33 (-39.8)	2.34 (5.74)
Biochar	2.07 $\pm$ 0.01	1.87 (-9.51)	3.56 (72.0)	1.98 (-4.28)
Dowex 50	3.16 $\pm$ 0.29	2.72 (-13.8)	5.67 (79.6)	3.45 (9.34)
Dowex Mac 3	4.07 $\pm$ 0.10	3.49 (-14.3)	5.37 (31.8)	3.71 (-9.02)

### A3. FIGURES

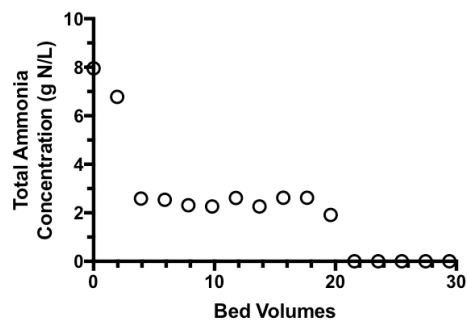


**Figure A1.** Elution curve for regeneration of Dowex Mac 3. The mass of ammonium eluted can be determined by numerically integrating the elution curve (Equation A1).

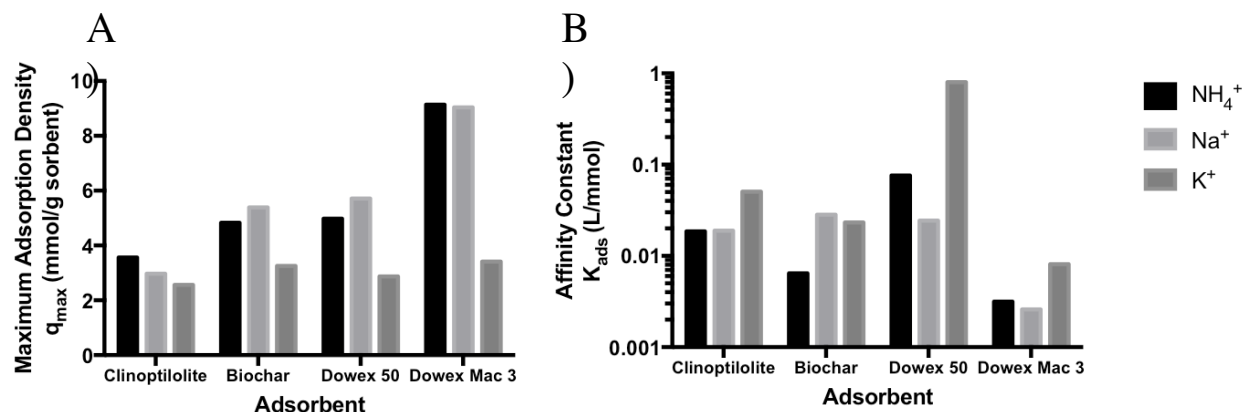


**Figure A2.** Comparison of Langmuir parameters (a)  $q_{\max}$  and (b)  $K_{\text{ads}}$  for  $\text{NH}_4\text{Cl}$ ,  $\text{NaCl}$ , and  $\text{KCl}$  without pH adjustment.

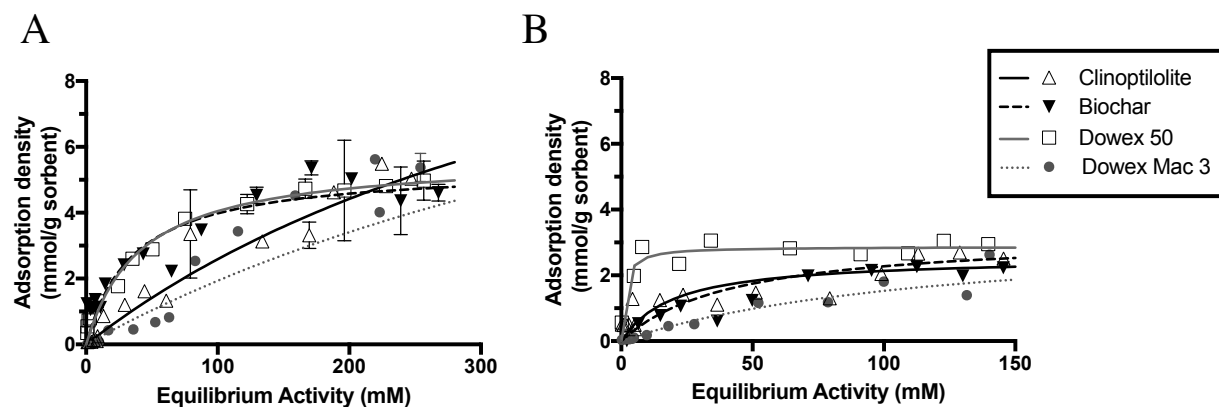


**Figure A3.** Adsorption for (a)  $\text{NaCl}$  and (b)  $\text{KCl}$  without pH adjustment. Error bars show dilution triplicates ( $n=3$ ) for high activities ( $> 100$  mM). Curves are Langmuir lines of best fit based on non-linear regression of experimental data. Best-fit parameters are in Table A4.

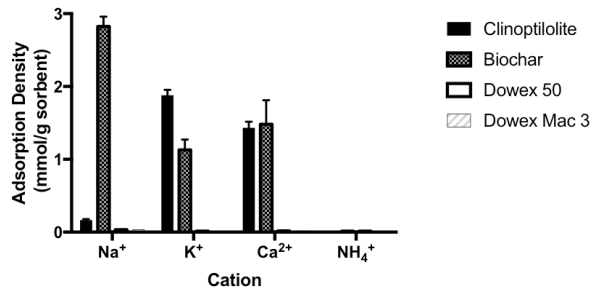


**Figure A4.** Estimated initial adsorption density of virgin adsorbents. Initial adsorption density was calculated based on aqueous concentrations after equilibrium with 0.65% H<sub>2</sub>SO<sub>4</sub> (0.015 g adsorbent in 5 mL). Here we assumed that all cations were desorbed ( $q_f=0$ ). Error bars show experimental triplicates (n=3).

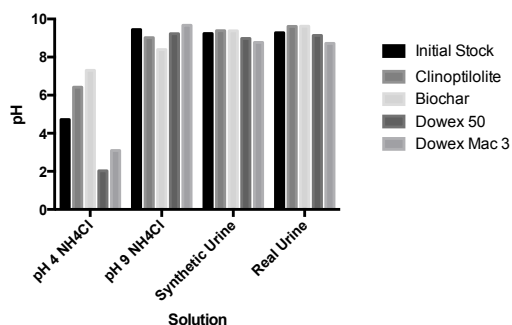


**Figure A5.** Comparison of pH of initial stock solutions (without adsorbent) and solution/adsorbent mixtures after 24-hour adsorption period. Results are shown for the highest concentrations tested: (i) 9000 mg N/L NH<sub>4</sub>Cl at pH 4, (ii) 9000 mg N/L NH<sub>4</sub>Cl at pH 9, (iii) undiluted synthetic urine, and (iv) undiluted real urine.

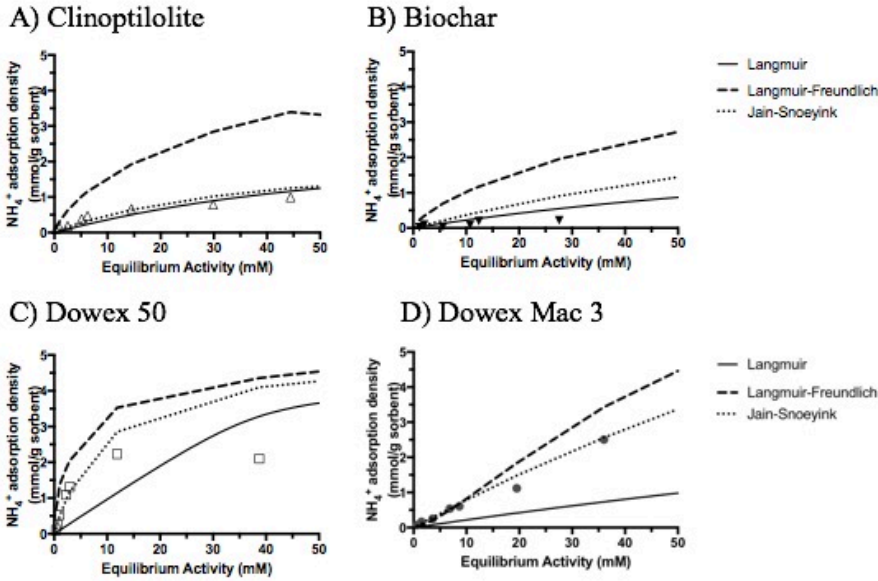


**Figure A6.** Comparison of synthetic urine adsorption data and competitive Langmuir, competitive Langmuir-Freundlich, and Jain-Snoeyink models for (a) clinoptilolite, (b) biochar, (c) Dowex 50, and (d) Dowex Mac 3. Data shown is for <50 mM. Full data set is in Figure 2.2.

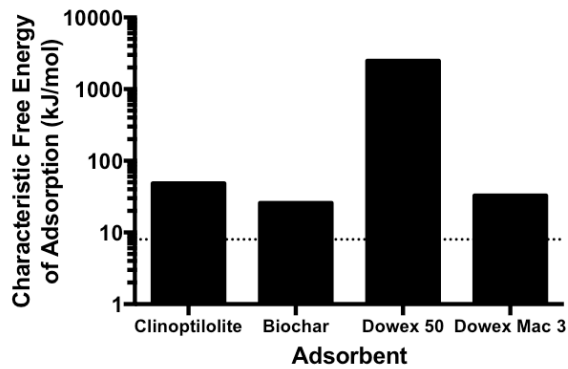


**Figure A7.** Free energies of adsorption determined from Dubinin-Radushkevich isotherm. If  $E > 8$  kJ/mol (dotted line), considered ion exchange.

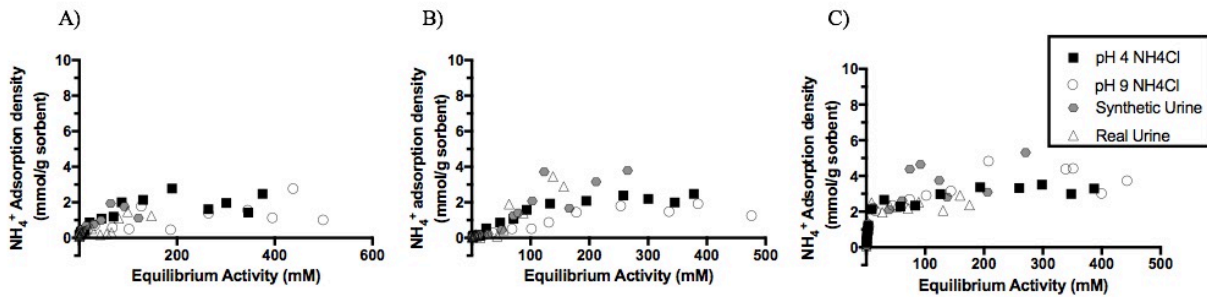


**Figure A8.**  $\text{NH}_4^+$  adsorption in all solutions for (a) clinoptilolite, (b) biochar, and (c) Dowex 50.

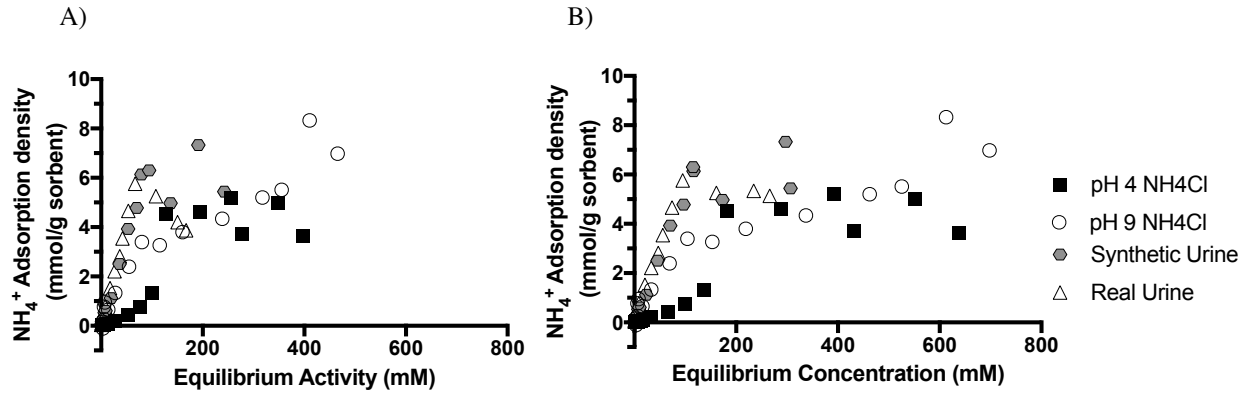


**Figure A9.** Comparison of adsorption curves relative to (a) activity (Figure 3b) and (b) concentration. The difference between figures can be attributed to ionic strength effects.

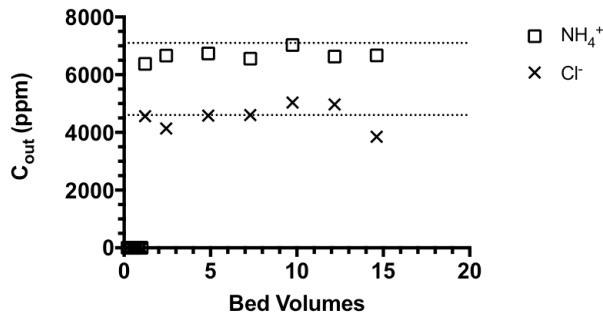


**Figure A10.** Ammonium and chloride concentrations in a control column with no resin. Measured concentrations are within 5% of influent concentrations (dotted lines, upper is  $\text{NH}_4^+$ , lower is  $\text{Cl}^-$ ).

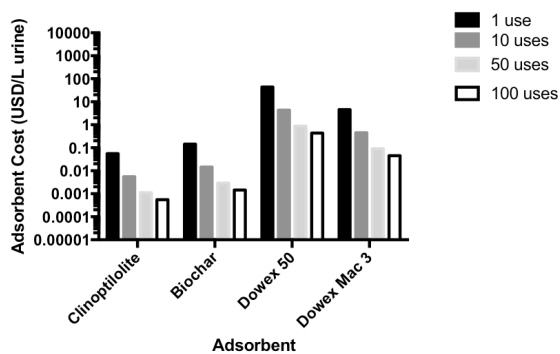


**Figure A11.** Recovery cost comparison of all four adsorbents (in USD/L urine) assuming 100% regeneration ( $r=1$ ). Urine total ammonia concentration assumed to be 7500 mg N/L.



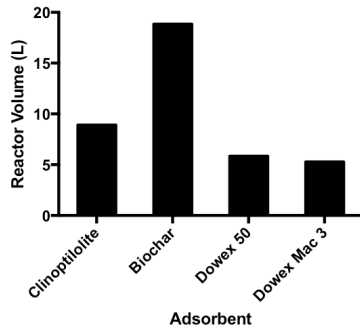


**Figure A12.** Required reactor volume (L) for each adsorbent based on adsorption density and bulk density. Volume of urine was 28 L, approximating the urine produced from four people in one week (1 L/person/day). Urine total ammonia concentration assumed to be 7500 mg N/L.

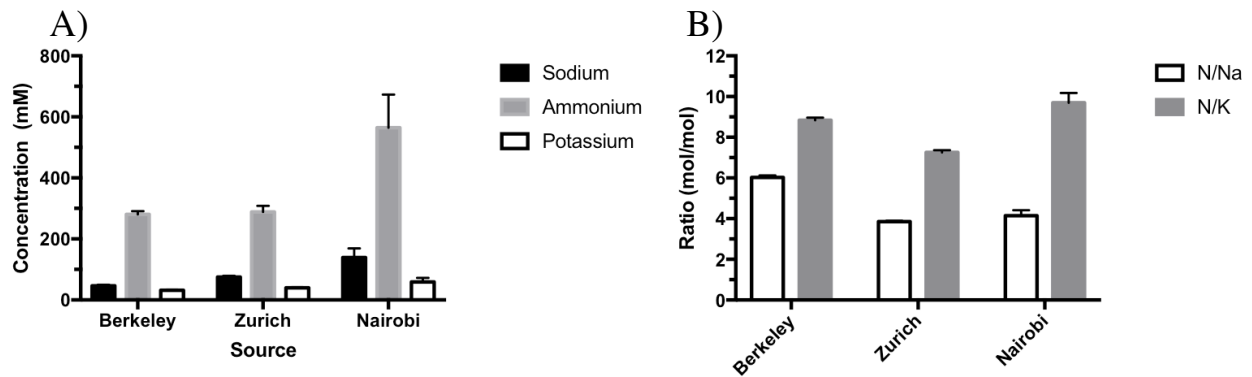


**Figure A13.** (a) Cation concentrations in urine collected in Berkeley, Zurich (Eawag), and Nairobi (Sanergy). (b) Cation concentration ratios from the same urine samples. Error bars reflect standard error of mean (n=5 Berkeley, n=3 Zurich, n=9 Nairobi).

## B. EFFECTS OF OPERATING AND DESIGN PARAMETERS ON ION EXCHANGE COLUMNS FOR NUTRIENT RECOVERY FROM URINE.

### B1. EQUATIONS

#### B1.1 Adsorption and Regeneration in Columns

Breakthrough curves and elution curves were generated from continuous adsorption and regeneration experiments, respectively. Integration of both curves allowed for calculation of the mass of ammonium adsorbed or eluted. Numerical integration was performed using the trapezoid rule:

$$\int C(BV)dBV \approx \sum_1^n \{ (BV_n - BV_{n-1}) * \frac{1}{2} * [C(BV_n) + C(BV_{n-1})] \} \quad (B1)$$

Where n is the number of data points, BV is number of bed volumes, and C(BV) is the concentration at a given number (BV) of bed volumes. For adsorption experiments, the mass of ammonium adsorbed was proportional to the area above the ammonium breakthrough curve and below the chloride tracer curve. For regeneration, the mass of ammonium eluted is proportional to the area below the elution curve. The equations for adsorption density (Equation B2) and regeneration efficiency (Equation B3) are:

$$q = \frac{\int [C_{Cl,ads}(BV) - C_{N,ads}(BV)] dBV * PV}{W * MW_N} \quad (B2)$$

$$\eta_{regen} = \frac{\int C_{N,elution}(BV) dBV}{\int [C_{Cl,ads}(BV) - C_{N,ads}(BV)] dBV} \quad (B3)$$

Where PV is pore volume (L bed volume<sup>-1</sup>), the volume of liquid retained by a column full of resin, W is resin mass (g resin), q is adsorption density (mmol N g resin<sup>-1</sup>), and the subscripts on concentration C(BV) denote adsorption or elution. Pore volume was calculated by subtracting the mass of a column full of dry resin from the same column filled with resin and distilled water. The number of bed volumes to 90% elution was calculated via interpolation of elution curve data points and cumulative area under the elution curve compared to total area (Equation B4):

$$BV_{90} = BV \left| \frac{\int_0^x C_{N,elution}(BV) dBV}{\int_0^f C_{N,elution}(BV) dBV} = 0.9 \right. \quad (B4)$$

Where x denotes cumulative bed volumes and f denotes the final bed volumes (end of experiment). Thus, bed volumes to 90% elution was calculated as the number of bed volumes at which 90% of the total mass eluted was reached, regardless of overall regeneration efficiency.

#### B1.2 Predicting phosphate adsorption density

Phosphate adsorption density was predicted based on a Freundlich model of best fit determined from batch experiments in real hydrolyzed urine (Equation B5):<sup>97</sup>

$$q_e = K_f C_e^{1/n} \quad (B5)$$

Where q<sub>e</sub> is equilibrium adsorption density (mg P g resin<sup>-1</sup>), C<sub>e</sub> is equilibrium phosphate concentration (mg P L<sup>-1</sup>), and K<sub>f</sub> (mg<sup>1-1/n</sup> L<sup>1/n</sup> g<sup>-1</sup>) and 1/n (unitless) are Freundlich constants. The

Freundlich model was combined with a mass balance (Equation B6) to predict equilibrium adsorption density.

$$\frac{W}{V}(q_e - q_0) = C_0 - C_e \quad (\text{B6})$$

In Equation B5, W/V is resin dose (g resin L<sup>-1</sup>), q is adsorption density (mg P g resin<sup>-1</sup>), C is aqueous phosphate concentration (mg P L<sup>-1</sup>), and subscripts denote equilibrium (e) and initial (0) conditions.

Equations B5 and B6 were combined to predict adsorption density assuming no initial P on the resin (q<sub>0</sub>=0), a resin dose of 10.036 g L<sup>-1</sup>,<sup>97</sup> Freundlich best-fit parameters from Sendrowski and Boyer 2013 (n=0.353, K<sub>f</sub>=0.999), and an initial phosphate concentration of 430 g P<sup>-1</sup> (measured in this study). The predicted value for q<sub>e</sub> was 0.255 mmol P g resin<sup>-1</sup>, which was reported in section 3.1.1 of the main manuscript.

### B1.3 Up-concentration in ammonium sulfate product

Concentrations of ammonium sulfate fertilizer product were determined by determining the maximum of the quotient of the area under the elution curve and elution time using Equation B6 (results in Table B9).

$$C_{product} = \text{Max} \left\{ \frac{\int C_{N,elution}(BV)dBV}{BV} \right\} \quad (\text{B7})$$

Available liquid ammonium sulfate is most often 8-9% N,<sup>108,109</sup> which is 80.7-89.6 g N L<sup>-1</sup> as calculated in Equation B7.

$$\frac{8 \text{ g N}}{100 \text{ g AS solution}} * \frac{100 \text{ g AS}}{21 \text{ g N}} * \frac{1 \text{ g solution}}{\text{mL solution}} * \frac{1000 \text{ mL solution}}{1 \text{ L solution}} * \frac{1 \text{ mol AS}}{132.14 \text{ g AS}} * \frac{2 \text{ mol N}}{1 \text{ mol AS}} * \frac{14 \text{ g N}}{1 \text{ mol N}} = 80.7 \text{ g N L}^{-1} \quad (\text{B8})$$

Where AS is ammonium sulfate, which is 21% N (molecular formula (NH<sub>4</sub>)<sub>2</sub>SO<sub>4</sub>).

The number of bed volumes required for up-concentration (BV<sub>U</sub>) was calculated according to Equation B9:

$$BV_U = \frac{q*W*MW_N}{C_{urine}*P} \quad (\text{B9})$$

where q is adsorption density (mmol N g resin<sup>-1</sup>), W is resin mass (g resin), MW<sub>N</sub> is the molar mass of nitrogen (mg N mmol N<sup>-1</sup>), C<sub>urine</sub> is the total ammonia concentration in urine (mg N L<sup>-1</sup>), and P is the pore volume (mL bed volume<sup>-1</sup>). Based on several experimental runs, the resin mass was estimated at 50 g, C<sub>urine</sub> at 5000 mg N L<sup>-1</sup>, and adsorption density at 4.9 mmol N g resin<sup>-1</sup>, giving an estimate of 8 bed volumes.

## B2. TABLES

**Table B1:** Adsorbent characteristics.

Adsorbent	Particle size (mm)	Pore structure <sup>a</sup>	Functional Group	Operating pH	Highest Reported Adsorption Density (mmol N/g. mmol P/g)
Dowex Mac 3	0.3-1.2 <sup>69</sup>	Macroporous	Carboxylate	5 <sup>69</sup>	4.9 <sup>69</sup>
LayneRT	0.3-1.2	Macroporous	Hydrous Iron Oxide	5.5-8.5	0.31 <sup>97</sup>

<sup>a</sup>The cut-off between macropores and micropores is 2 nm.<sup>158</sup>

**Table B2:** Composition of synthetic and real urine. Synthetic urine parameters based on recipe; real urine measured from samples used in these experiments.

	Synthetic Urine
<b>pH</b>	8.87
<b>Total Ammonia Nitrogen (mg N L<sup>-1</sup>)</b>	7950
<b>Sodium (mg Na L<sup>-1</sup>)</b>	2560
<b>Potassium (mg Na L<sup>-1</sup>)</b>	2200
<b>Chloride (mg Cl L<sup>-1</sup>)</b>	4180
<b>Total Phosphate (mg P L<sup>-1</sup>)</b>	542
<b>Total Sulfate (mg SO<sub>4</sub> L<sup>-1</sup>)</b>	472
<b>Total Inorganic Carbon (mg C L<sup>-1</sup>)</b>	3250
<b>COD (mg O<sub>2</sub> L<sup>-1</sup>)</b>	8000

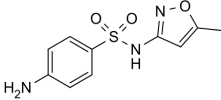
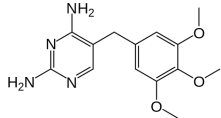
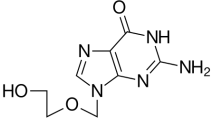
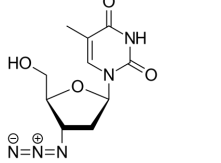
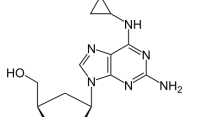
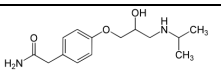
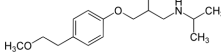
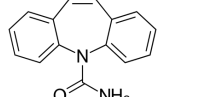
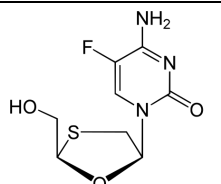
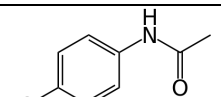
**Table B3:** Synthetic Urine Recipe in 1 L nanopure water. Assumes urea completely hydrolyzed, struvite and hydroxyapatite precipitated, no volatilization, and no citrate/oxalate complexation.<sup>23</sup>

Substance	Amount	
	[g]	[ml]
Na <sub>2</sub> SO <sub>4</sub> anhydrous	2.30	
NaH <sub>2</sub> PO <sub>4</sub> anhydrous	2.10	
NaCl	3.60	
KCl	4.20	
NH <sub>4</sub> Ac	9.60	
NH <sub>4</sub> OH solution (25% NH <sub>3</sub> )		13.0
NH <sub>4</sub> HCO <sub>3</sub>	21.40	

**Table B4.** Stock regenerant concentrations from Alibaba.com (accessed May 11, 2016). For NaCl, a saturated solution was assumed based on the solubility of NaCl at 25° C (359 g NaCl L<sup>-1</sup>).<sup>164</sup>

<i>Regenerant</i>	<i>C<sub>stock</sub> (M)</i>
<i>H<sub>2</sub>SO<sub>4</sub></i>	18.21
<i>HCl</i>	10.35
<i>HNO<sub>3</sub></i>	15.47
<i>NaCl</i>	6.143

**Table B5:** Properties of trace organic contaminants

Abbrev	Compound	Structure	Function	MW (g/mol)	pKa	Log K <sub>ow</sub>	Predominant Charge at pH 9
SMX	Sulfamethoxazole		Antibiotic	253.28	1.7, 5.6	0.89 <sup>165</sup>	Negative
TMP	Trimethoprim		Antibiotic	290.32	7.4	0.79 <sup>165</sup>	Positive
ACY	Acyclovir		Antiviral	225.21	2.3, 9.3	-1.76 <sup>165</sup>	Neutral
ZDV	Zidovudine		Antiretroviral	267.24	9.7	-0.53 <sup>165</sup>	Neutral
ABA	Abacavir		Antiretroviral	286.33	5.01	0.72 <sup>165</sup>	Positive
ATE	Atenolol		Beta blocker	266.34	9.6	0.16 <sup>166</sup>	Positive
MET	Metoprolol		Beta blocker	267.37	9.5	1.76 <sup>167</sup>	Positive
CBZ	Carbamazepine		Antiepileptic	236.27	13.9	2.67 <sup>167</sup>	Positive
FTC	Emitricitabine		Antiretroviral	247.25	14.3	-3.96 <sup>167</sup>	Neutral
ACE	Acetaminophen		Pain reliever	151.16	9.7	0.34 <sup>165</sup>	Neutral

<sup>a</sup>Deborde et al 2008<sup>168</sup> (pH 7)<sup>b</sup>Barazesh et al 2016<sup>169</sup> (pH 8)

**Table B6.** Bed volumes to 90% elution, breakthrough curve slopes, and adsorption density for phosphate adsorption in real urine. \* denotes significant difference between two rows.

	Bed volumes to 90% elution	Slope (BV <sup>-1</sup> )	Adsorption density (mmol P g resin <sup>-1</sup> )
In series	10.6 ± 0.21	1.13 ± 0.20*	0.50 ± 0.04
Mixed bed	7.70 ± 0.23	0.69 ± 0.08*	0.53 ± 0.04

**Table B7.** Bed volumes to 90% elution, breakthrough curve slopes, and adsorption density for ammonium adsorption in real urine. \* denotes significant difference between two rows.

	Bed volumes to 90% elution	Slope (BV <sup>-1</sup> )	Adsorption density (mmol N g resin <sup>-1</sup> )
In series	16.1 ± 0.6	0.20 ± 0.05	5.44 ± 0.91
Mixed bed	18.3 ± 0.5	0.19 ± 0.02	6.76 ± 0.50*
Struvite supernatant	18.4 ± 0.8	0.34 ± 0.06	2.54 ± 0.57*
Cation exchange only	14.7 ± 1.4	0.26 ± 0.04	4.10 ± 0.17

**Table B8.** Henry's law constant for selected gases (M/atm).

<i>Compound</i>	<i>K<sub>H</sub> (M atm<sup>-1</sup>)</i>
<i>N<sub>2</sub></i>	6.3 x 10 <sup>-4</sup>
<i>NO</i>	1.9 x 10 <sup>-3</sup>
<i>N<sub>2</sub>O</i>	2.5 x 10 <sup>-2</sup>
<i>O<sub>2</sub></i>	1.3 x 10 <sup>-3</sup>
<i>CO<sub>2</sub></i>	3.4 x 10 <sup>-2</sup>
<i>NH<sub>3</sub></i>	59

**Table B9.** Ammonium recovery efficiencies, and stoichiometric efficiencies, and bed volumes to 90% elution for elution experiments at high concentration and low flow rate. Resin was exhausted during adsorption with synthetic urine. TAN is total ammonia nitrogen.

H <sub>2</sub> SO <sub>4</sub> Concentration (M)	Flow rate (mL/min)	Bed volumes to 90% elution	Stoichiometric Efficiency (%)	Recovery Efficiency (%)	Final Eluent TAN (g N L <sup>-1</sup> )
2	3	3.37	52.2	89.1	20.9
3	2	3.02	33.3	81.4	22.3
6	2	2.78	19.1	101	22.2

**Table B10.** Potassium recovery efficiencies, stoichiometric efficiencies, and bed volumes to 90% elution for triplicate elution experiments with various regenerants. Resin was exhausted during adsorption with synthetic urine. Recovery efficiencies greater than 100% are due to variability of measuring low K concentrations in eluent.

	Bed volumes to 90% elution	Stoichiometric Efficiency (%)	Recovery Efficiency (%)
HNO <sub>3</sub>	18.2 ± 1.8	7.2 ± 0.7	134 ± 7.3
HCl	25.4 ± 5.0	6.2 ± 1.2	136 ± 6.7
NaCl	17.3 ± 1.3	8.2 ± 0.7	87.6 ± 9.5
H <sub>2</sub> SO <sub>4</sub>	16.6 ± 0.9	8.0 ± 0.8	111 ± 1.8



### B3. FIGURES

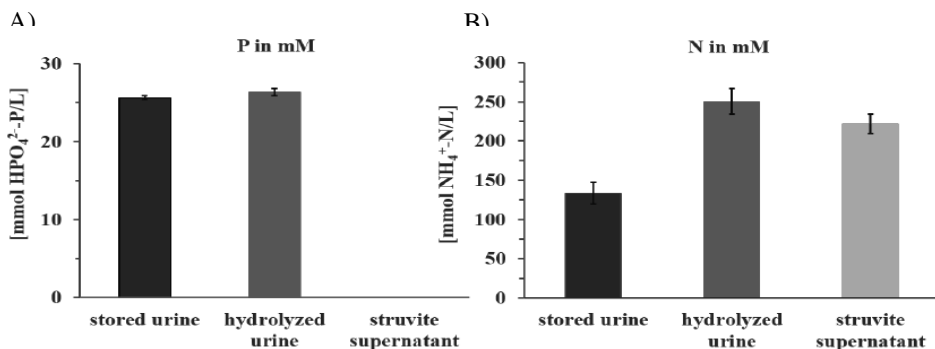


**Figure B1.** Phosphorus (P) and total ammonia nitrogen (N) concentrations for stored urine, hydrolyzed urine after urease addition, and struvite supernatant (after  $MgCl_2$  addition, mixing, and settling). Error bars represent  $\pm$  one standard deviation for experimental triplicates.

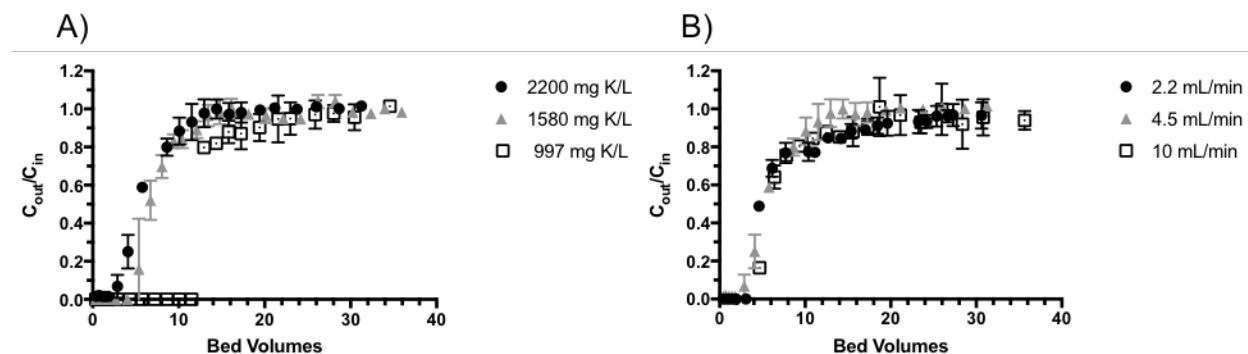


**Figure B2.** Potassium breakthrough curves with synthetic urine influent for (a) varying influent concentrations and (b) varying flow rate. Error bars represent  $\pm$  one standard deviation for experimental triplicates. Error bars not shown are smaller than symbol.

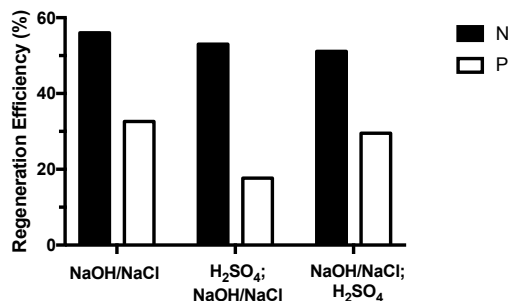


**Figure B3.** Regeneration efficiencies for nitrogen and phosphorus from mixed bed column. Regenerants used were 0.122 M  $H_2SO_4$  and 2% NaOH/ 2% NaCl (0.5 M NaOH/0.342 M NaCl). Semicolon denotes switching regenerants halfway through regeneration experiment (150 min of each solution).

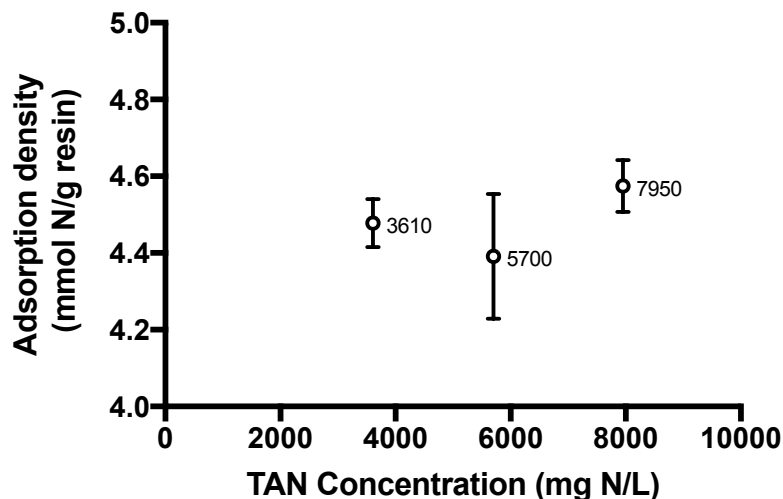


**Figure B4.** Ammonium adsorption densities vs. concentration for adsorption with synthetic urine at  $4.5 \text{ mL min}^{-1}$ . Error bars are  $\pm 1$  standard deviation. Point labels are TAN concentrations.

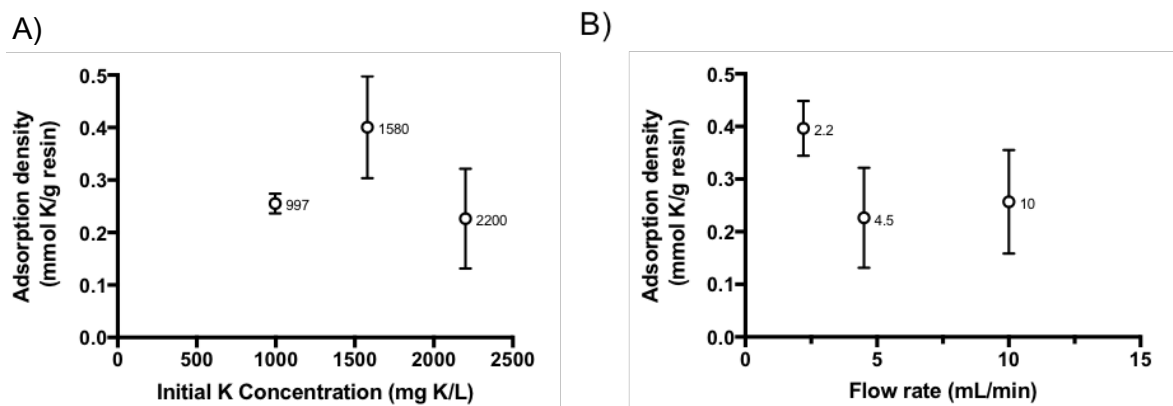


**Figure B5.** Potassium adsorption densities for varying (a) concentration and (b) flow rate with synthetic urine. Error bars are  $\pm 1$  standard deviation.

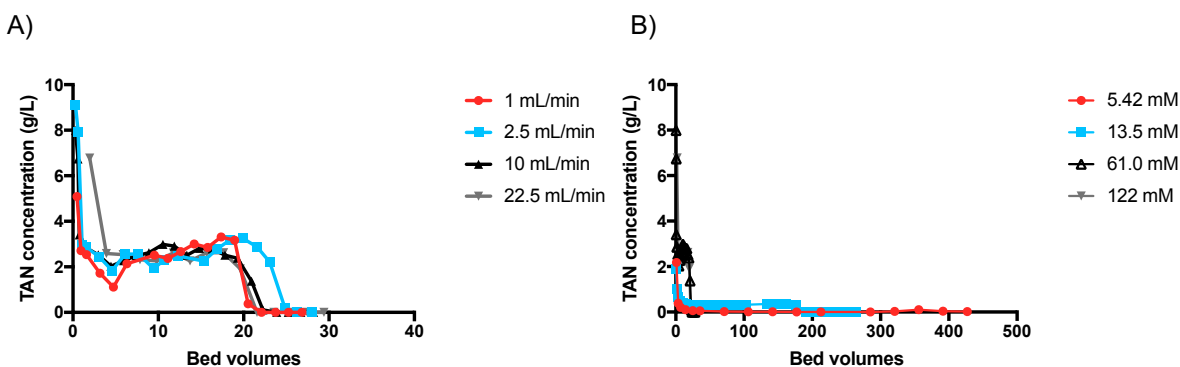


**Figure B6.** Elution curves for varying (a) flow rate and (b) acid concentration. Flow rate experiments conducted with  $122 \text{ mM H}_2\text{SO}_4$  and concentration experiments conducted at  $22.5 \text{ mL min}^{-1}$ .

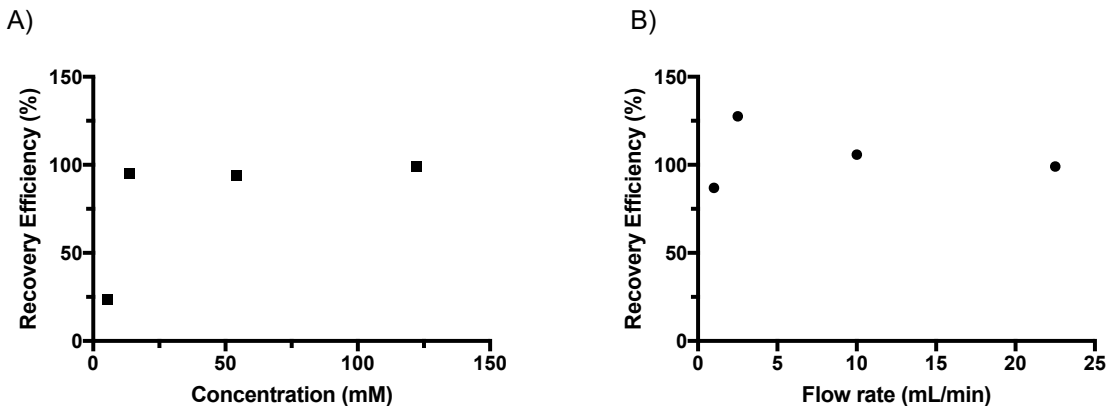


**Figure B7.** Nitrogen recovery efficiency during elution for varying (a) concentration and (b) flow rate was consistently above 90% for all flow rates tested (1-22.5 mL min<sup>-1</sup>) and for concentrations greater than or equal to 13.6 mM.

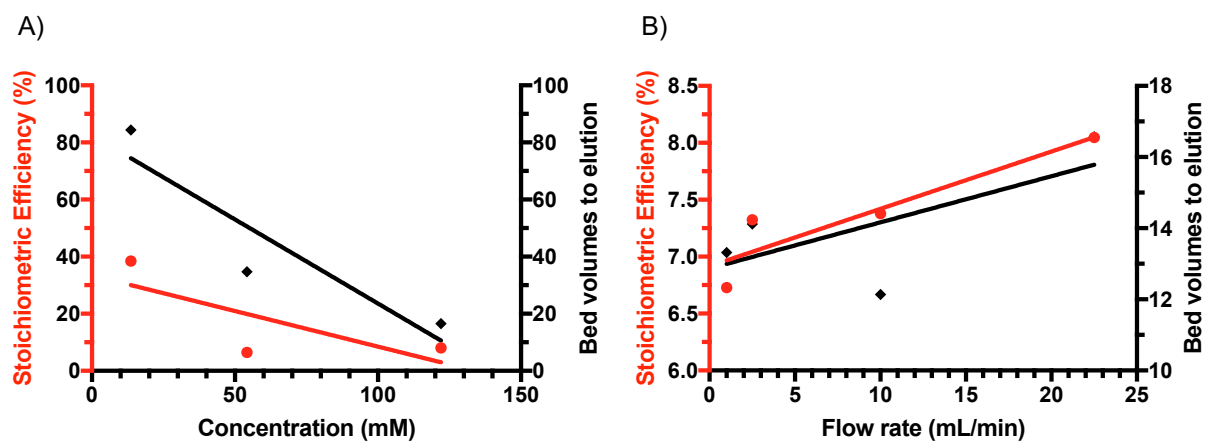


**Figure B8.** Sulfuric acid use efficiency compared to stoichiometric exchange for potassium elution and column regeneration with (a) varying concentration and (b) varying flow rate. Linear regression lines show slope of each correlation. Resin was exhausted during adsorption with synthetic urine. Lowest concentration excluded because potassium concentrations were below detection limit.

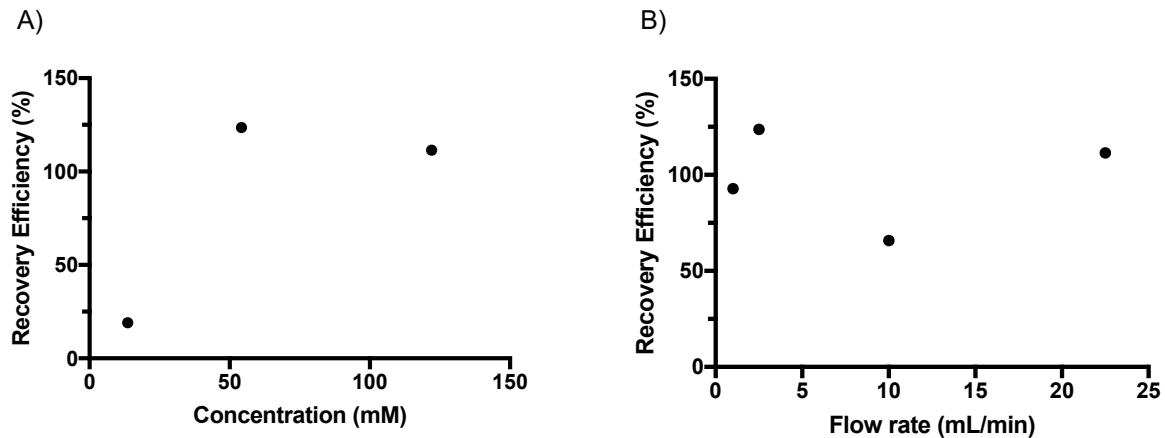


**Figure B9.** Potassium recovery efficiency for (a) varying regenerant concentration and (b) varying elution flow rate.

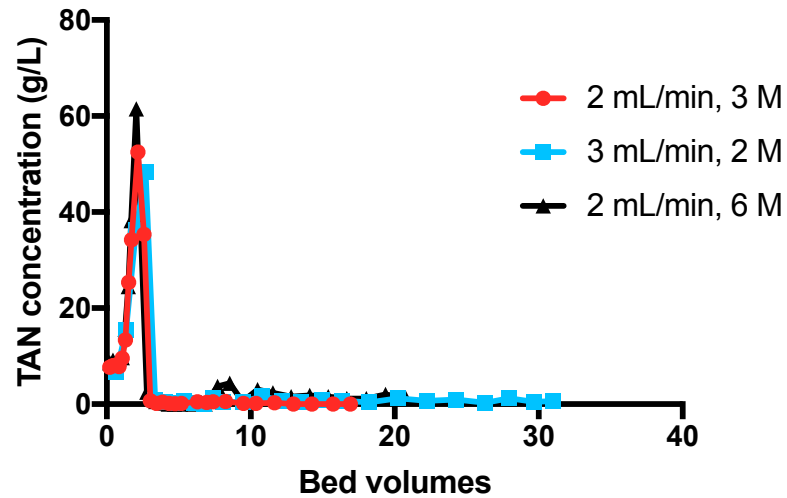


**Figure B10.** Sulfuric acid elution curves for high concentration and low flow rate. Bed volumes to elution, stoichiometric efficiencies, and regeneration efficiencies in Table B9.

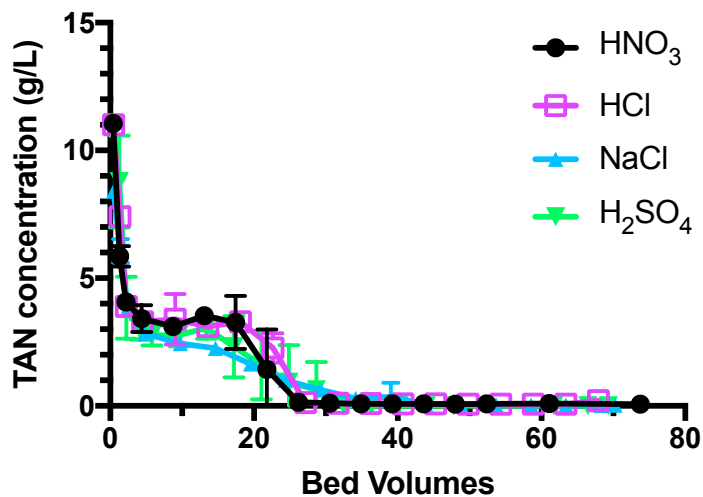


**Figure B11.** Elution curves for equinormal (0.244 N) regenerants. Error bars are  $\pm 1$  standard deviation; some error bars too small to see.

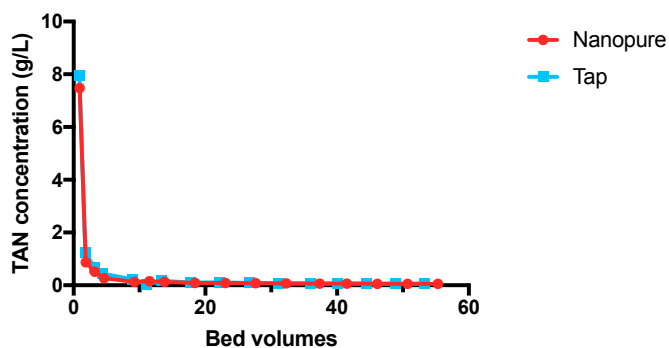


**Figure B12.** Elution curves for nanopure and tap water. Concentration decreases immediately as synthetic urine elutes from column.

## C. ELECTROCHEMICAL STRIPPING TO RECOVER NITROGEN FROM URINE

### C1. EQUATIONS

#### C1.1 Batch Experiment Nitrogen Recovery

Equation C1: In batch experiments, Recovery efficiency (R, in %) calculated by dividing TAN concentration in trap chamber at end of experiment ( $C_{T,F}$ , g N L<sup>-1</sup>) by initial TAN concentration in anode chamber ( $C_{A0}$ ).

$$R = \frac{C_{T,F}}{C_{A0}} * 100\% \quad (C1)$$

#### C1.2 Continuous Experiment Calculations

##### Energy Input

Energy input per mass of nitrogen ( $E_N$ , MJ kg N<sup>-1</sup>) was calculated according to Desloover 2012.<sup>122</sup>

$$E_N = \frac{V * I_{applied} * 1000 \frac{g N}{kg N} * 60 \frac{min}{hr} * 60 \frac{s}{min} * 24 \frac{hr}{d}}{3.6E6 \frac{J}{MJ} * J_{N,AC}} \quad (C2)$$

Where V is measured cell voltage,  $I_{applied}$  is applied current density (A m<sup>-2</sup>), and  $J_{N,AC}$  is nitrogen flux from anode to cathode (g N m<sup>-2</sup> d<sup>-1</sup>).

##### Fluxes

Nitrogen flux from anode to cathode was calculated by mass balance, as in Desloover 2012<sup>122</sup>:

$$J_{N,AC} = \frac{Q_A(C_{A,in} - C_{A,out})}{A} \quad (C3)$$

Where  $J_{N,AC}$  is nitrogen flux from anode to cathode (g N m<sup>-2</sup> d<sup>-1</sup>),  $Q_A$  (L d<sup>-1</sup>) is anode flow rate, A (m<sup>2</sup>) is cation exchange membrane surface area, and  $C_{A,in}$  and  $C_{A,out}$  (both g N L<sup>-1</sup>) are steady-state influent and effluent anode concentrations.

Nitrogen flux from cathode to trap ( $J_{N,CT}$ , g N m<sup>-2</sup> d<sup>-1</sup>) was calculated as according to equation c. Both trap and cathode chamber solutions were recirculated in batch mode.

$$J_{N,CT} = \frac{Q_A C_{T,F}}{A} \quad (C4)$$

where  $C_{T,F}$  is steady state TAN concentration in trap chamber ( $\text{g N L}^{-1}$ ),  $Q_A$  ( $\text{L d}^{-1}$ ) is anode flow rate, and  $A$  ( $\text{m}^2$ ) is polypropylene membrane surface area.

### Removal and recovery efficiencies

Removal efficiencies across the cation exchange membrane (from anode to cathode) were calculated as:

$$\eta_{removal} = \frac{C_{A,in} - C_{A,out}}{C_{A,in}} * 100\% \quad (C5)$$

Recovery efficiencies across the gas permeable membrane (from cathode to trap) were calculated as

$$\eta_{recovery} = \frac{C_{T,F}}{C_{A,in} - C_{A,out}} * 100\% \quad (C6)$$

Where  $C_{T,F}$  is steady state TAN concentration in trap chamber ( $\text{g N L}^{-1}$ ) and  $C_{A,in}$  and  $C_{A,out}$  (both  $\text{g N L}^{-1}$ ) are steady-state influent and effluent anode concentrations.

### Current Efficiency

Current efficiency is defined as the proportion of electrons transported that are matched by a transformation or transport of interest. Current efficiency (CE, %) for ammonia was also calculated according to Desloover 2012.<sup>122</sup>

$$CE_N = \frac{J_{N,AC} * z_{NH_4^+} * F}{MW_N * 60 \frac{\text{min}}{\text{hr}} * 60 \frac{\text{s}}{\text{min}} * 24 \frac{\text{hr}}{\text{d}} * I_{applied}} * 100\% \quad (C7)$$

Where  $J_{N,AC}$  is nitrogen flux from anode to cathode ( $\text{g N m}^{-2} \text{d}^{-1}$ ),  $z_{NH_4^+}$  is charge of ammonium ion,  $F$  is Faraday's constant,  $MW_N$  is molecular weight of nitrogen, and  $I_{applied}$  is applied current density ( $\text{A m}^{-2}$ ).

Current efficiency for chloride oxidation was calculated based on measured HOCl concentrations in a 1 hr experiment with ammonium sulfate adjusted to pH 9 (Figure C7). The slope of the linear regression was the chlorine production rate:  $0.0003853 \pm 1.133 \times 10^{-5} \text{ mg Cl}_2 \text{ equiv coulomb}^{-1}$ . This rate was converted to a current efficiency for chlorine according to the equation:

$$\frac{0.0003853 \text{ mg Cl}_2 \text{ equiv}}{\text{coulomb}} * \frac{\text{mmol Cl}_2 \text{ equiv}}{70.9 \text{ mg Cl}_2 \text{ equiv}} * \frac{\text{mmol Cl}_2 \text{ equiv}}{70.9 \text{ mg Cl}_2 \text{ equiv}} * \frac{\text{mol Cl}_2 \text{ equiv}}{1000 \text{ mmol Cl}_2 \text{ equiv}} * \frac{\text{coulomb}}{6.242 \times 10^{18} e^-} * \frac{6.02 \times 10^{23} e^-}{\text{mol } e^-} * 100\% = \mathbf{0.052 \% \text{ Current efficiency for HOCl production (C8)}}$$



## C2. TABLES

**Table C1:** Product information for cation exchange membrane (CEM) and gas permeable membrane (GPM)

Function	Manufacturer	Model Number	Active layer	Support Material	Nominal Pore Size ( $\mu\text{m}$ )	Thickness ( $\mu\text{m}$ )
Gas permeable membrane	3M	0.2 micron	Polypropylene	No	0.59	110
Cation exchange membrane	Membranes International, Inc.	CMI-7000	Polystyrene, divinylbenzene	No	0.002 (varies)	450

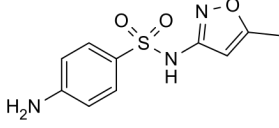
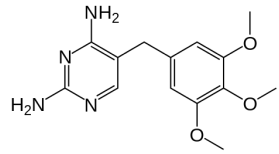
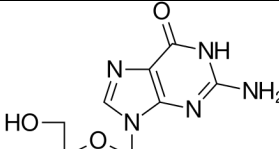
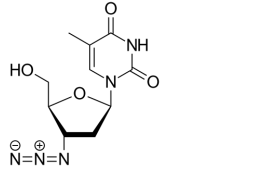
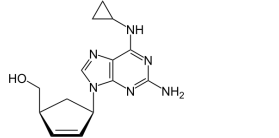
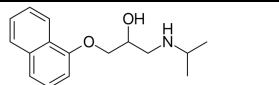
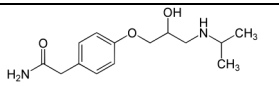
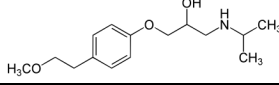
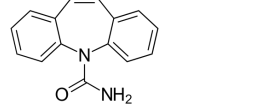
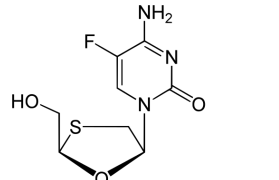
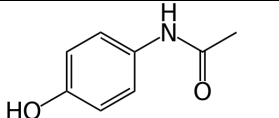
**Table C2.** Composition of influents. Synthetic urine is according to recipe in Table C2; diluted synthetic urine was used as influent to more closely match TAN in synthetic and real urine

	$(\text{NH}_4)_2\text{SO}_4$	Synthetic Urine	Synthetic Urine (diluted)	Real Urine
pH	9.44	8.87	9.13	8.99
Total Ammonia Nitrogen (mg N/L)	3400	7950	3740	3820
Sodium (mg Na/L)	0	2560	1200	1620
Potassium (mg Na/L)	0	2200	1030	1470
Chloride (mg Cl/L)	0	4180	1960	3060
Total Phosphate (mg P/L)	0	542	255	169
Total Sulfate (mg $\text{SO}_4/\text{L}$ )	2980	472	222	1680
Total Inorganic Carbon (mg C/L)	0	3250	1530	1860
COD (mg $\text{O}_2/\text{L}$ )	0	8000	3760	3460

**Table C3.** Synthetic Urine Recipe in 1 L nanopure water. Assumes urea completely hydrolyzed, struvite and hydroxyapatite precipitated, no volatilization, and no citrate/oxalate complexation<sup>23</sup>

Substance	Amount	
	[g]	[ml]
$\text{Na}_2\text{SO}_4$ anhydrous	2.30	
$\text{NaH}_2\text{PO}_4$ anhydrous	2.10	
NaCl	3.60	
KCl	4.20	
$\text{NH}_4\text{Ac}$	9.60	
$\text{NH}_4\text{OH}$ solution (25% $\text{NH}_3$ )		13.0
$\text{NH}_4\text{HCO}_3$	21.40	

**Table C4. Properties of trace organic contaminants**

Abbrev.	Compound	Structure	Function	MW (g/mol)	pKa	$k_{\text{HOCl}}$ at pH 7 ( $\text{M}^{-1}\text{s}^{-1}$ )	Log $K_{\text{ow}}$
SMX	Sulfamethoxazole		Antibiotic	253.28	1.7, 5.6	$1.8 \times 10^{3a}$	$0.89^{165}$
TMP	Trimethoprim		Antibiotic	290.32	7.4	$58^a$	$0.79^{165}$
ACY	Acyclovir		Antiviral	225.21	2.3, 9.3	$9.9^b$	- $1.76^{165}$
ZDV	Zidovudine		Antiretroviral	267.24	9.7	--	- $0.53^{165}$
ABA	Abacavir		Antiretroviral	286.33	5.01	$7.1^b$	$0.72^{165}$
PRO	Propranolol		Beta blocker	259.34	9.1	Fast <sup>a</sup>	$3.12^{166}$
ATE	Atenolol		Beta blocker	266.34	9.6	Fast <sup>a</sup>	$0.16^{166}$
MET	Metoprolol		Beta blocker	267.37	9.5	Fast <sup>a</sup>	$1.76^{167}$
CBZ	Carbamazepine		Antiepileptic	236.27	13.9	$2.6 \times 10^{-2b}$	$2.67^{167}$
FTC	Emitricitabine		Antiretroviral	247.25	14.3	--	- $3.96^{167}$
ACE	Acetaminophen		Pain reliever	151.16	9.7	$13^a$	$0.34^{165}$

<sup>a</sup>Deborde et al 2008<sup>168</sup> (pH 7)<sup>b</sup>Barazesh et al 2016<sup>169</sup> (pH 8)

**Table C5.** Relevant literature values for nitrogen flux across cation exchange membrane (CEM) and current densities (applied for electrochemical cells, produced for microbial fuel cells) in microbial fuel cells (MFCs) and electrochemical cells (ECs)

Study	CEM Flux (g N/m <sup>2</sup> *d)	Current density (A/m <sup>2</sup> )	Influent	Cell Type
Desloover 2014 <sup>170</sup>	47	10	Anaerobic digestate	EC
Luther 2015 <sup>121</sup>	500	50	Synthetic Urine	EC
Desloover 2013 <sup>122</sup>	120	20	Anaerobic digestate	EC
Kuntke 2012 <sup>171</sup>	3.29	0.5	Real Urine	MFC
Rodriguez Arredondo 2016 <sup>124</sup>	300	50	Real Urine	EC
This study	1710	100	Real Urine	EC

**Table C6.** Relevant literature values for nitrogen recovery efficiency in microbial fuel cells (MFCs) and electrochemical cells (ECs)

Study	Recovery Efficiency (%)	Influent, notes	Cell Type
Ledezma 2017	50	Synthetic Urine	MFC
Luther 2015	57	Real Urine, EC and absorption tower	EC
Luther 2015	79	Real Urine, also strip head space	EC
Desloover 2015	28	Anaerobic digestate	EC
Kuntke 2016	42	Real Urine	MFC
This study	61 <sup>a</sup>	CEM, real urine	EC
This study	50 <sup>a</sup>	GPM, real urine	EC

**Table C7.** Relevant literature values for required energy input in microbial fuel cells (MFCs) and electrochemical cells (ECs). Negative values indicate energy produced

Study	Energy Input (MJ/kg N)	Influent	Cell Type
Ledezma 2017 <sup>172</sup>	8.58	Synthetic Urine	MFC
Luther 2015 <sup>121</sup>	43.2	Real Urine	EC
Kuntke 2012 <sup>171</sup>	-3.46	Real Urine	MFC
Desloover 2014 <sup>170</sup>	61.2	Anaerobic digestate	EC
This study	30.6	Real Urine	EC

**Table C8.** Second order rate constants for reactions with chlorine

Species	$k_{\text{HOCl}}$ (1/(M*s))	pKa
Ammonia	$3.39 \times 10^6$	9.25
Ammonium	-*	9.25
Phenol	0.36	9.99
Phenolate	$2.86 \times 10^4$	9.99
Acetate	$1 \times 10^{-6}$	4.76

\*All rate constants from Deborde and von Gunten 2008<sup>168</sup>

**Table C9.** Detection limits of measured ions by ion chromatography with CC16 column for cations and AC14 column for anions

Compound	Detection Limit (mg/L)
Li <sup>+</sup>	0.05
Na <sup>+</sup>	0.1
NH <sub>4</sub> <sup>+</sup>	0.05
K <sup>+</sup>	0.05
Mg <sup>2+</sup>	0.05
Ca <sup>2+</sup>	0.05
F <sup>-</sup>	0.03
C <sub>2</sub> H <sub>3</sub> O <sub>2</sub> <sup>-</sup>	1.0
Cl <sup>-</sup>	0.11
NO <sub>2</sub> <sup>-</sup>	0.08
Br <sup>-</sup>	0.08
NO <sub>3</sub> <sup>-</sup>	0.29
HPO <sub>4</sub> <sup>2-</sup>	0.52
SO <sub>4</sub> <sup>2-</sup>	0.49

**Table C10.** Maximum Contaminant Levels (MCLs) for five metals monitored in this study

Compound	MCL (ppb)
Cr	100
Cu	1300
As	10
Se	50
Cd	5

### C3. FIGURES

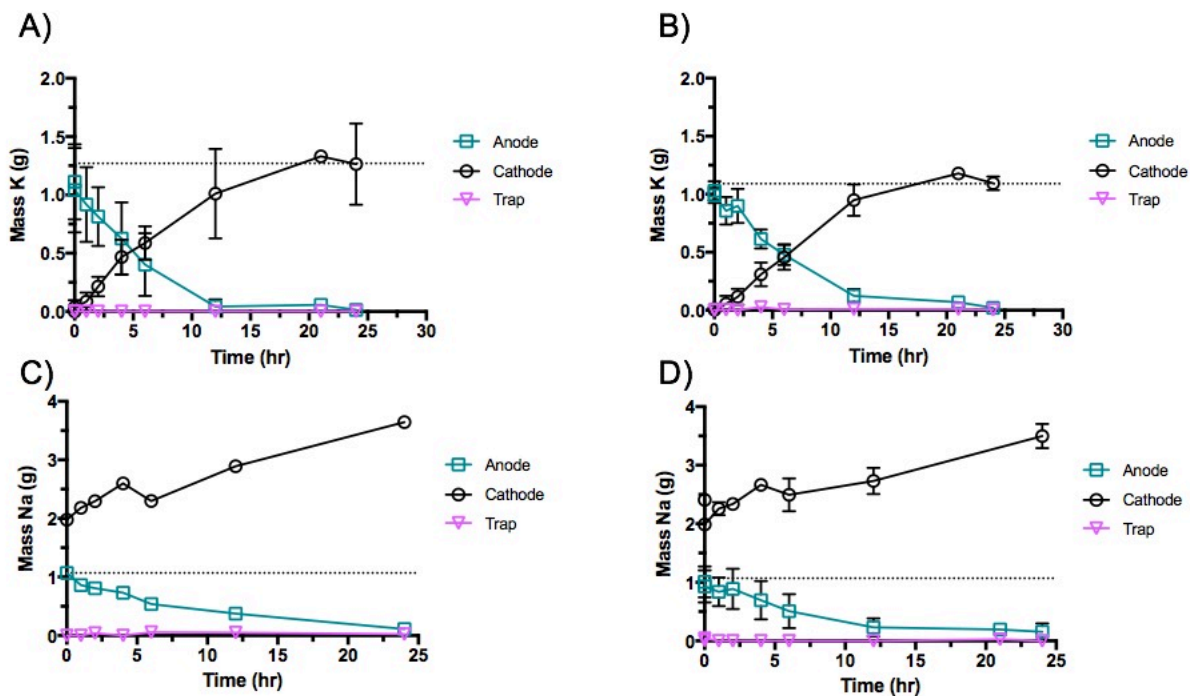


**Figure C1.** Mass balance for potassium (K) recovery in (a) real and (b) synthetic urine; mass balance for sodium (Na) recovery in (c) real and (d) synthetic urine. Na in cathode is higher than in anode because catholyte was 0.1 M NaCl. Error bars represent  $\pm$  one standard deviation. Error bars not shown are too small to be shown, expect for 21 hours (n=1). Large standard deviations in (a) due to varying real urine sodium concentrations from different batches.

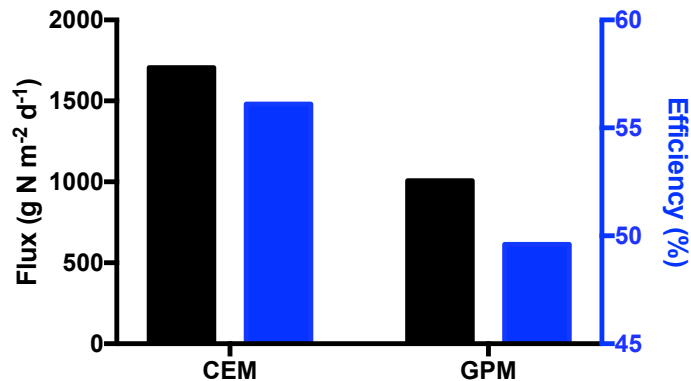


**Figure C2.** Transmembrane fluxes and nitrogen removal efficiencies for cation exchange membrane (CEM, anode to cathode) and gas permeable membrane (GPM, cathode to trap).

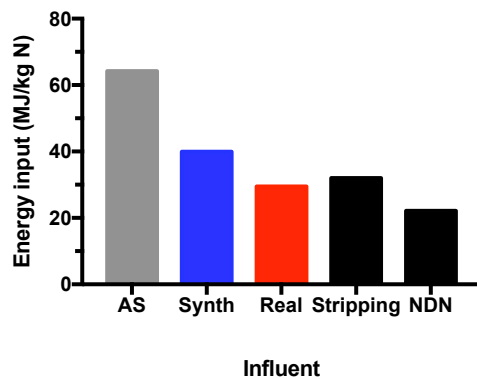


**Figure C3.** Energy input (MJ/kg N) for varied influents in continuous flow experiment, compared to conventional ammonia stripping<sup>173</sup> and nitrification-denitrification with methanol addition (NDN).

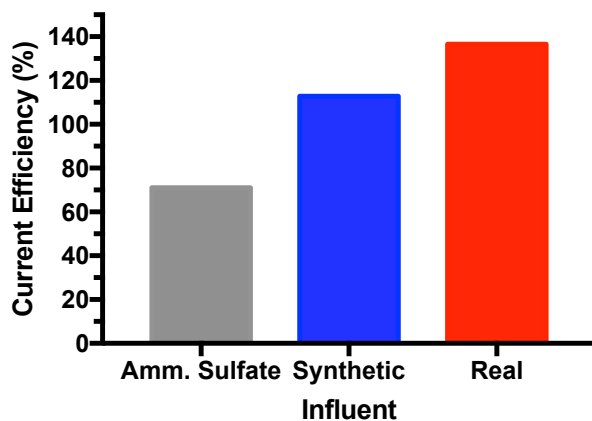


**Figure C4.** Current efficiency for total ammonia in varied influents.

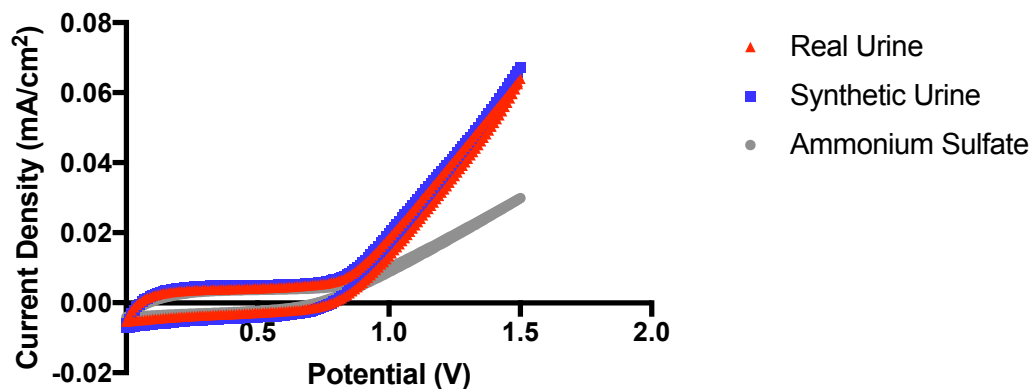


**Figure C5.** Cyclic voltammetry of varied influents. Potential measured vs. Ag/AgCl reference electrode.

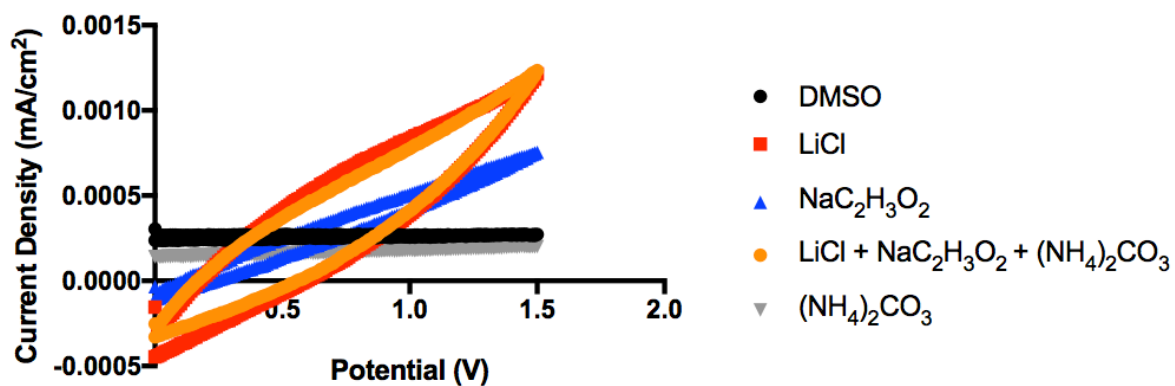


**Figure C6.** Cyclic voltammetry of varied influents in dimethyl sulfoxide (DMSO), an aprotic solvent that excluded water oxidation. All solutions 10 mM; potential measured vs. Ag/AgCl reference electrode.

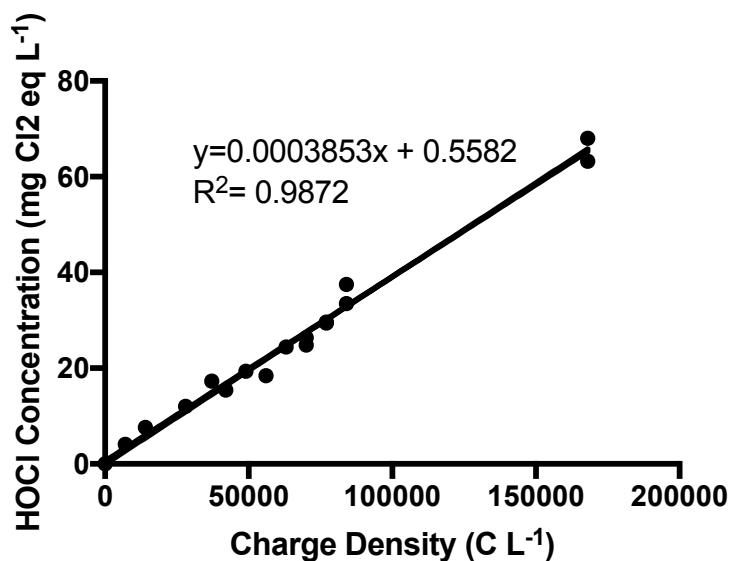


**Figure C7.** Chlorine production vs. applied charge density. Equation and correlation coefficient are for line of best fit.

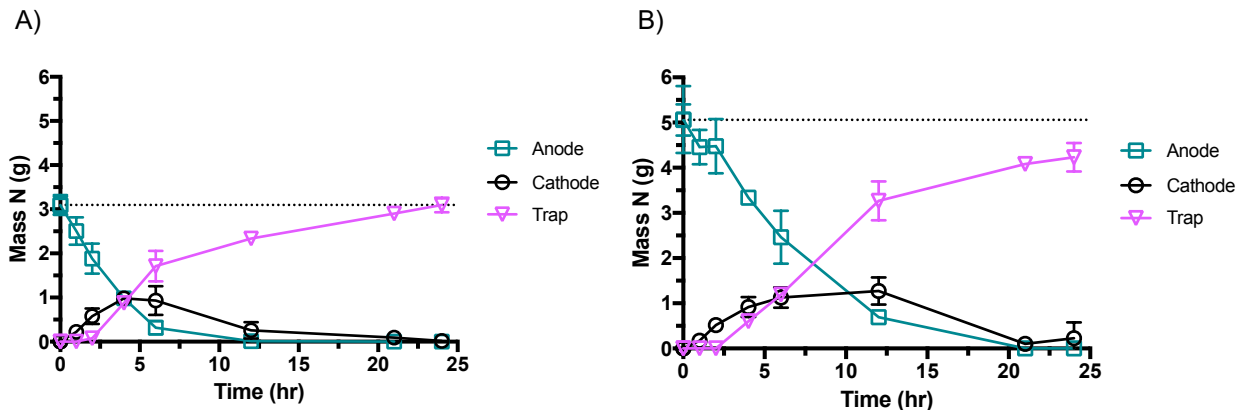


**Figure C8.** Mass balance line graph TAN for (a) ammonium sulfate and (b) synthetic urine. Error bars represent  $\pm$  one standard deviation.

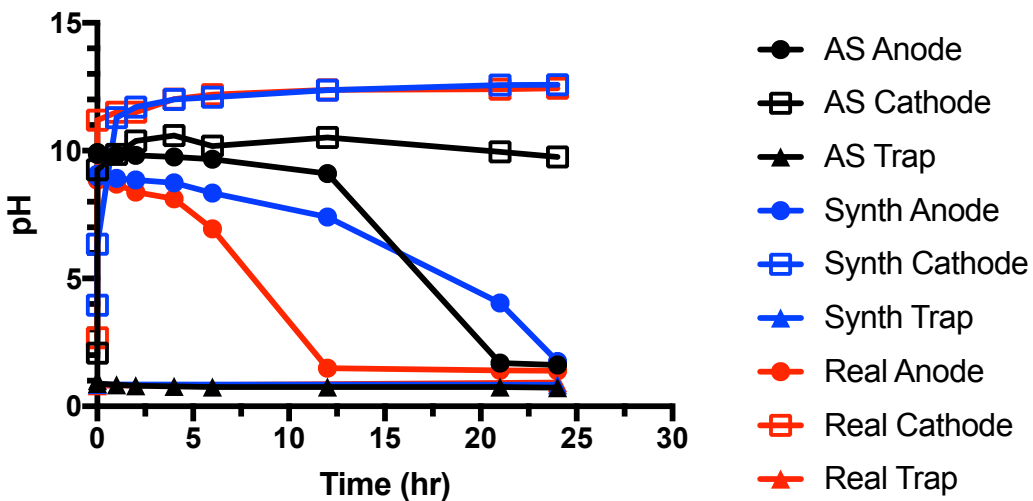


**Figure C9.** pH values for each chamber and influent during batch experiments (AS= ammonium sulfate, Synth=synthetic urine, Real= real urine).



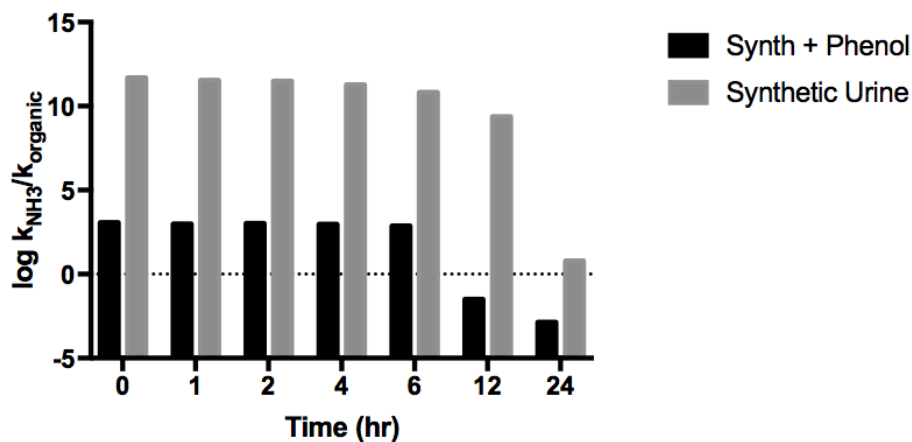


**Figure C10.** Time series of branching ratio of first-order rate constant for chlorine-ammonia vs. chlorine-organic. Organic in synthetic urine was acetate; organic in synthetic urine with phenol was phenol. Changes are due to decreases in pH and TAN due to electrochemical oxidation of water (produced protons) and  $\text{NH}_4^+$  migration due to electrochemical stripping process. Horizontal dashed line denotes equal rate constants for both reactions.

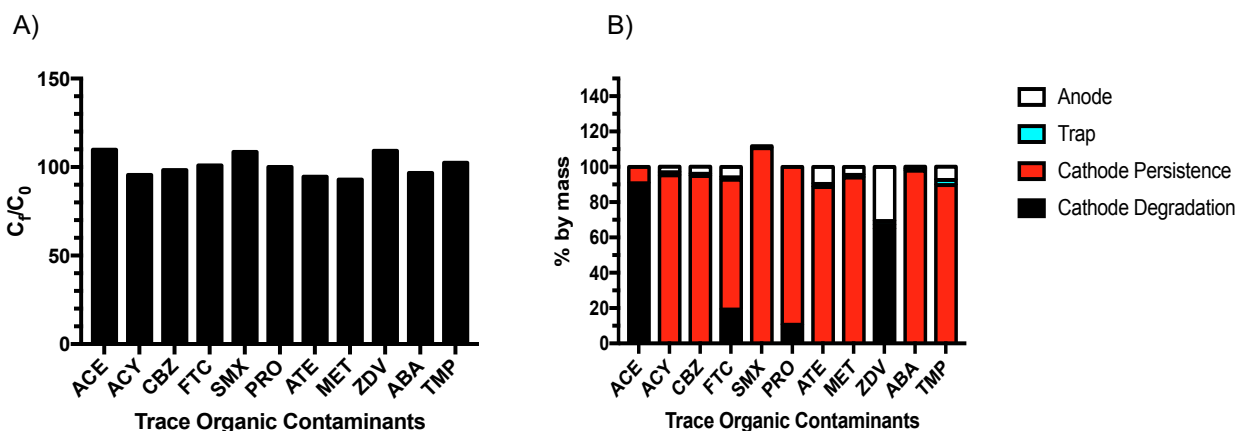


**Figure C11.** TrOC control experiments. (controls) (a) trap concentrations at 24 hours relative to initial concentrations for 20 ppb TrOCs added to 1 M  $\text{H}_2\text{SO}_4$ . (b) fate of TrOCs when added to the cathode at 20 ppb.

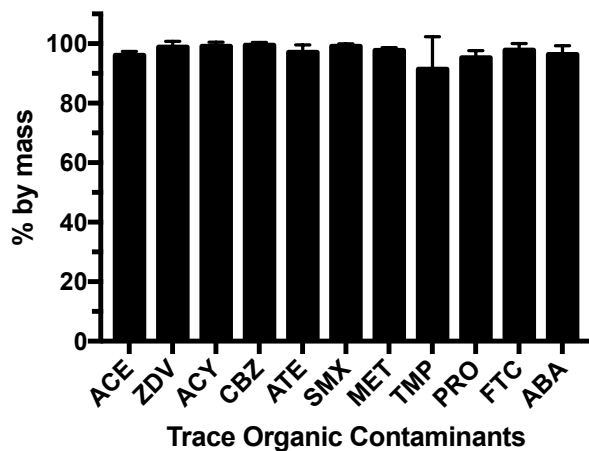


Figure C12. Anodic degradation for trace organic contaminants in synthetic urine.

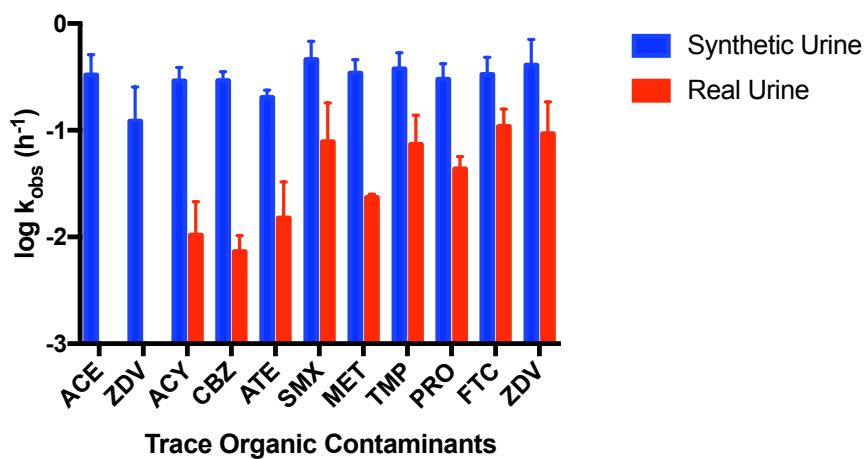


Figure C13. First-order rate constant for anodic degradation of trace organic contaminants in synthetic and real urine. Error bars represent  $\pm$  one standard deviation.

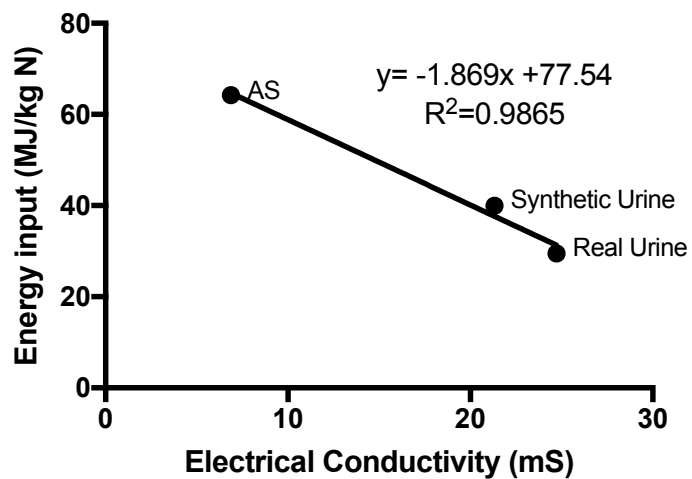
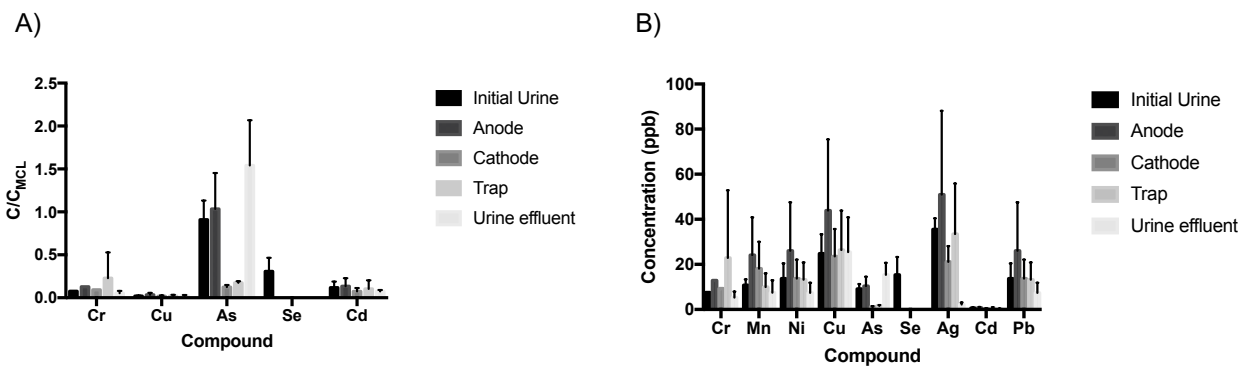


Figure C14. Conductivity vs. energy input for different influents. AS= ammonium sulfate.



**Figure C15.** (a) Concentrations in each chamber and influent and effluent urine of trace elements relative to their MCLs. (b) Concentrations of trace elements in each chamber, influent urine, and effluent urine. Error bars denote standard deviation.

## D. EVALUATING ION EXCHANGE FOR NITROGEN RECOVERY FROM SOURCE-SEPARATED URINE IN NAIROBI, KENYA

### D1. EQUATIONS

#### D1.1 Continuous Experiments

Breakthrough curves from column adsorption experiments were integrated to calculate the mass of ammonium adsorbed or eluted. Numerical integration was performed using the trapezoid rule:

$$\int C(BV)dBV \approx \sum_1^n \{ (BV_n - BV_{n-1}) * \frac{1}{2} * [C(BV_n) + C(BV_{n-1})] \} \quad (D1)$$

Where n is the number of data points, BV is number of bed volumes, and C(BV) is the concentration at a given number (BV) of bed volumes. For adsorption experiments, the mass of ammonium adsorbed was proportional to the area above the ammonium breakthrough curve and below the chloride tracer curve. For regeneration, the mass of ammonium eluted was calculated based on the total volume and concentration of the cumulative eluent. The equations for adsorption density (Equation D2) and regeneration efficiency (Equation D3) are:

$$q = \frac{\int [C_{Cl,ads}(BV) - C_{N,ads}(BV)] dBV * PV}{W * MW_N} \quad (D2)$$

$$\eta_{regen} = \frac{V_{eluent} C_{N,eluent}}{\int [C_{Cl,ads}(BV) - C_{N,ads}(BV)] dBV} \quad (D3)$$

Where PV is pore volume (mL/bed volume), the volume of liquid retained by a column full of resin, W is adsorbent mass (g adsorbent), q is adsorption density (mmol N/g adsorbent),  $V_{eluent}$  is the total volume of eluent after column regeneration (L),  $C_{N,eluent}$  is concentration in the final eluent (mmol N/L), and the subscripts on concentration C(BV) denote adsorption. Pore volume was calculated by subtracting the mass of a column full of dry resin from the same column filled with resin and distilled water.

#### D1.2 Calculation of Average Urine Collected in Sanergy Toilet

Sanergy collects approximately 5,000 L of urine each day from 781 toilets.<sup>150</sup>

$$\frac{5,000 \text{ L urine}}{\text{day}} * \frac{1}{781 \text{ toilets}} = \frac{6.40 \text{ L urine}}{\text{toilet} * \text{day}} \quad (D4)$$

#### D1.3 Jain-Snoeyink isotherm

An adapted Jain-Snoeyink isotherm<sup>98</sup> was used to predict ammonium adsorption density from initial ammonium concentration in Nairobi urine. This three-solute adaptation was developed in previous work on equilibrium isotherms for Dowex Mac 3. Of several models applied to batch

data in real urine, the Jain-Snoeyink model had the smallest error from experimental data. To predict batch adsorption in undiluted real urine, we used initial cation activities and model parameters to solve a system of six equations containing model predictions for each cation and mass balances on each cation:

$$q_{f,N} = \frac{q_{max,K}K_{ads,N}\{A_N\}}{1+K_{ads,K}\{A_K\}+K_{ads,Na}\{A_{Na}\}+K_{ads,N}\{A_N\}} + \frac{(q_{max,Na}-q_{max,K})K_{ads,N}\{A_N\}}{1+K_{ads,Na}\{A_{Na}\}+K_{ads,N}\{A_N\}} + \frac{(q_{max,N}-q_{max,Na})K_{ads,N}\{A_N\}}{1+K_{ads,N}\{A_N\}} \quad (D5)$$

$$q_{f,Na} = \frac{q_{max,K}K_{ads,Na}\{A_{Na}\}}{1+K_{ads,K}\{A_K\}+K_{ads,Na}\{A_{Na}\}+K_{ads,N}\{A_N\}} + \frac{(q_{max,Na}-q_{max,K})K_{ads,Na}\{A_{Na}\}}{1+K_{ads,K}\{A_K\}+K_{ads,Na}\{A_{Na}\}} \quad (D6)$$

$$q_{f,K} = \frac{q_{max,K}K_{ads,K}\{A_K\}}{1+K_{ads,K}\{A_K\}+K_{ads,Na}\{A_{Na}\}+K_{ads,N}\{A_N\}} \quad (D7)$$

$$q_{f,K} = \frac{V_L}{W} (C_{0,K} - C_{f,K}) \quad (D8)$$

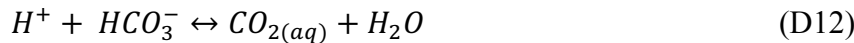
$$q_{f,Na} = \frac{V_L}{W} (C_{0,Na} - C_{f,Na}) \quad (D9)$$

$$q_{f,N} = \frac{V_L}{W} (C_{0,N} - C_{f,N}) \quad (D10)$$

where  $V_L$  is solution volume (L),  $C_0$  is initial concentration of adsorbate (mg  $\text{NH}_4^+$ -N,  $\text{Na}^+$ , or  $\text{K}^+$ /L),  $C_f$  is adsorbate concentration at equilibrium (mg  $\text{NH}_4^+$ -N,  $\text{Na}^+$ , or  $\text{K}^+$ /L),  $W$  is adsorbent mass (g), and  $q_0$  is the initial adsorption density (mg  $\text{NH}_4^+$ -N,  $\text{Na}^+$ , or  $\text{K}^+$ /g adsorbent). Maximum adsorption densities and affinity constants ( $q_{max}$  and  $K_{ads}$  for each cation) were determined from single-solute Langmuir isotherms.<sup>98</sup> For Nairobi urine, average composition of the sampled toilets was used (439 mM N, 139 mM Na, 59 mM K; data shown in Figure D2).

#### D1.4 Changes in urine composition during storage

During urine storage, volatile species such as  $\text{NH}_3$ ,  $\text{CO}_2$ , and volatile organic compounds diffuse out of the aqueous phase into the gas phase. Equilibrium reactions for ammonia and carbon dioxide are as follows:



As ammonia and carbon dioxide volatilize out of the aqueous phase, Equations D11 and D12 shift rightward. For ammonia, electrical conductivity is expected to remain the same because one mole of  $\text{H}^+$  is produced for each mole of  $\text{NH}_4^+$  that is consumed to maintain equilibrium. For carbon dioxide, electrical conductivity decreases because two moles of charged species ( $\text{H}^+$  and  $\text{HCO}_3^-$ ) are consumed for every mole of  $\text{CO}_{2(aq)}$  produced to preserve equilibrium.

#### D1.5 Calculating ion exchange cost

The total treatment costs ( $P_T$ ) were calculated as the sum of costs for adsorbent (resin), regenerant, cartridge manufacturing, cartridge collection, fertilizer bottling, renting facility space, and miscellaneous costs (e.g., pump and equalization tank manufacturing, pump operation and all material transportation for infrastructure construction). Based on previous work for life cycle cost assessment in San Francisco, the most expensive components were renting facility space, resin, and regenerant. Facility space is ample in the Sanergy case, so was neglected along with the other components that were less costly. In the field site studied here, cartridge collection is already included and cartridge manufacturing was inexpensive for the columns that were constructed in Nairobi. With these simplifications, the total treatment cost was approximated as the sum of adsorbent costs ( $P_A$ ) and regenerant costs ( $P_R$ ).

$$P_T = P_A + P_R \quad (D13)$$

Adsorbent costs per  $m^3$  urine ( $P_A$ ) were calculated according to Equation D14, where  $P_{\text{adsorbent}}$  is specific adsorbent price (USD/kg resin),  $[NH_3]_{\text{tot}}$  is total ammonia concentration in urine (g N/L,  $[NH_3]_{\text{tot}} = [NH_4^+] + [NH_3]$ , assumed 7.5),<sup>23</sup>  $N$  is number of uses before adsorbent replacement,  $q_0$  is adsorption capacity (mmol N/g resin, 4.9 for Dowex Mac 3),<sup>98</sup> and  $MW_N$  is the molecular weight of nitrogen.

$$P_A = \frac{P_{\text{adsorbent}}[NH_3]_{\text{tot}}*1000}{Nq_0MW_N} \quad (D14)$$

Regenerant cost ( $P_R$ ) was added to resin costs to calculate total treatment costs ( $P_T$ ) according to Equation D15 using the price of regenerant ( $P_{\text{regenerant}}$ , USD/L), volume of regenerant used per cycle ( $U_{\text{regenerant}}$ , L/(g resin\* cycle)), total ammonia concentration in urine ( $[NH_3]_{\text{tot}}$ , g N/L), number of uses before adsorbent replacement ( $N$ ), adsorption capacity ( $q_0$ , mmol N/g resin), and molecular weight of nitrogen ( $MW_N$ ).

$$P_T = P_A + \frac{P_{\text{regenerant}}U_{\text{regenerant}}[NH_3]_{\text{tot}}*N*(1000)^2}{q_0MW_N} \quad (D15)$$

Sulfuric acid (regenerant) cost was calculated from an average of 40 sulfuric acid costs from Alibaba.com: 0.285 USD/L 98% sulfuric acid.<sup>174</sup> The volume of regenerant used was calculated assuming stoichiometric exchange of both protons in  $H_2SO_4$  for  $NH_4^+$  on loaded resin (0.000135 L 98% sulfuric acid/g resin).

Costs for urine exhaustion, resin, regenerant, and total ion exchange treatment costs were converted from USD/ $m^3$  urine to USD/kg N ( $P_N$ ) using Equation D16. Total ammonia concentration ( $[NH_3]_{\text{tot}}$ ) in urine is 7.5 g N/L, or 7.5 kg N/ $m^3$  urine.

$$P_N = \frac{P_U}{[NH_3]_{\text{tot}}} \quad (D16)$$

## D1.6 Calculating value of Evergrow premium

The value of a hypothetical Evergrow premium fertilizer containing supplemental nitrogen recovered from urine via ion exchange was calculated based on approximate application rates for common crops ( $A_N$ , kg N acre<sup>-1</sup>), Evergrow application rates (kg Evergrow acre<sup>-1</sup>), the nitrogen content of Evergrow (3% by mass), and the price of nitrogen fertilizer (USD/kg N, see section D1.7). Urea was used for this calculation because it contains only nitrogen, as does the urine-derived nitrogen supplement. The additional value ( $P_p$ , USD kg Evergrow<sup>-1</sup>) of Evergrow premium compared to standard Evergrow ( $P_s$ ) was calculated as:

$$P_p = \frac{(A_N - A_S N_S) * P_N}{A_S} - P_S \quad (D17)$$

## D1.7 Calculating fertilizer cost

DAP price in Kenya, 2012: 3000 KES/50 kg DAP= 60 KES/kg DAP<sup>175</sup>

$$\frac{60 \text{ KES}}{\text{kg DAP}} * \frac{\text{USD}}{102.8 \text{ KES}} * \frac{1 \text{ kg DAP}}{1000 \text{ g DAP}} * \frac{132 \text{ g DAP}}{\text{mol DAP}} * \frac{1 \text{ mol DAP}}{2 \text{ mol N}} * \frac{1 \text{ mol N}}{14 \text{ g N}} * \frac{1000 \text{ g N}}{1 \text{ kg N}} = \frac{2.75 \text{ USD}}{\text{kg N}} \quad (D8)$$

Urea price in Kenya: 2 USD /kg urea<sup>176</sup> (average price from market survey in western Kenya)

$$\frac{2 \text{ USD}}{\text{kg urea}} * \frac{1 \text{ kg urea}}{1000 \text{ g urea}} * \frac{60 \text{ g urea}}{\text{mol urea}} * \frac{1 \text{ mol urea}}{2 \text{ mol N}} * \frac{1 \text{ mol N}}{14 \text{ g N}} * \frac{1000 \text{ g N}}{1 \text{ kg N}} = \frac{4.29 \text{ USD}}{\text{kg N}} \quad (D9)$$

Global urea price, averaged from 2010-2014: 350.6 USD/metric tonne urea<sup>177</sup>

$$\frac{350.6 \text{ USD}}{\text{metric tonne urea}} * \frac{1 \text{ metric tonne urea}}{10^6 \text{ g urea}} * \frac{60 \text{ g urea}}{\text{mol urea}} * \frac{1 \text{ mol urea}}{2 \text{ mol N}} * \frac{1 \text{ mol N}}{14 \text{ g N}} * \frac{1000 \text{ g N}}{1 \text{ kg N}} = \frac{0.75 \text{ USD}}{\text{kg N}} \quad (D10)$$

Global DAP (diammonium phosphate) price, averaged from 2010-2014: 426.4 USD/metric tonne DAP<sup>177</sup>

$$\frac{426.4 \text{ USD}}{\text{metric tonne DAP}} * \frac{1 \text{ metric tonne DAP}}{10^6 \text{ g DAP}} * \frac{132 \text{ g DAP}}{\text{mol DAP}} * \frac{1 \text{ mol DAP}}{2 \text{ mol N}} * \frac{1 \text{ mol N}}{14 \text{ g N}} * \frac{1000 \text{ g N}}{1 \text{ kg N}} = \frac{2.0 \text{ USD}}{\text{kg N}} \quad (D11)$$

DAP in Kenya is 37.5% more expensive in Kenya than the global average; urea is 472% more expensive.

## D2. TABLES

**Table D1:** Composition of synthetic urine.

	Synthetic Urine
pH	8.87
Total Ammonia Nitrogen (mg N/L)	7950
Sodium (mg Na/L)	2560
Potassium (mg Na/L)	2200
Chloride (mg Cl/L)	4180
Total Phosphate (mg P/L)	542
Total Sulfate (mg SO <sub>4</sub> /L)	472
Total Inorganic Carbon (mg C/L)	3250
COD (mg O <sub>2</sub> /L)	8000

**Table D2:** Application rates of standard Evergrow and suggested application rates for nitrogen fertilizers.

Crop	Evergrow application rate (kg Evergrow acre <sup>-1</sup> )	Suggested N application rate (kg N acre <sup>-1</sup> ) <sup>a</sup>
Corn	--	85.7 <sup>178-180</sup>
Tomatoes	750	71.7 <sup>181-184</sup>
Onions	400	60.9 <sup>185,186</sup>
French beans	400	22.6 <sup>180,187</sup>
Capsicum (bell pepper)	800	95.4 <sup>180,188,189</sup>
Cabbage	400	70.9 <sup>180,190,191</sup>

<sup>a</sup> Application rates were averaged from the sources shown.



### D3. FIGURES

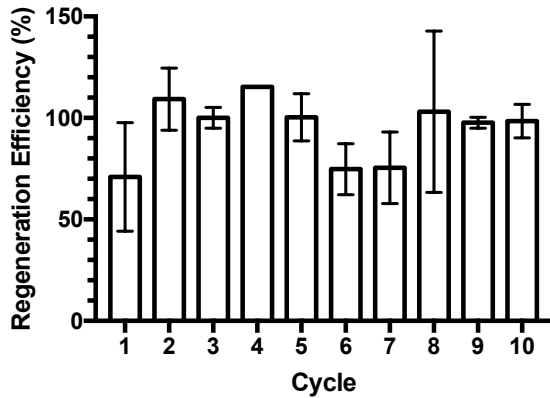


**Figure D1:** Regeneration efficiency vs. cycle. Error bars indicate one standard deviation above and below mean for experimental triplicates.

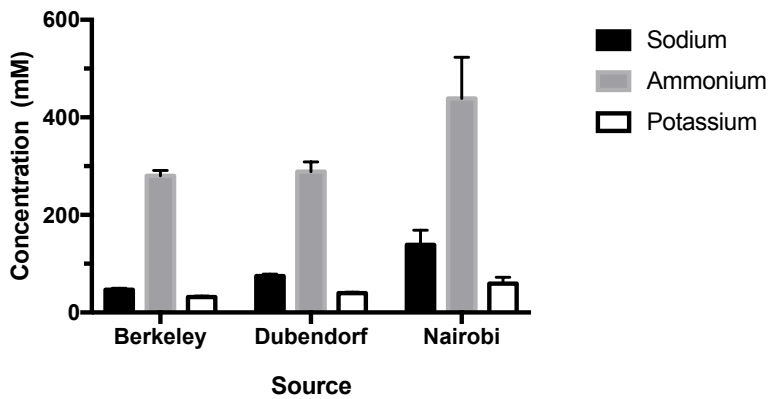


**Figure D2.** Cation concentrations in urine collected in Berkeley, Dubendorf (Eawag), and Nairobi (Sanergy).

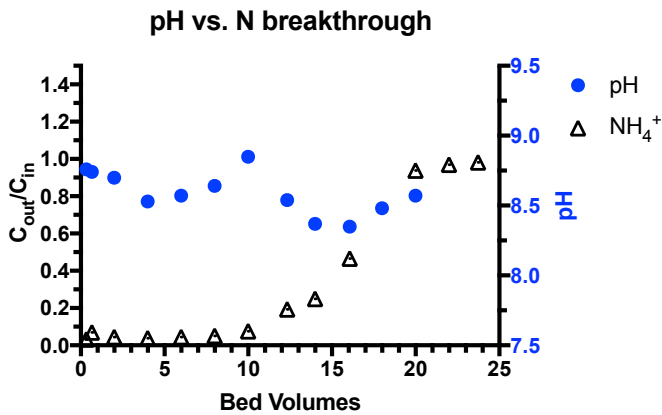


**Figure D3.** pH vs. ammonium breakthrough curve.

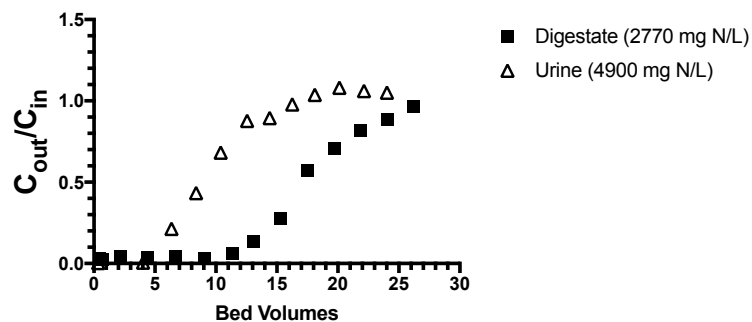


**Figure D4.** Digestate vs. urine ammonium breakthrough curves. Influent total ammonia nitrogen concentration in parentheses in legend. Calculated adsorption densities: 3.10 mmol N/g resin (digestate), 4.12 mmol N/g resin (real urine, average of triplicate columns shown in this graph).